Thyroid Hormone and Insulin Metabolic Actions on Energy and Glucose Homeostasis

Thyroid Hormone and Insulin Metabolic Actions on Energy and Glucose Homeostasis

A dissertation presented

by

Jessica Ann Hall

to

The Division of Medical Sciences

in partial fulfillment of the requirements

for the degree of

Doctor of Philosophy

in the subject of

Biological and Biomedical Sciences

Harvard University

Cambridge, Massachusetts

April 2014

Dissertation Advisor: Dr. Pere Puigserver **Jessica Ann Hall**

Thyroid Hormone and Insulin Metabolic Actions on Energy and Glucose Homeostasis

ABSTRACT

Faced with an environment of constantly changing nutrient availability, mammals have adapted complex homeostatic mechanisms to maintain energy balance. Deviations from this balance are largely corrected through a concerted, multi-organ effort that integrates hormonal signals with transcriptional regulatory networks. When these relationships are altered, as with over-nutrition and insulin resistance, metabolic disease ensues. Here, I present data concerning two distinct transcriptional pathways—one for thyroid hormone (TH) and one for insulin—that confer hormone responsiveness on metabolic gene programs that preserve energy homeostasis.

In brown adipose tissue (BAT), localized amplification of TH signaling by type 2 deiodinase (D2) is necessary for the acute thermogenic response to cold. Using mice lacking D2 (D2KO), we show that absence of D2-medaited TH signaling during BAT development decreases expression of the transcriptional program that defines BAT identity and underlies the thermogenic defects found in these mice in adulthood. Further, differentiation of D2KO brown adipocytes *in vitro* uncovered defective adipogenesis and decreased oxidative capacity consequent to enhanced oxidative stress and reduced insulin signaling. We hypothesized that impaired thermogenic potential of D2KO brown adipocytes alters metabolic response to high-fat feeding. Indeed, at thermoneutrality, D2KO mice exhibit increased susceptibility to obesity with glucose intolerance and hepatic steatosis. Interestingly, this phenotype was masked under room temperature thermal stress due to compensatory elevation of D2KO BAT sympathetic signaling.

These discoveries highlight the importance of local activation of TH signaling in BAT development and function, with significant ramifications for diet-induced thermogenesis and energy homeostasis control.

When nutrients and insulin signaling are low, hepatic forkhead transcription factor FoxO1 maintains glucose homeostasis by inducing expression of gluconeogenic enzymes. In an effort to understand posttranslational modifications that alter FoxO1 activity, we identified deubiquitinating enzyme USP7. We show that USP7-mediated mono-deubiquitination of FoxO1 suppresses FoxO1 transcriptional activity by decreasing gene promoter occupancy. Knockdown of USP7 in hepatocytes elevated gluconeogenic genes in a FoxO1-dependent manner. Conversely, overexpression of USP7 suppressed gluconeogenic gene expression in hepatocyte cells and in mouse liver, decreasing hepatic glucose production. Insight into this pathway might aid in designing therapies to restore glucose metabolic control in those with type 2 diabetes.

Table of Contents

List of Figures

List of Tables

Acknowledgements

My path to the Ph.D. has been a long and rewarding journey that has pushed my growth intellectually and emotionally. First and foremost, I would like to thank my advisor, Pere Puigserver. Through his guidance, patience, and support, he has helped transform my understanding of science. He has taught me how to think critically as an independent researcher and how to approach hypotheses with flexibility. Pere's excitement for unraveling new and important metabolic pathways is invigorating, and I am truly grateful to have been able to share in and contribute to his quest. I would also like to acknowledge my former mentor, Tony Bianco, who helped provide the foundation for my training as a scientist.

I am thankful to the members of my dissertation advisory committee, Bruce Spiegelman, John Blenis, Wade Harper, David Cohen, and Tony Hollenberg, for their invaluable advice and selfless commitment to my success. Also, I would like to express my sincere appreciation to the BBS program office, especially Kate Hodgins and Maria Bollinger, for their support and encouragement over the years and even across state-lines.

During my graduate studies, I have had the fortunate privilege of working with really talented, compassionate colleagues who have contributed to an academically enriching—and fun—lab environment. And although all have undoubtedly helped shape the scientist that I am today, there are some who deserve particular mention. To that end, I would like to thank Sharon Blättler, Helen Chim, John Dominy, Zach Gerhart-Hines, Tim Kelly, Yoonjin Lee, Ji-Hong Lim, Chi Luo, Joe Rodgers, Mitsu Tabata, Kiko Verdeguer, Rutger Vogel, Renata Grozovsky, John Harney, Brian Kim, Scott Ribich, Matt Rosene, Cintia Ueta, and Ann Marie Zavacki. Their friendship and guidance not only left a positive impact on my science, but also on my well-being.

I would also like to thank my friends outside of the lab. I am extremely lucky to have made some wonderful, lasting friendships in the BBS program, including Shariya Terrell, Monica Markovski, Alison Taylor, and Caitlin Reavey. Our shared graduate school experiences provided the strength and support that I needed to overcome the challenges and made the successes all the sweeter. I am also deeply grateful to my dear friends, Jamie Pool and Ale Schneider Leupold, for their encouragement, counsel, and humor. The laughs that we shared provided a most-welcomed escape from my life in the lab. I will always be thankful for their support and solidarity.

Most importantly, I am indebted to the constant love and unwavering support from my family. I am immensely appreciative of my siblings, Elizabeth, Christopher, and Rebecca. Our silly adventures together have helped me keep life in perspective and rejuvenate the soul. Elizabeth, my courageous sister with type 1 diabetes, has also been a source of inspiration for my commitment toward diabetes research—I hope and trust that one day there will be a cure. Finally, I would like to express my deepest gratitude to my parents, Bill and Ilona. My dad's calming advice and my mom's care packages have helped brighten even the darkest days. They have been my biggest supporters every step of what has been a rather long and, at times, challenging graduate career. To them I extend a heartfelt thank you for their encouragement, for their sacrifices, and for always believing in me.

Chapter 1

Introduction

A constant supply of energy is an essential requirement for life in all organisms. We obtain this energy from our environment, process what we need for immediate use, and store the rest. For mammals, extensive endocrine and neural signals coordinate the actions of multiple organ systems to maintain energy homeostasis despite fluctuating nutrient levels and varying degrees of energy demand. When these connections are damaged, however, balance is disrupted and a variety of common metabolic disorders may result. Throughout this work, I will provide data to suggest key pathways at the intersection of hormonal and transcriptional control that affect metabolic gene programs and alter organismal homeostasis. Namely, I will 1) examine a role for type 2 deiodinase in brown adipose tissue development and protection from obesity, and I will 2) characterize the function of deubiquitinating enzyme USP7 in hepatic gluconeogenesis and whole body glucose metabolism.

BROWN FAT ACTIVATION IN THE CONTROL OF ENERGY HOMEOSTASIS

In this section, I first will introduce the obesity epidemic and discuss activation of brown adipose tissue as a possible therapeutic approach to increase energy expenditure and promote weight loss. Next, I will review our current understanding of the process by which precursor brown fat cells differentiate into mature adipocytes. Finally, I will discuss the importance of thyroid hormone signaling and the deiodinase enzymes in brown adipose tissue function.

"The body is a ship which must not be overloaded" – Plutarch

The obesity epidemic and weight loss strategies

We are a population with a growing healthcare concern as blatantly obvious as our expanding waistlines. Obesity, or corpulency as it was once referred to, results when energy

intake exceeds energy expenditure, which leads to a massive expansion of adipose tissue that has adverse health consequences. Using a function of weight and height, obesity is characterized as having a body mass index (BMI) of 30 or above. With this criterion in mind, the most recent data on obesity prevalence in the United States reveals an alarming statistic: 34.9% of American adults are obese (1). However, the obesity epidemic is not just a national concern, and the World Health Organization (WHO) estimates that more than half a billion adults worldwide are obese. These figures are nearly double that from 30 years ago, and the forecast for the future does not look promising. The excess weight carries with it a higher risk for an onslaught of comorbid conditions, including type 2 diabetes, cardiovascular disease, and some cancers, thereby reducing life expectancy and placing a massive burden on global healthcare (2). The challenge that lies ahead for the medical and scientific communities is to safely shrink our growing midsections and mitigate the comorbidities for those who have already tipped the scale.

A central tenet of obesity management is to avoid a positive energy balance by decreasing food intake and increasing energy expenditure. Modest weight loss of 5–10% of initial body weight achieved through intensive lifestyle modification is considered clinically meaningful, as it reduces cardiovascular disease risk factors, prevents or delays type 2 diabetes, and improves other health consequences of obesity (3). However, strong evolutionary pressure to avoid starvation in cases of famine has crafted our homeostatic mechanisms to favor energy storage over expenditure; evolution did not prepare us for an industrialized world with unrestricted food access (4). Indeed, fluctuations by 10% in body weight are accompanied by corresponding corrections in energy expenditure, making it difficult to deviate from one's "usual" weight (5). Studies have shown that only about 20% of individuals who lose 10% of

their initial body weight are able to maintain this weight loss for at least 1 year post-treatment (6), which is associated with a decline in mitigated risk (7).

Given the challenges of long-term weight maintenance, there is a medical need for adjunctive therapies in the weight-loss battle. Currently, all of the available pharmacotherapies tackle the energy intake side of the obesity equation (8). By suppressing appetite or limiting absorption of dietary fats, use of these agents in combination with lifestyle intervention can provide greater weight loss than diet and exercise alone. However, none of these obesity medications has been shown to decrease cardiovascular morbidity or mortality (9). On the contrary, several anti-obesity drugs have actually been withdrawn from the U.S. marketplace or are prescribed with caution due to increased risk of cardiovascular complications or alterations in hepatic function (10). And of the therapies available, unacceptable side effects often preclude a broader use (11). For extreme cases of obesity, bariatric surgery has documented success in causing long-term weight loss as well as complete remission of diabetes in many individuals, but surgical intervention is not practical on a global scale (12).

Considering the difficulty and apparent limitations of altering energy intake, the obvious alternative is to target energy expenditure. Some components here are within our control, such as physical activity, but others are not, such as the energy expended for obligatory cellular processes that are necessary for maintaining life and limb. Another component of energy expenditure is thermogenesis—the production of heat energy—which occurs in all cells as a byproduct of inefficiencies in mitochondrial adenosine triphosphate (ATP) production and biochemical ATP use (i.e. “futile” metabolic cycles). However, *adaptive* thermogenesis, by transforming chemical energy into heat, has evolved as a defense to cold exposure and caloric

excess for some organisms (13). And one organ has made this its prime prerogative: brown adipose tissue (BAT).

Brown adipose tissue function

BAT was first discovered in 1551 by the Swiss naturalist Konrad Gessner (14), but it was not recognized for its dominant role in heat production until the latter half of the 20th century, when it was demonstrated as the major site for non-shivering thermogenesis of cold-exposed rats (15). Indeed, BAT is well documented in mammals where shivering is an inefficient means of heat generation, such as those with a high surface area to volume ratio and those that cannot afford the convective heat loss from body movement. These include small rodents and human infants. Hibernating mammals also use BAT to rapidly elevate body temperature during bouts of arousal from hibernation. In rodents, BAT is present in the interscapular, axillary, and perinephric depots. The interscapular depot, being the largest, is the one most commonly studied. Scientific understanding of BAT has greatly increased since its description as the "hibernating organ," and it is now appreciated for having roles in both cold- and diet-induced thermogenesis (16).

The functional unit of BAT is the brown adipocyte, which is a highly specialized cell capable of dissipating stored chemical energy in the form of heat. On a cellular level, brown adipocytes differ from white adipocytes in that they are multilocular (numerous small lipid inclusions as opposed to one large vacuole), contain a nucleus that is spherical and centrally located (as opposed to flattened against the periphery), and have a high concentration of iron-containing mitochondria (providing the "brown" color from which they get their name). Mitochondria in brown adipocytes are unique in that they harbor a capacity to uncouple fuel

oxidation from ATP generation. Specifically, brown adipocytes express a BAT-specific protein called uncoupling protein 1 (UCP1) that sits in the inner mitochondrial membrane. When activated, UCP1 catalyzes a proton leak from the intermembrane space into the mitochondrial matrix. This short-circuits the electrochemical gradient that drives ADP phosphorylation. Combustion of substrates accelerates to offset the falling ATP levels, with a net result being the generation of heat (16).

Both the sympathetic nervous system and thyroid hormone engage in a vital crosstalk to maintain BAT function. Sympathethic signaling increases in the cold, and chronic cold exposure leads to the recruitment (proliferation and differentiation) as well as activation of the mature adipocyte (17). Norepinephrine release from sympathethic nerve terminals stimulates β-adrenergic receptors (β-AR), which results in a rapid accumulation of cyclic AMP (cAMP), a second messenger responsible for eliciting thermogenic effects in the brown adipocyte (18). One such effect is elevated transcription of the *UCP1* gene, which occurs subsequent to binding of protein kinase A (PKA)-activated cAMP response element binding protein (CREB) to four cAMP response elements (CREs) in the *UCP1* promoter and enhancer (19). Mice in which all three known β-ARs are lost ("β-less" mice) exhibit defective cold- and diet-induced thermogenesis, highlighting the requirement for β-adrenergic signaling (20). That thyroid hormone also plays a crucial role is seen by the inability of hypothyroid animals to survive in the cold (21, 22). This is related to the finding that inadequate levels of thyroid hormone render BAT incapable of heat generation upon norepinephrine stimulation (22, 23). Indeed, the appropriate thermogenic transcriptional response is mediated through several thyroid hormone-sensitive genes, including *UCP1* (24). These processes are further intertwined, as sympathetic stimulation leads to a tissue-level thyrotoxicosis through type 2 deiodinase (D2), which is encoded by the

cAMP-dependent *Dio2* gene and is responsible for amplifying thyroid hormone signaling (discussed in detail below). Of note, both thyroid hormone and catecholamines exert prominent effects on the basal metabolic rate, generating heat through obligatory thermogenesis, as well (25).

The potential for brown fat to have an anti-obesity effect has been highlighted in recent years. Certain high caloric diets that encourage overeating in rodents were found to stimulate BAT expansion and thermogenesis as a supposed physiological adaptation to thwart weight gain (26). This became known as "diet-induced thermogenesis" and led to the assumption that BAT normally functions to counter obesity by lowering metabolic efficiency. In support of this notion, brown fat ablation in transgenic mice with a *UCP1* promoter-driven toxigene led to the development of obesity (27). The role of UCP1 *per se* in controlling body weight was further supported by additional studies using conventional knockout technology to delete UCP1. When these UCP1-deficient mice were housed at thermoneutrality (28–30°C), they too showed a propensity toward body weight gain (28). It is important to note that UCP1 knockout mice failed to show an obese phenotype when reared under the chronic thermal stress of standard "room temperature" conditions (18–22°C) (29, 30). Together, these studies emphasize the potential for BAT activation in the context of promoting and sustaining weight loss by increased energy expenditure.

Brown adipose tissue in humans

Until recently, the minimal BAT present in adult humans was considered vestigial—likened to an organ of as questionable importance as the appendix. BAT was believed to be largely absent and metabolically irrelevant in healthy adults, appearing only under extreme

conditions of chronic cold exposure, as with the Finnish lumberjack, or in pheochromocytoma patients with pathological excess of catecholamines (31, 32). Moreover, the existence of brown fat in adult humans was so thoroughly denied that many cautioned against extrapolating the functional significance of BAT from rodent studies to man (33).

This position changed when a combination of whole-body imaging with molecular techniques finally allowed for definitive proof of BAT in adult humans. Early reports of high symmetric uptake of ^{18}F-fluorodeoxyglucose (^{18}F-FDG) in the neck/thoracic region of patients undergoing positron-emission tomography (PET) to detect tumors/metastases baffled oncologists (34). These symmetric "false positives" were deemed putative BAT after analysis with combined PET and computed tomography (CT; PET-CT) and recognizing the ability of norepinephrine to stimulate glucose uptake in BAT (35-37). However, debate in the scientific community persisted until 2009, when three groups determined that the tracer uptake in the supraclavicular and spinal regions was consistent with brown fat, with the detection of UCP1-positive cells serving as definitive proof (38-40). Moreover, these studies demonstrated that brown fat activity correlates inversely with age and obesity, generating excitement for a potential role of BAT in adult human metabolism. The presence and activity of BAT in the adult population means that it may be used as a target for interventions aimed at modulating energy expenditure.

In rodents, the thermogenic capacity of BAT to defend against obesity is impressive, but its potential to alter energy balance in adult humans is still unclear. Rothwell and Stock (1983) famously postulated that in humans, as little as 40–50 g of maximally active BAT could contribute up to 20% of basal energy consumption (41). However, this is most likely an overestimation for the oxidative capacity of human BAT (42). In mice at least, reduced BAT activity has been associated with predisposition to obesity (43, 44) and abnormal glucose

homeostasis (45). Although its predominant fuel source is lipid, its ability to catabolize glucose means that activation of BAT could have anti-obesity as well as anti-diabetic effects (46). The potential for inducing even small amounts of brown fat in adult humans to increase energy expenditure could provide a new therapeutic approach to curb the obesity crisis.

In the 1930s, the chemical uncoupler 2,4-dinitophenol (DNP) was widely used as an anti-obesity pill. Like activated UCP1, DNP promotes proton leakage across the mitochondrial membrane, albeit in a non-tissue-specific manner. Unfortunately for DNP, the pharmacologically effective dose is very close to that which leads to dangerous side effects, including death by hyperthermia, ultimately precluding its use today (8). Despite its failings, DNP treatment provides proof-of-concept support for targeting uncoupled respiration for weight loss and highlights the possible clinical utility of BAT activation therapy. The goal then should be to develop strategies that safely enhance respiratory uncoupling by exploiting the mechanisms naturally evolved to do so, as with the recruitment and activation of brown fat.

Brown adipose tissue development

BAT appears earlier during embryonic development than other fat depots and reaches its maximum mass shortly after birth (2–4% of birth weight in humans), with only small mammals maintaining large amounts of BAT into adulthood (47). In mice, an interscapular BAT depot is first observed around embryonic day 15 (E15). The rapidly expanding fat mass is accompanied by cell proliferation, increased triglyceride content, and a rise in mitochondrial number and activity, obtaining peak differentiation and functional activity postnatally (48). In humans, histomorphological studies have shown that immature brown adipocytes can be detected in the interscapluar region as early as in the 29th week of gestation (49). More recently, through a

combined use of high-resolution imaging and biochemical analysis, this interscapular depot of human infants has been confirmed to be bona fide brown fat, similar to rodents (50). Thus, late fetal development of rodent BAT provides a unique model to study brown adipocyte differentiation *in vivo*.

Transcriptional control of brown adipocyte differentiation

Differentiation, also known as adipogenesis, is the process by which precursor cells (preadipocytes) in adipose tissue undergo a transcriptional program to become mature adipocytes. Despite differences in function and developmental origin, the differentiation process for white and brown adipocytes involves many of the same factors, and much of what we know about brown adipocyte differentiation comes from studies of cultured white adipose cell lines originally developed by Howard Green and colleagues in the 1970s (51, 52). The differentiation of preadipocytes into adipocytes involves growth arrest, clonal expansion, and terminal differentiation. Adipogenesis is regulated by a coordinated transcriptional cascade, including the sequential activation of members of the CCAAT/enhancer-binding proteins (C/EBP) family of basic region leucine zipper (bZIP) transcription factors and the nuclear hormone receptor peroxisome proliferator-activated receptor γ (PPARγ) (53).

PPARγ is the transcriptional master regulator of adipocyte differentiation and is absolutely required for adipogenesis (54). Key to the function of both brown and white adipocytes, PPARγ binds to and regulates a large number of genes that span the gamut of adipocyte metabolism, including those involved in fatty acid uptake, binding, and storage. This includes adipocyte fatty-acid-binding protein (FABP4, also known as aP2), a marker of terminally differentiated adipocytes (55, 56). Most pro-adipogenic transcription factors act, to

some extent, by inducing PPARγ expression and activity. The temporal expression of C/EBPβ, C/EBPδ, and C/EBPα are crucial in this role (57). Interestingly, C/EBPβ also has a unique function in brown adipocytes; it is enriched in brown adipose relative to white adipose, and it aids in controlling the brown fat-selective gene signature (58). Furthermore, although PPARγ is not exclusive to BAT, it does activate the *UCP1* enhancer only in brown fat cells (59).

There are also many negative regulators of adipogenesis. A widely accepted marker of both brown and white preadipocytes is preadipocyte factor 1 (Pref1; also known as Dlk1 or *Drosophila* Homolog-like 1). Its expression is high in preadipocytes and declines with differentiation (60). Mice lacking Pref1 exhibit several abnormalities including accelerated adiposity (61), whereas Pref1 overexpression in adipose results in decreased fat pad size (62). Other notable inhibitors of adipogenic differentiation include several members of the GATA-binding and forkhead transcription factor families, as well as Wnt signaling family members (53). Many of these anti-adipogenic factors show decreased expression over the course of differentiation, highlighting the importance for their repression under a pro-adipogenic environment.

The final stages of brown adipocyte differentiation are unique for their preferential expression of a number of genes, such as PPARγ coactivator 1α (PGC-1α) and numerous genes involved in mitochondrial biogenesis (63). PGC-1 (now known as PGC-1α) was first identified in brown fat as a cold-inducible coactivator of PPARγ and thyroid hormone receptor β (TRβ) on the *UCP1* promoter (64). The importance of PGC-1α extends well beyond its role in brown adipocyte biology, being hailed as a master regulator of mitochondrial biogenesis and oxidative metabolism in most tissues and coactivating numerous transcription factors for a key role in many areas of energy homeostasis (65).

PGC-1α is essential for cold- and cAMP-induced thermogenic gene expression. Two independent PGC-1α whole body knockout mouse lines were found to develop severe hypothermia when challenged with cold (66, 67), and PGC-1α knockout brown fat cells fail to mount a normal thermogenic response when treated with cAMP (68). Similarly, forced expression of PGC-1α in white fat cells induces the mitochondrial and thermogenic gene programs (64, 69). However, brown adipocytes lacking PGC-1α have the same adipogenic capacity as wildtype cells and express many BAT-selective markers, suggesting that the identity of brown fat cells does not require PGC-1α (68). Thus, while critical for the thermogenic function, PGC-1α does not dictate commitment to the brown fat fate.

While searching for a transcription factor that uniquely regulates all aspects of the specific brown adipocyte transcriptome, Seale and colleagues discovered the zinc-finger containing PR-domain-containing protein-16 (PRDM16) (70). Surprisingly, knockdown of PRDM16 from brown fat cells was shown to not only ablate the entire brown fat character, but it also uncovered a cell fate switch into muscle (70, 71). These discoveries and others (72, 73) challenged the preexisting belief that brown and white adipocytes originate from the same precursor population and provoked a paradigm shift in our understanding of preadipocyte lineage commitment. Specifically, current data support a new model where muscle and brown fat—but not white fat—derive from the same precursors (74). In addition, muscle-specific lineage tracing studies revealed that not *all* UCP1-containing cells originate from muscle precursors (71). Those that emerge in white fat depots upon chronic cold exposure or treatment with β-agonists, a process commonly referred to as "browning," express a transcriptional signature distinct from "classical" interscapular brown adipocytes (75). These so-called "beige" or "recruitable BAT" cells have received considerable attention from the scientific community, especially given recent

studies indicating that the UCP1-positive cells in adult humans share more characteristics with rodent beige adipocytes than brown adipocytes (74, 76).

Thyroid hormone signaling

Thyroid hormone is critical for the time- and tissue-specific regulation of numerous developmental and metabolic processes (77). The thyroid gland is responsible for producing thyroid hormone, of which it secretes two varieties. The majority secreted is in the form of the biologically-inactive prohormone thyroxine (T4). Its triply iodinated derivative, 3,5,3′-triiodothyronine (T3), is the active form capable of binding the nuclear TRs responsible for thyroid hormone signaling within a cell. This transcriptional response is aided by extrathyroidal production of T3, which contributes about 80% of the body's daily T3 in humans (78). When systemic levels of thyroid hormone are low, the anterior pituitary releases thyroid stimulating hormone (TSH), which binds to the TSH receptor of the thyroid follicular cell to activate synthesis and secretion of thyroid hormone, providing a feedback mechanism to ensure steady levels of thyroid hormone in the plasma (79). This tight regulation reflects the necessity of thyroid hormone for the proper functioning of many physiological systems, and one's health mandates that serum thyroid hormone levels stay within a normal euthyroid range.

Cells acquire T3 from two different sources: plasma T3 and intracellular 5′ monodeiodination of T4 in tissue. This deiodination of thyroid hormone is catalyzed by the iodothyronine deiodinases[1], which selectively activate or inactivate thyroid hormone through removal of an iodide moiety from the phenolic (outer) or tyrosil (inner) ring of the

[1]Note that type 1, 2, and 3 iodothyronine deiodinases are distinct from iodotyrosine deiodinase I. Throughout this body of work whenever "deiodinase" is mentioned, it is in reference to the iodothyronine deiodinases.

iodothyronines, respectively (Figure 1.1) (77). Type 2 deiodinase (D2) is the main deiodinase to catalyze local activation of thyroid hormone, whereas type 3 deiodinase (D3) is the main deiodinase to catalyze local inactivation of T3 and T4. Comparatively, type 1 deiodinase (D1) is kinetically inefficient and is the only deiodinase capable of both activating and inactivating T4 (80). Together the deiodinases modulate thyroid hormone signaling in a tissue-specific manner despite a relatively constant level of thyroid hormone in plasma (80).

The extent of thyroid hormone signaling within a cell depends on the net occupation of T3-bound TRs. TRs bind to distinct DNA sequences known as thyroid hormone response elements (TREs) in the promoters of thyroid hormone-responsive genes, leading to transcriptional modification of these genes. Liganded TRs will activate genes with positive TREs and downregulate genes with negative TREs; however, the mechanism of negative regulation is not well understood. Importantly, the unliganded TR is not a passive bystander, as it can act as an aporeceptor and repress basal transcription through recruitment of corepressors (81, 82). For positively regulated T3-genes, T3 binding to the TR alters this transcriptional complex, remodeling chromatin to promote transcription (83). TR occupancy is dependent on the intracellular T3 concentration, which in the majority of tissues is similar to the serum free T3 concentration (84). However, tissues expressing the deiodinases have either higher or lower levels of T3 concentration and TR saturation due to additional T3 (in the case of D2) or inactivation of T3 (in the case of D3) (80). An example of this is BAT, which upon cold-induced adrenergic stimulation increases intracellular T3 by ~5-fold through a ~50-fold increase in D2 activity (85), eliciting the transcription of T3-responsive thermogenic genes (77). As a consequence, the amount of TR occupancy is much higher in D2-expressing cells (70–90% compared to 40–50% in most tissues) (80).

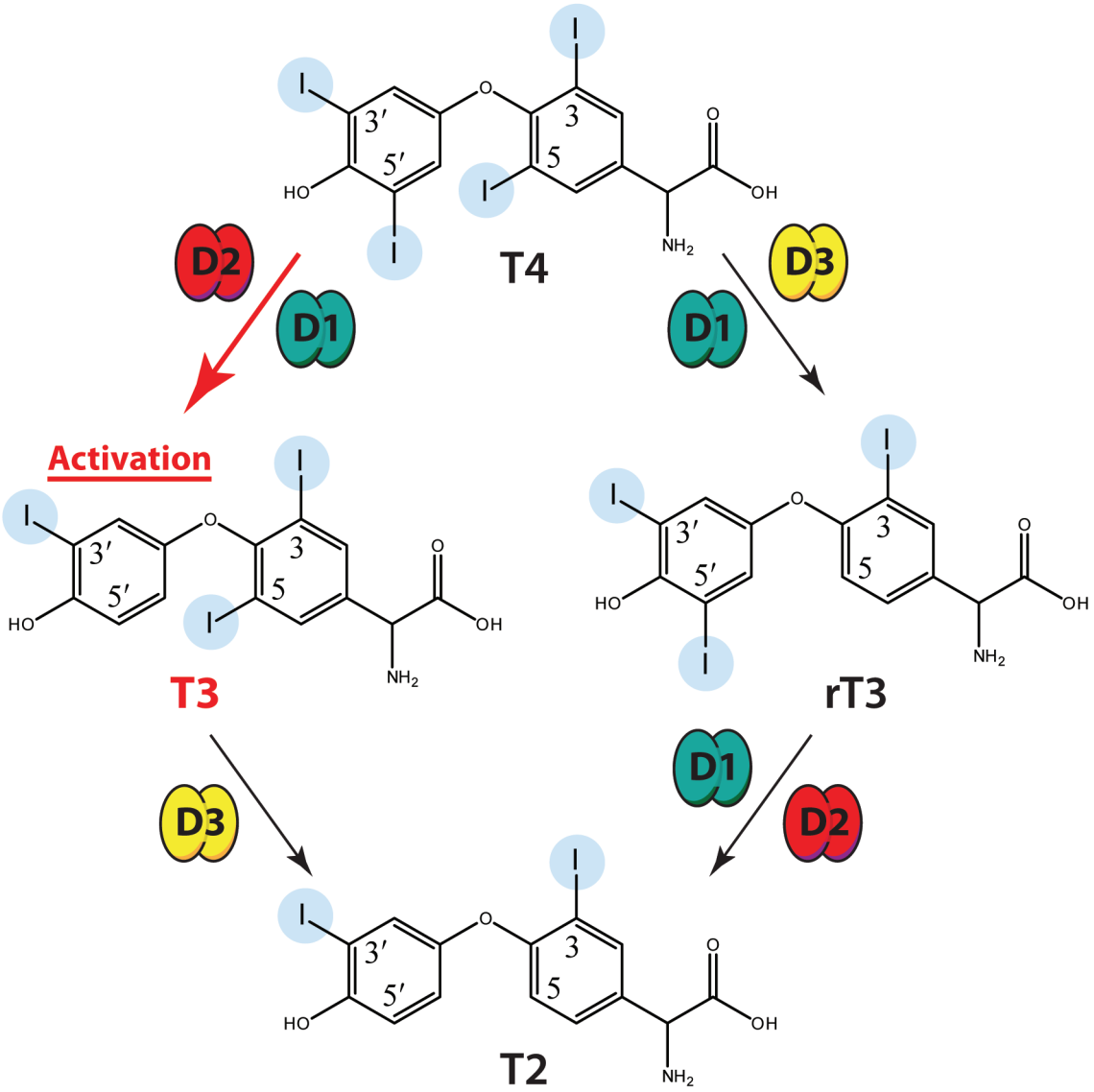

Figure 1.1. Thyroid hormone deiodination. Outer ring deiodination of T4 by D2 or D1 produces T3, the biologically active form of thyroid hormone. T4 can be inactivated by D3 or D1 to generate rT3. T2 is an inactive metabolite common to both pathways. Adapted from (80).

Type 2 deiodinase

There are certain key features of D2 that endow it with the privileged capacity to specifically and transiently elevate nuclear TR occupancy by T3. In common to all three deiodinases, D2 is a thioredoxin-fold-containing enzyme that catalyzes the deiodination reaction through a vital selenocysteine in its active center (86, 87). Also integral to its catalytic activity is a homodimerization event that renders a proper conformation for its active center (88). D2 is located in the endoplasmic reticulum, which, given its close proximity to the nuclear compartment, provides D2 with a spatial advantage for easy access of its deiodinated substrate to the nucleus (78). This is perhaps best reflected by the longer nuclear retention time of D2-generated T3 compared to T3 from the plasma (hours *vs*. minutes, respectively) (89). In addition, D2 is subjected to multiple levels of control that are both transcriptional and posttranslational to ensure tight regulation of its activity (90). As mentioned earlier, *Dio2* is responsive to cAMP, as seen during cold exposure. Unique to BAT, *Dio2* expression also increases in a feed-forward manner with T3 stimulation, highlighting the similarities between the *Dio2* and *UCP1* transcriptional response (91). D2 is subject to ubiquitination and proteasomal degradation and has a short half-life (approximately 40 minutes), which is further decreased (to approximately 20 minutes) upon exposure to substrate such as T4. The potency of substrate inhibition after catalysis provides a mode of negative feedback regulation that efficiently controls cellular T3 production (92, 93).

D2 in adaptive thermogenesis

It is by now well established that D2 plays a critical role in BAT thermogenesis. The cold-induced activation of BAT thermogenic function relies on a cAMP-mediated increase in

D2-generated T3 (94), which increases T3-sensitive genes, such as *UCP1*. It is worth emphasizing that the increased T3 signaling of the cold-stimulated brown fat occurs in an isolated fashion; circulating T3 levels remain constant despite the local thyrotoxicosis in BAT (95). The role here of D2 has been further clarified by studies of mice with targeted disruption of the *Dio2* gene [D2KO mouse (96)]. Upon cold exposure, D2KO mice exhibit a mild hypothermia that is otherwise offset by compensatory shivering, which is an unusual thermogenic behavior in mice (97). That these mice have impaired adaptive thermogenesis was clearly shown by a decreased thermal response of interscapular BAT to norepinephrine (97). Further, isolated brown adipocytes from D2KO mice had diminished norepinephrine-induced *UCP1* expression, which could be rescued when mice were given a TR-saturating dose of T3 (97). A follow-up study revealed that D2KO mice are able to survive cold exposure due to increased sympathetic activity, which elevates to overcompensate for a decreased adrenergic responsiveness of the D2KO BAT (98). Since the D2KO mouse is systemically euthyroid, these results lend further support to the prevailing hypothesis that tissue-specific control of thyroid hormone signaling in BAT is important for increasing energy expenditure. In addition, supplementation of diet with bile acids mediates a resistance to diet-induced obesity in mice via upregulation of D2 activity in BAT, indicating that D2's role in brown fat might extend beyond cold-induced thermogenesis (99).

Deiodinases and development

Deiodinase-catalyzed temporal and spatial modulation of thyroid hormone signaling plays an essential role in the development of various tissues (80). The timing of deiodinase activity is crucial for a diverse set of developmental events, including D3 in proper rotation of

the retina in *Xenopus laevis* (100), ubiquitination and subsequent inactivation of D2 in the tibial growth plate of developing chickens (101), as well as D2 in a critical period of cochlear development in mammals (102, 103). The coordinated action of the deiodinases in modulating thyroid hormone signaling has been suggested to play a role in the switch between proliferation and differentiation in different cell models, such as in chondrocytes and keratinocytes, where activation of D3 and inactivation of D2 lead to a cellular hypothyroidism that enhances proliferation (101, 104). Thus, D3 is thought to promote proliferation by limiting intracellular T3, and D2, by increasing T3, is regarded as being pro-differentiative.

Thyroid hormone has long been known as an adipogenic factor for white preadipocytes based on studies in which cells were cultured under non-physiological conditions of hypo- or hyperthyroidism. T3 is frequently used in adipogenic cocktails at supra-physiological levels to induce differentiation and is absolutely required for terminal differentiation of some white preadipocyte cell lines (105-107). D3 has recently been recognized for its high expression and association with brown adipocyte proliferation (108), calling attention to a possible role for the deiodinases in brown adipocyte development. Notably, D3 is encoded in the same locus as the anti-adipogenic Pref1. Since imprinting is coordinately regulated (109), it seems likely that D3 is an additional member of this imprinted gene network that regulates differentiation of fat cells.

Brown fat development is unique in that it reaches its maximum T3-binding capacity and TR expression prior to birth, which is unlike other thyroid hormone-sensitive tissues that attain maximum T3-resposniveness postnatal (110). With the exception of the thyroid gland, tissue T3 concentration is higher in BAT than in any other tissue of the developing fetus. This is especially remarkable in light of the low prenatal circulating T3 levels (111). In fact, this tissue-specific increase in T3 most likely reflects the ontogenic profile of BAT D2 activity, which has been

shown to dramatically increase during late fetal life of rats and mice (110, 112, 113). But a precise role for D2 in the developing BAT remained unclear.

Objectives

There is an urgent need for new drugs to treat a growing population of obese individuals, and a better understanding of brown adipose tissue development and function may offer safe alternatives to increase energy expenditure as an anti-obesity therapy. D2 has previously been recognized for its important role in the acute thermogenic response to cold. In Chapter 2, I expand the role of D2 to brown fat development and adipogenesis. Using mice with inactivation of the D2 pathway (D2KO), we found that a lack of D2-generated T3 results in impaired BAT development that contributes to the thermogenic defect observed in adult mice. In Chapter 3, we tested whether defective thermogenesis of D2KO mice increases their susceptibility to diet-induced obesity. When mice are reared at an ambient temperature that minimizes thermal stress, they become obese with glucose intolerance and hepatic steatosis. These findings provide novel insight into the role of D2 in brown fat development and function.

HEPATIC GLUCONEOGENESIS IN THE CONTROL OF GLUCOSE HOMEOSTASIS

In this section, I will introduce type 2 diabetes, a chronic metabolic disease that is increasing globally in parallel with the rising obesity epidemic. Diabetes results from a failure to regulate glucose homeostasis, and I will discuss how this is predominantly due to uncontrolled elevation in hepatic gluconeogenesis. I will review the current scientific understanding of the transcriptional regulation of gluconeogenesis and the key role played by FoxO1 in conferring insulin sensitivity onto the expression of gluconeogenic genes. I will also discuss the known

posttranslational modifications that control FoxO1 activity with particular emphasis on ubiquitination. Finally, I will introduce the deubiquitinating enzyme USP7.

"Corpulence is not only a disease itself, but the harbinger of others" – Hippocrates

Type 2 diabetes

Type 2 diabetes is one of obesity's most distinct comorbidities. The conditions are so intimately tied that over 80% of people with type 2 diabetes are obese (114). Following the global epidemic of obesity, 439 million people are projected to suffer from diabetes mellitus by 2030—a staggering 7.7% of the adult world population (115). Diabetes mellitus, more commonly referred to as diabetes, is a group of diseases marked by hyperglycemia due to defective insulin production, action, or both. Consequences of diabetes include both micro- and macrovascular complications, which can lead to blindness, renal insufficiency, cardiovascular disease, or stroke. Type 2 diabetes, also known as adult-onset diabetes, comprises approximately 90–95% of diabetes cases worldwide and is characterized by peripheral insulin resistance, which is when the body fails to respond appropriately to insulin. It should not be confused with type 1 diabetes, also known as juvenile diabetes, which is an insulin-dependent form of diabetes caused by autoimmune destruction of insulin-producing pancreatic beta cells (116). Diabetes results from impaired glucose utilization, and achieving glucose homeostasis is paramount to the management of this disease.

Maintenance of glucose homeostasis

Blood glucose must be kept within a narrow range to ensure vitality. This is especially important for the brain and red blood cells, which almost exclusively rely on glucose for energy.

Glucose levels remain relatively stable through the opposing actions of pancreatic hormones glucagon and insulin, which coordinate a synchronous effort from multiple tissues to facilitate glucose disposal in times of excess and production in times of scarcity. However, it is primarily the liver that carries the metabolic burden of safeguarding blood glucose levels and maintaining glucose homeostasis (117).

During fasting, glucagon rises to initiate hepatic glucose production in order to replace scarce glucose. Initially, short-term needs of fasting are met by glycogen breakdown (glycogenolysis). After glycogen stores have been depleted, longer fasting requires gluconeogenesis, which entails the production of glucose from non-carbohydrate precursors, mainly lactate, pyruvate, glycerol, and alanine. Conversely, under fed conditions when dietary carbohydrates are sufficient to meet energy demands, insulin release stimulates glucose uptake in the muscle and fat, while repressing glucose output from the liver. However, in diabetes, where there is insulin insufficiency or insulin resistance, glucose is overproduced by the liver and underutilized by other organs; the diabetic is in a mode of biochemical starvation (117). Increased hepatic glucose production is one of the main contributors to the hyperglycemia in diabetes, which can be attributed predominantly to elevated gluconeogenesis (118, 119). Thus, a deeper understanding of the molecular mechanisms that regulate gluconeogenesis has the ability to provide key insight into treatments for diabetes.

Transcriptional control of gluconeogenesis

Gluconeogenesis is largely controlled at the transcriptional level, whereby hormonal cues are relayed through a vast and complex regulatory network that converges on the transcription of key rate limiting enzymes, glucose-6-phosphatase (*G6Pc*; G6Pase) and phosphoenolpyruvate

carboxykinase (*Pck1*; PEPCK) (Figure 1.2). During fasting, glucagon activates the cAMP/PKA pathway, which initiates a wave of transcriptional events that enhance the gluconeogenic gene program. Initially, PKA-activated CREB directly binds to CREs within the promoters of *G6Pc* and *Pck1*, stimulating their expression (120-122). Assisting the CREB response, cAMP-mediated dephosphorylation of CREB regulated transcription coactivator 2 (CRTC2, also known as TORC2) promotes its nuclear localization and coactivation of CREB (123). In a feed-forward manner, CREB/CRTC2 stimulates expression of *PGC-1α*, which plays a key role during the later phase of fasting (120, 123, 124). Namely, elevated levels of PGC-1α robustly amplify and maintain gluconeogenic gene expression through the coactivation of gluconeogenic transcription factors, such as forkhead box O1 (FoxO1) (125, 126). FoxO1 induces expression of *G6Pc* and *Pck1* by interacting with an insulin responsive element (IRE) on their promoters (127-130). The promoter region of *G6Pc* contains at least three IRE motifs and the promoter region of *Pck1* contains at least one IRE motif (131, 132).

Insulin adds another layer to the richness and complexity of gluconeogenic transcriptional control. In the hepatic response to feeding, insulin initiates a linear signaling cascade through the phosphatidylinositol 3-kinase (PI3K) pathway that results in phosphorylation and activation of the serine/threonine kinase Akt, which is a central node responsible for the insulin-induced suppression of *G6Pc* and *Pck1* expression (133, 134). Although Akt antagonizes the fasting response in several ways, quite arguably the most important route by which insulin/Akt suppresses hepatic production of glucose is through phosphorylation of FoxO1 at Thr24, Ser256, and Ser319 of the human protein, resulting in its inactivation (125, 128, 135, 136). This phosphorylation event induces a nuclear-cytoplasmic shuttling by aid of the chaperone protein 14-3-3, which sequesters FoxO1 in the cytoplasm and,

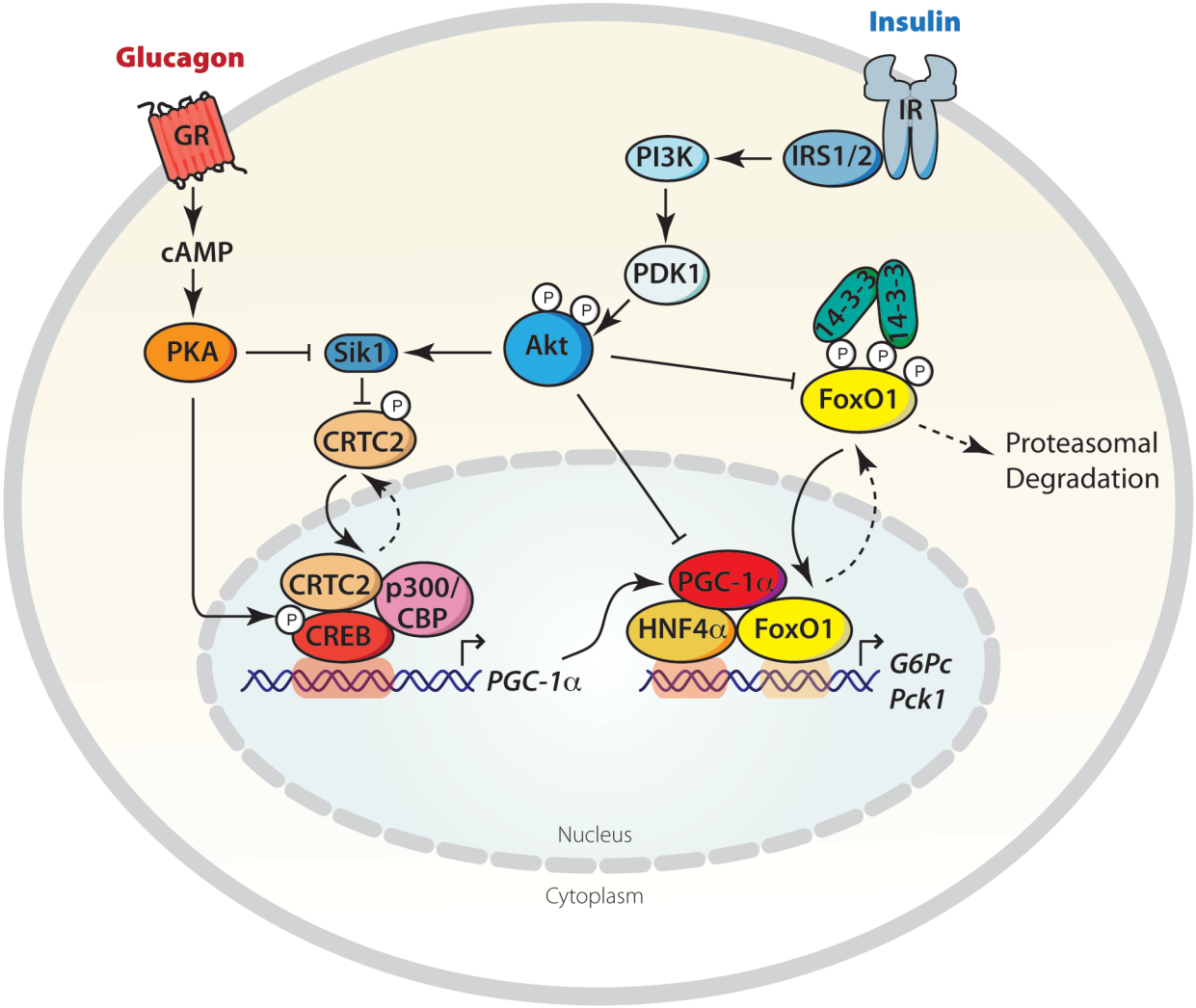

Figure 1.2. Glucagon and insulin signaling on the gluconeogenic program in the hepatocyte. Glucagon signaling through cAMP/PKA activates CREB/CRTC2 that stimulates expression of *PGC-1α*. PGC-1α coactivates HNF4α and FoxO1 at cognate elements in the promoters of *G6Pc* and *Pck1*, leading to increased gluconeogenesis. Insulin suppresses gluconeogenic gene expression by signaling through Akt. Akt activates salt-inducible kinase 1 (Sik1), which promotes the cytoplasmic translocation of CRTC2 (123). Akt also directly inhibits PGC-1α (137). Akt-mediated phosphorylation of FoxO1 induces cytoplasmic localization, association with 14-3-3 proteins, and ubiquitination followed by proteasomal degradation. See the text for more details and references.

hence, reduces its transcriptional activity (138). Once rendered cytoplasmic by insulin, FoxO1 becomes polyubiquitinated and degraded by the proteasome (139). By conferring insulin sensitivity onto the expression of gluconeogenic genes, FoxO1 is a critical regulator of hepatic gluconeogenesis.

Several mouse models have demonstrated the importance of FoxO1 in glucose metabolism. Liver-specific deletion of FoxO1 results in a mouse with reduced gluconeogenic gene expression and reduced hepatic glucose output (both glycogenolysis and gluconeogenesis) as measured by hyperinsulinemic euglycemic clamp (140). However, a more profound phenotype is realized on a diabetic background. Using diabetic *db/db* mice, hepatic expression of a dominant negative FoxO1 decreases gluconeogenic gene expression and reduces glucose levels to that of non-diabetic mice (141). Moreover, in mice with genetically-induced diabetes—with either deletion of the insulin receptor (140), insulin receptor substrates IRS1 and IRS2 (142), or Akt1 and Akt2 (143)—the added deletion of FoxO1 rescues their hyperglycemia. There is also an emerging story of FoxO1 control in hepatic lipid metabolism, although its precise role remains unclear (144). Together, these studies strongly suggest that inhibition of FoxO1 could be a promising strategy to reverse hyperglycemia associated with insulin-resistant diabetes. Therefore, it is important to gain a better understanding of how FoxO1 is regulated.

FoxO family of transcription factors

FoxO1 belongs to a family of transcription factors within a larger family of Forkhead proteins, which are so-called based on their characteristic “forkhead box” DNA binding domain. In addition to FoxO1, the mammalian FoxO subfamily contains at least three other members, including FoxO3, FoxO4, and FoxO6 (145, 146). All FoxOs bind as monomers to the same

target consensus motif (that is 5′-TTGTTTAC-3′) (147). This consensus motif differs slightly from the IRE [5′-T(G/A)TTTTG-3′], which FoxOs bind to with lower affinity (148). FoxO1, FoxO3, and FoxO4 contain the same evolutionarily conserved Akt phosphorylation motifs, and all three are expressed in the adult mouse liver—albeit to a lesser extent for FoxO4 (138, 148-150). FoxO6 lacks the third Akt phosphorylation motif, has slightly different nuclear-cytoplasmic shuttling kinetics, and is expressed predominantly in neural cells (146). Given their similarities, FoxO proteins consequently display some level of redundancy (147). However, they appear to have unique functions as well (151). This is best realized upon global deletion of the specific FoxOs. Whereas mice lacking FoxO1 are embryonic lethal, FoxO3- and FoxO4-null mice are viable (152), thus, attesting to their functional diversity. Together, the FoxO family members are responsible for orchestrating gene expression programs involved in a broad spectrum of biological processes, including cell survival, growth, and metabolism (153).

Posttranslational modifications of FoxO proteins

Contributing to their functional breadth, the activity of FoxO proteins can be altered by posttranslational modifications, including phosphorylation, acetylation, methylation, glycosylation, and ubiquitination (Figure 1.3). In response to various cellular signals, specific enzymes catalyze attachment of these moieties at defined residues, which leads to alterations in subcellular localization, DNA-binding ability, or molecular half-life (157). Phosphorylation of FoxOs by Akt has been discussed above and is a prime example of an inhibitory modification on FoxO activity. FoxOs can also be phosphorylated in an activating manner, such as with mammalian Ste20-like kinase (MST1). Under oxidative stress, MST1 phosphorylates FoxO proteins on a conserved site within the forkhead domain that prevents association with 14-3-3

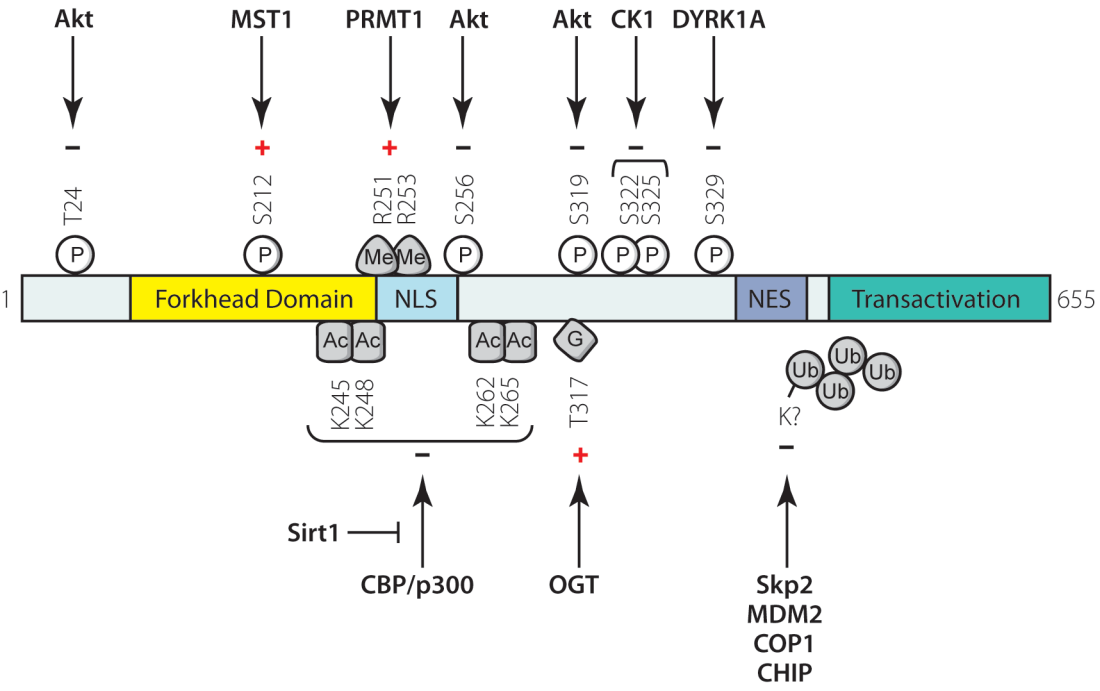

Figure 1.3. Posttranslational modifications of FoxO1. The functional domains of human FoxO1 are shown together with the sites of modification and the responsible modifying/demodifying enzymes. Modifications that inhibit FoxO1 transcriptional activity are indicated with a (-). Activating modifications are indicated with a (+). The site(s) of polyubiquitination are unknown and are denoted by a question mark. See the text for references with the exception of dual-specificity tyrosine-phosphorylation-regulated kinase 1A (DYRK1A) (154), CK1 (155), and *O*-linked glycosylation with *N*-acetylglucosamine (*O*-GlcNac) transferase (OGT) (156). Phosphorylation (P); Methylation (Me); Acetylation (Ac); *O*-GlcNac (G); Ubiquitination (Ub); Nuclear localization sequence (NLS); Nuclear export sequence (NES).

proteins, rendering FoxO nuclear and active (158). In addition, there are modifications that can protect FoxOs from Akt-mediated inactivation, with an example being the methylation of arginine residues within its Akt consensus site as catalyzed by protein arginine methyltransferase (PRMT) (159). Another important modification of FoxO proteins is the attachment of acetyl groups, which reduces DNA binding ability and promotes cytoplasmic localization (160). FoxOs are acetylated by histone acetyltransferases CREB binding protein (CBP) and its related protein p300 (CBP/p300) and deacetylated by class I-II and III histone deacetylases, including Sirt1, an NAD+-dependent deacetylase (161-163). Furthermore, in addition to these aforementioned small molecule modifications, the function of FoxO proteins can be altered by attachment of an entire protein, such as ubiquitin.

Ubiquitination is an important posttranslational modification for regulation of FoxO activity. Early studies focused on polyubiquitination of FoxO proteins, having found that FoxOs get polyubiquitinated and degraded by the proteasome in response to insulin (139, 164). This process was shown to require Akt-induced phosphorylation and cytosolic localization (139). Several E3 ligases responsible for FoxO polyubiquitination and degradation under various settings have been described, including Skp2, an F-box protein that is present in Skp1, Cullin-1, F-box protein complexes (165); mouse double minute 2 (MDM2) (166, 167); COP1, a Ring-Finger E3 ubiquitin ligase (168); and C-terminus of Hsc70-interacting protein (CHIP), a co-chaperone protein and functional E3 ubiquitin ligase (169). However, a potential role for monoubiquitination in the control of FoxO activity has recently received attention due to findings of oxidative stress-induced monoubiquitination of FoxO4 (170-172). In this scenario, monoubiquitination does not degrade FoxO4; instead, monoubiquitination actually promotes FoxO4 nuclear localization and enhances its transcriptional activity (170). Given that FoxO

family members share many of the same regulatory mechanisms, it will be informative to understand whether FoxO1 activity is also controlled by monoubiquitination.

Ubiquitination and deubiquitination

Posttranslational modification by ubiquitin (ubiquitination) provides a robust signaling mechanism that regulates numerous aspects of cell biology, including cell division, DNA damage repair, and transcription (173). Ubiquitin, as the name suggests, is a ubiquitously expressed protein found in essentially every cell of the body. Weighing in at about 8 kDa, this small, globular protein is comprised of a 76 amino acid sequence that is highly conserved from yeast to man (174). Key features of its structure include seven lysine (Lys) residues (at positions 6, 11, 27, 29, 33, 48, and 63) and an extended carboxyl tail with a C-terminal glycine residue. Through a sequential cascade of enzymatic reactions, this glycine residue most typically forms an isopeptide bond with the ε-amino group on a lysine of its target substrate. The covalent attachment of a single ubiquitin entity on one or multiple sites of a recipient protein results in mono- and multi-monoubiquitinated proteins, respectively. Ubiquitin itself can be subjected to this conjugation, with any one of its own lysine residues, or even its amino terminal methionine, serving as acceptor sites for another ubiquitin moiety. Sequential rounds of this process lead to the assembly of polyubiquitin chains on target substrates, which can vary in terms of linkage-type topology (174). Although all linkage types have been detected *in vivo,* Lys48 and Lys63 linked chains are the most abundant in both yeast and mammalian cells and the best studied (175-177); very little is known about the other "atypical" chains (178). A discussion of the distinct fates dictated by these various ubiquitin linkages goes beyond the scope of this introduction but is reflected in Figure 1.4. These modifications lead to diverse consequences for

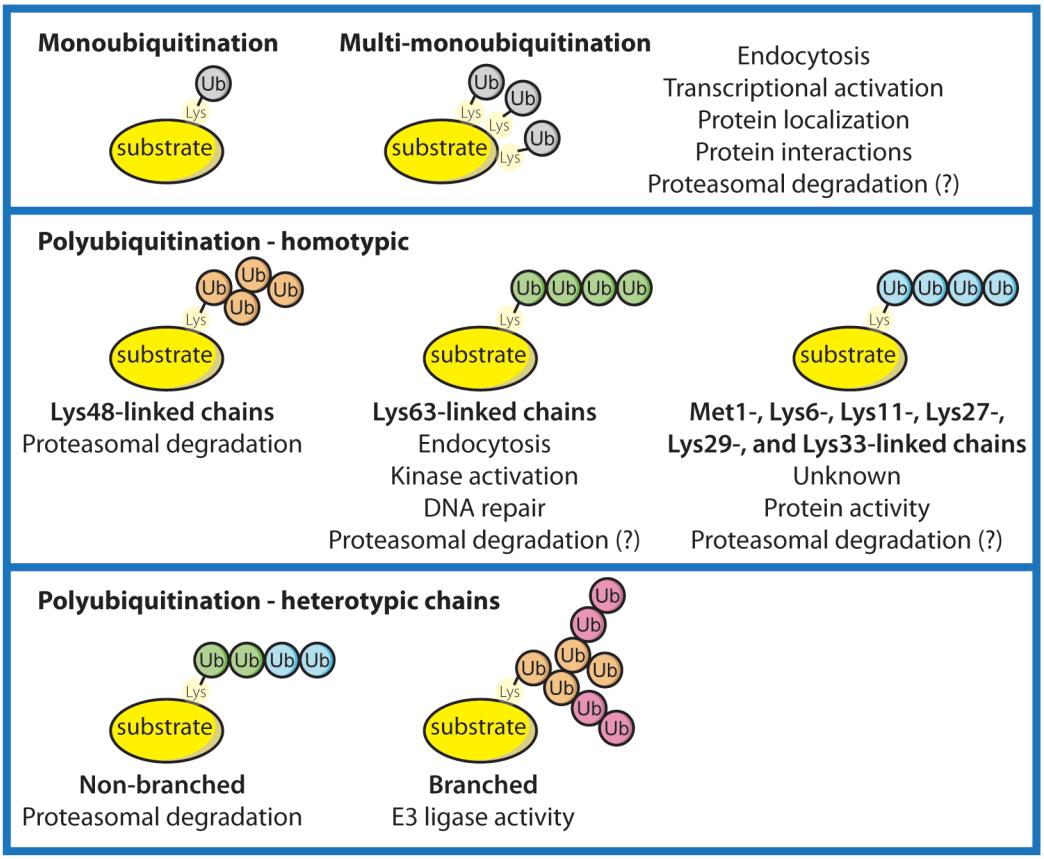

Figure 1.4. Diversity of ubiquitin modifications. Ubiquitin (Ub) can be attached as a single moiety (monoubiquitination) or multiple single Ub moieties (multi-monoubiquitination) to a substrate protein. In addition, all seven lysine residues of Ub (and the N-terminal methionine of Ub) are capable of accepting additional Ub moieties in formation of a polyubiquitin chain. These polyubiquitin chains can exist as homotypic chains (all of the same linkage) or as heterotypic chains comprised of different linkage types. Heterotypic chains are either branched or non-branched. The various Ub chain types lead to different outcomes as indicated. See the text for references and (174, 178).

the ubiquitinated protein, ranging from proteasome-dependent proteolysis to modulation of protein structure, assembly, localization, and/or function (174).

The process of ubiquitination is tightly regulated and occurs through a three-step catalytic cycle (Figure 1.5). First, the ubiquitin activating enzyme (E1) forms a thioester bond between its active site cysteine and the C-terminus of ubiquitin in an ATP-consuming reaction. The activated ubiquitin intermediate is transferred from E1 to the ubiquitin conjugating enzyme (E2) as a thioester and is subsequently attached to the target substrate by an ubiquitin ligase (E3), which confers specificity through substrate recognition (179). The details differ in this last step depending on the nature of the E3 involved, with homologous with E6-associated protein C-terminus (HECT) domain E3s forming a thioester intermediate with ubiquitin (180), whereas really interesting new gene (RING) domain E3s assist in direct transfer of ubiquitin from E2 to the recipient protein (181). The human genome encodes two E1 enzymes, about 40 E2 enzymes, and over 600 E3 ligases, attesting to the tight regulation and high level of specialization that surround this ubiquitin moiety (174). Indeed, ubiquitination is also a highly plastic posttranslational modification, and in one fell swoop the net action of the ubiquitin ligation machinery can be undone through a process of deubiquitination.

Deubiquitinating enzymes (also referred to as deubiquitinases or DUBs) modulate ubiquitin signaling through the removal of both mono- and polyubiquitin moieties. They are also responsible for generating the pool of free ubiquitin monomers by processing the polyubiquitin gene product and by recycling ubiquitin from leftover polyubiquitin chains of degraded proteins (182). The human genome encodes approximately 100 DUBs that belong to five gene families, four classes of which are cysteine proteases. The cysteine proteases include the ubiquitin C-terminal hydrolase (UCH), the ubiquitin specific protease (USP), the ovarian tumor domain

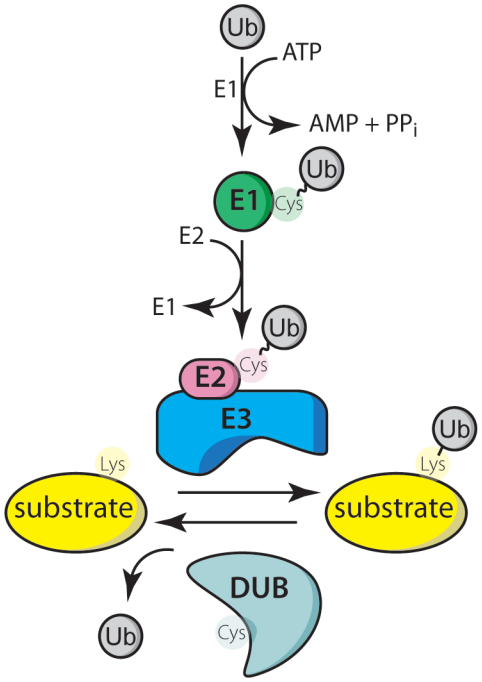

Figure 1.5. Enzymatic cascade leading to substrate ubiquitination and its reversal. Ubiquitin (Ub) is activated by Ub activating enzyme (E1) and is then passed to Ub conjugating enzyme (E2). A Ub ligase (E3) aids in the final attachment of Ub to a substrate protein. The process of ubiquitination can be reversed by deubiquitination through the action of deubiquitinating enzymes (DUBs). See the text for more details and references.

(OTU), and the Josephin domain (MJD) DUBs. The fifth family is comprised of the JAB1/MPN/Mov34 metalloenzyme (JAMM) domain DUBs that are zinc-dependent metalloproteases (183). For the cysteine proteases, activity depends on a vital catalytic triad composed of a cysteine, a histidine, and an aspartate. During the act of deubiquitination, the catalytic cysteine performs a nucleophilic attack on the carbonyl group of the protein-ubiquitin linkage, cleaving the crucial isopeptide bond and liberating the substrate protein (183). To prevent against fortuitous cleavage, the activity of DUBs is tightly regulated on the transcriptional and posttranslational level; they themselves are even prone to ubiquitination. Also, DUBs contain ubiquitin-binding domains and protein-protein interaction domains, which aid in selecting the appropriate substrate and in recognizing different ubiquitin chains (182). Although recent efforts have begun to unravel the increasing importance of DUBs in a variety of cellular processes, the specific targets and physiological roles of most DUBs remain poorly understood (184). However, one DUB, USP7, has been heavily studied because of its connection to the cancer field.

The deubiquitinating enzyme USP7

Ubiquitin specific protease 7 (USP7; also known as herpesvirus-associated USP, HAUSP) is a DUB that was first identified in 1997 as a protein interacting with herpes simplex virus type I immediate early protein, ICP0 (or Vmw110) (185). However, insight into its cellular function did not begin to materialize until an association with the tumor suppressor p53 was made five years later (186). Although the original findings suggested that USP7 deubiquitinates and stabilizes p53, subsequent studies have found that USP7 preferentially deubiquitinates and stabilizes HDM2 (the human ortholog of MDM2), an E3 ligase responsible for the

polyubiquitination and degradation of p53 (187, 188). Interest in this DUB has skyrocketed since then, finding that it makes critical connections with numerous proteins involved in tumor suppression, DNA repair, response to infection, and epigenetic regulation of gene expression (187). And with the advent of high-throughput proteomic analysis, the list of potential USP7 substrates continues to grow (189, 190).

USP7 has two other prominent tumor suppressor targets: phosphatase and tensin homologue (PTEN) and FoxO4. However, its regulation of these substrates is in a manner unrelated to protein turnover. Under both situations, USP7 deubiquitinates the monoubiquitinated protein, which leads to altered subcellular localization and activity (170, 191). Similar to its net effect on p53, knockdown of USP7 leads to functional changes in PTEN and FoxO4 that promote their tumor suppressor activities (170, 191). Notably, USP7 overexpression has been found to directly correlate with tumor aggressiveness in prostate cancer and possibly others (191, 192). Given the tractability of DUB inhibition, the therapeutic appeal of a USP7-targeted approach has not eluded drug companies. USP7 is the most studied DUB target, and several companies are actively pursuing USP7 drug discovery programs (193).

Objectives

Given the critical role of FoxO1 in gluconeogenesis, there is great interest in understanding enzymes that control its transcriptional activity, as they may provide potential drug targets in the treatment of hyperglycemia associated with insulin resistance. USP7 has been shown to inhibit the activity of FoxO4, which suggested that this deubiquitinating enzyme might also regulate FoxO1 and, therefore, impact gluconeogenesis. In Chapter 4, I describe FoxO1 as a novel target for USP7-mediated mono-deubiquitination and provide data that show USP7

inhibits FoxO1 transcription of gluconeogenic genes. These results expand USP7 to the context of glucose metabolic control and provide insight into an alternative pathway for the maintenance of glucose homeostasis.

REFERENCES

1. **Ogden CL, Carroll MD, Kit BK, Flegal KM** 2014 Prevalence of childhood and adult obesity in the United States, 2011-2012. JAMA 311:806-814

2. **Haslam DW, James WP** 2005 Obesity. Lancet 366:1197-1209

3. **Wing RR, Lang W, Wadden TA, Safford M, Knowler WC, Bertoni AG, Hill JO, Brancati FL, Peters A, Wagenknecht L, Look ARG** 2011 Benefits of modest weight loss in improving cardiovascular risk factors in overweight and obese individuals with type 2 diabetes. Diabetes Care 34:1481-1486

4. **Bellisari A** 2008 Evolutionary origins of obesity. Obesity reviews : an official journal of the International Association for the Study of Obesity 9:165-180

5. **Leibel RL, Rosenbaum M, Hirsch J** 1995 Changes in energy expenditure resulting from altered body weight. N Engl J Med 332:621-628

6. **Wing RR, Hill JO** 2001 Successful weight loss maintenance. Annu Rev Nutr 21:323-341

7. **Look ARG, Wing RR** 2010 Long-term effects of a lifestyle intervention on weight and cardiovascular risk factors in individuals with type 2 diabetes mellitus: four-year results of the Look AHEAD trial. Arch Intern Med 170:1566-1575

8. **Harper ME, Green K, Brand MD** 2008 The efficiency of cellular energy transduction and its implications for obesity. Annu Rev Nutr 28:13-33

9. **Yanovski SZ, Yanovski JA** 2014 Long-term drug treatment for obesity: a systematic and clinical review. JAMA 311:74-86

10. **Balkon N, Balkon C, Zitkus BS** 2011 Overweight and obesity: pharmacotherapeutic considerations. Journal of the American Academy of Nurse Practitioners 23:61-66

11. **Melnikova I, Wages D** 2006 Anti-obesity therapies. Nature reviews Drug discovery 5:369-370

12. **Tharakan G, Tan T, Bloom S** 2011 Emerging therapies in the treatment of 'diabesity': beyond GLP-1. Trends in pharmacological sciences 32:8-15

13. **Lowell BB, Spiegelman BM** 2000 Towards a molecular understanding of adaptive thermogenesis. Nature 404:652-660

14. **Cannon B, Nedergaard J** 2008 Developmental biology: Neither fat nor flesh. Nature 454:947-948

15. **Foster DO, Frydman ML** 1979 Tissue distribution of cold-induced thermogenesis in conscious warm- or cold-acclimated rats reevaluated from changes in tissue blood flow: the dominant role of brown adipose tissue in the replacement of shivering by nonshivering thermogenesis. Canadian journal of physiology and pharmacology 57:257-270

16. **Cannon B, Nedergaard J** 2004 Brown adipose tissue: function and physiological significance. Physiological reviews 84:277-359

17. **Klingenspor M** 2003 Cold-induced recruitment of brown adipose tissue thermogenesis. Experimental physiology 88:141-148

18. **Bartness T, Vaughan C, Song C** 2010 Sympathetic and sensory innervation of brown adipose tissue. International journal of obesity (2005) 34 Suppl 1:42

19. **Kozak UC, Kopecky J, Teisinger J, Enerback S, Boyer B, Kozak LP** 1994 An upstream enhancer regulating brown-fat-specific expression of the mitochondrial uncoupling protein gene. Mol Cell Biol 14:59-67

20. **Bachman E, Dhillon H, Zhang C-Y, Cinti S, Bianco A, Kobilka B, Lowell B** 2002 betaAR signaling required for diet-induced thermogenesis and obesity resistance. Science (New York, NY) 297:843-845

21. **Sellers EA, You SS** 1950 Role of the thyroid in metabolic responses to a cold environment. Am J Physiol 163:81-91

22. **Bianco A, Silva J** 1987 Intracellular conversion of thyroxine to triiodothyronine is required for the optimal thermogenic function of brown adipose tissue. The Journal of clinical investigation 79:295-300

23. **Ribeiro M, Lebrun F, Christoffolete M, Branco M, Crescenzi A, Carvalho S, Negrão N, Bianco A** 2000 Evidence of UCP1-independent regulation of norepinephrine-induced thermogenesis in brown fat. American journal of physiology Endocrinology and metabolism 279:22

24. **Cassard-Doulcier AM, Larose M, Matamala JC, Champigny O, Bouillaud F, Ricquier D** 1994 In vitro interactions between nuclear proteins and uncoupling protein gene promoter reveal several putative transactivating factors including Ets1, retinoid X receptor, thyroid hormone receptor, and a CACCC box-binding protein. J Biol Chem 269:24335-24342

25. **Bianco A, McAninch E** 2013 The role of thyroid hormone and brown adipose tissue in energy homoeostasis. The lancet Diabetes & endocrinology 1:250-258

26. **Rothwell N, Stock M** 1997 A role for brown adipose tissue in diet-induced thermogenesis. Obesity research 5:650-656

27. **Lowell BB, V SS, Hamann A, Lawitts JA, Himms-Hagen J, Boyer BB, Kozak LP, Flier JS** 1993 Development of obesity in transgenic mice after genetic ablation of brown adipose tissue. Nature 366:740-742

28. **Feldmann HM, Golozoubova V, Cannon B, Nedergaard J** 2009 UCP1 ablation induces obesity and abolishes diet-induced thermogenesis in mice exempt from thermal stress by living at thermoneutrality. Cell Metab 9:203-209

29. **Liu X, Rossmeisl M, McClaine J, Riachi M, Harper ME, Kozak LP** 2003 Paradoxical resistance to diet-induced obesity in UCP1-deficient mice. J Clin Invest 111:399-407

30. **Enerback S, Jacobsson A, Simpson EM, Guerra C, Yamashita H, Harper ME, Kozak LP** 1997 Mice lacking mitochondrial uncoupling protein are cold-sensitive but not obese. Nature 387:90-94

31. **Huttunen P, Hirvonen J, Kinnula V** 1981 The occurrence of brown adipose tissue in outdoor workers. European journal of applied physiology and occupational physiology 46:339-345

32. **Ricquier D, Nechad M, Mory G** 1982 Ultrastructural and biochemical characterization of human brown adipose tissue in pheochromocytoma. J Clin Endocrinol Metab 54:803-807

33. **Cunningham S, Leslie P, Hopwood D, Illingworth P, Jung RT, Nicholls DG, Peden N, Rafael J, Rial E** 1985 The characterization and energetic potential of brown adipose tissue in man. Clinical science 69:343-348

34. **Barrington SF, Maisey MN** 1996 Skeletal muscle uptake of fluorine-18-FDG: effect of oral diazepam. J Nucl Med 37:1127-1129

35. **Hany TF, Gharehpapagh E, Kamel EM, Buck A, Himms-Hagen J, von Schulthess GK** 2002 Brown adipose tissue: a factor to consider in symmetrical tracer uptake in the neck and upper chest region. European journal of nuclear medicine and molecular imaging 29:1393-1398

36. **Tatsumi M, Engles JM, Ishimori T, Nicely O, Cohade C, Wahl RL** 2004 Intense (18)F-FDG uptake in brown fat can be reduced pharmacologically. J Nucl Med 45:1189-1193

37. **Yeung HW, Grewal RK, Gonen M, Schoder H, Larson SM** 2003 Patterns of (18)F-FDG uptake in adipose tissue and muscle: a potential source of false-positives for PET. J Nucl Med 44:1789-1796

38. **Cypess AM, Lehman S, Williams G, Tal I, Rodman D, Goldfine AB, Kuo FC, Palmer EL, Tseng YH, Doria A, Kolodny GM, Kahn CR** 2009 Identification and importance of brown adipose tissue in adult humans. N Engl J Med 360:1509-1517

39. **van Marken Lichtenbelt WD, Vanhommerig JW, Smulders NM, Drossaerts JM, Kemerink GJ, Bouvy ND, Schrauwen P, Teule GJ** 2009 Cold-activated brown adipose tissue in healthy men. N Engl J Med 360:1500-1508

40. **Virtanen KA, Lidell ME, Orava J, Heglind M, Westergren R, Niemi T, Taittonen M, Laine J, Savisto NJ, Enerback S, Nuutila P** 2009 Functional brown adipose tissue in healthy adults. N Engl J Med 360:1518-1525

41. **Rothwell NJ, Stock MJ** 1983 Luxuskonsumption, diet-induced thermogenesis and brown fat: the case in favour. Clinical science 64:19-23

42. **Carey A, Kingwell B** 2013 Brown adipose tissue in humans: therapeutic potential to combat obesity. Pharmacology & therapeutics 140:26-33

43. **Himms-Hagen J, Desautels M** 1978 A mitochondrial defect in brown adipose tissue of the obese (ob/ob) mouse: reduced binding of purine nucleotides and a failure to respond to cold by an increase in binding. Biochem Biophys Res Commun 83:628-634

44. **Trayhurn P, Thurlby PL, James WP** 1977 Thermogenic defect in pre-obese ob/ob mice. Nature 266:60-62

45. **Hamann A, Benecke H, Le Marchand-Brustel Y, Susulic VS, Lowell BB, Flier JS** 1995 Characterization of insulin resistance and NIDDM in transgenic mice with reduced brown fat. Diabetes 44:1266-1273

46. **Bartelt A, Bruns OT, Reimer R, Hohenberg H, Ittrich H, Peldschus K, Kaul MG, Tromsdorf UI, Weller H, Waurisch C, Eychmuller A, Gordts PL, Rinninger F, Bruegelmann K, Freund B, Nielsen P, Merkel M, Heeren J** 2011 Brown adipose tissue activity controls triglyceride clearance. Nat Med 17:200-205

47. **Symonds ME, Mostyn A, Pearce S, Budge H, Stephenson T** 2003 Endocrine and nutritional regulation of fetal adipose tissue development. The Journal of endocrinology 179:293-299

48. **Houstěk J, Kopecký J, Rychter Z, Soukup T** 1988 Uncoupling protein in embryonic brown adipose tissue--existence of nonthermogenic and thermogenic mitochondria. Biochimica et biophysica acta 935:19-25

49. **Aherne W, Hull D** 1966 Brown adipose tissue and heat production in the newborn infant. The Journal of pathology and bacteriology 91:223-234

50. **Lidell M, Betz M, Dahlqvist Leinhard O, Heglind M, Elander L, Slawik M, Mussack T, Nilsson D, Romu T, Nuutila P, Virtanen K, Beuschlein F, Persson A, Borga M, Enerbäck S** 2013 Evidence for two types of brown adipose tissue in humans. Nature medicine 19:631-634

51. **Green H, Kehinde O** 1975 An established preadipose cell line and its differentiation in culture. II. Factors affecting the adipose conversion. Cell 5:19-27

52. **Green H, Kehinde O** 1976 Spontaneous heritable changes leading to increased adipose conversion in 3T3 cells. Cell 7:105-113

53. **Farmer S** 2006 Transcriptional control of adipocyte formation. Cell metabolism 4:263-273

54. **Rosen ED, Sarraf P, Troy AE, Bradwin G, Moore K, Milstone DS, Spiegelman BM, Mortensen RM** 1999 PPAR gamma is required for the differentiation of adipose tissue in vivo and in vitro. Molecular cell 4:611-617

55. **Tontonoz P, Hu E, Graves RA, Budavari AI, Spiegelman BM** 1994 mPPAR gamma 2: tissue-specific regulator of an adipocyte enhancer. Genes Dev 8:1224-1234

56. **Tontonoz P, Graves RA, Budavari AI, Erdjument-Bromage H, Lui M, Hu E, Tempst P, Spiegelman BM** 1994 Adipocyte-specific transcription factor ARF6 is a heterodimeric complex of two nuclear hormone receptors, PPAR gamma and RXR alpha. Nucleic Acids Res 22:5628-5634

57. **Rosen E, MacDougald O** 2006 Adipocyte differentiation from the inside out. Nature reviews Molecular cell biology 7:885-896

58. **Kajimura S, Seale P, Kubota K, Lunsford E, Frangioni J, Gygi S, Spiegelman B** 2009 Initiation of myoblast to brown fat switch by a PRDM16-C/EBP-beta transcriptional complex. Nature 460:1154-1158

59. **Sears I, MacGinnitie M, Kovacs L, Graves R** 1996 Differentiation-dependent expression of the brown adipocyte uncoupling protein gene: regulation by peroxisome proliferator-activated receptor gamma. Molecular and cellular biology 16:3410-3419

60. **Smas C, Sul H** 1993 Pref-1, a protein containing EGF-like repeats, inhibits adipocyte differentiation. Cell 73:725-734

61. **Moon Y, Smas C, Lee K, Villena J, Kim K-H, Yun E, Sul H** 2002 Mice lacking paternally expressed Pref-1/Dlk1 display growth retardation and accelerated adiposity. Molecular and cellular biology 22:5585-5592

62. **Lee K, Villena J, Moon Y, Kim K-H, Lee S, Kang C, Sul H** 2003 Inhibition of adipogenesis and development of glucose intolerance by soluble preadipocyte factor-1 (Pref-1). The Journal of clinical investigation 111:453-461

63. **Kajimura S, Seale P, Spiegelman BM** 2010 Transcriptional control of brown fat development. Cell Metab 11:257-262

64. **Puigserver P, Wu Z, Park C, Graves R, Wright M, Spiegelman B** 1998 A cold-inducible coactivator of nuclear receptors linked to adaptive thermogenesis. Cell 92:829-839

65. **Handschin C, Spiegelman B** 2006 Peroxisome proliferator-activated receptor gamma coactivator 1 coactivators, energy homeostasis, and metabolism. Endocrine reviews 27:728-735

66. **Leone TC, Lehman JJ, Finck BN, Schaeffer PJ, Wende AR, Boudina S, Courtois M, Wozniak DF, Sambandam N, Bernal-Mizrachi C, Chen Z, Holloszy JO, Medeiros DM, Schmidt RE, Saffitz JE, Abel ED, Semenkovich CF, Kelly DP** 2005 PGC-1alpha deficiency causes multi-system energy metabolic derangements: muscle dysfunction, abnormal weight control and hepatic steatosis. PLoS Biol 3:e101

67. **Lin J, Wu P-H, Tarr P, Lindenberg K, St-Pierre J, Zhang C-Y, Mootha V, Jäger S, Vianna C, Reznick R, Cui L, Manieri M, Donovan M, Wu Z, Cooper M, Fan M, Rohas L, Zavacki A, Cinti S, Shulman G, Lowell B, Krainc D, Spiegelman B** 2004 Defects in adaptive energy metabolism with CNS-linked hyperactivity in PGC-1alpha null mice. Cell 119:121-135

68. **Uldry M, Yang W, St-Pierre J, Lin J, Seale P, Spiegelman BM** 2006 Complementary action of the PGC-1 coactivators in mitochondrial biogenesis and brown fat differentiation. Cell Metab 3:333-341

69. **Tiraby C, Tavernier G, Lefort C, Larrouy D, Bouillaud F, Ricquier D, Langin D** 2003 Acquirement of brown fat cell features by human white adipocytes. J Biol Chem 278:33370-33376

70. **Seale P, Kajimura S, Yang W, Chin S, Rohas L, Uldry M, Tavernier G, Langin D, Spiegelman B** 2007 Transcriptional control of brown fat determination by PRDM16. Cell metabolism 6:38-54

71. **Seale P, Bjork B, Yang W, Kajimura S, Chin S, Kuang S, Scime A, Devarakonda S, Conroe HM, Erdjument-Bromage H, Tempst P, Rudnicki MA, Beier DR, Spiegelman BM** 2008 PRDM16 controls a brown fat/skeletal muscle switch. Nature 454:961-967

72. **Lepper C, Fan C-M** 2010 Inducible lineage tracing of Pax7-descendant cells reveals embryonic origin of adult satellite cells. Genesis (New York, NY : 2000) 48:424-436

73. **Timmons J, Wennmalm K, Larsson O, Walden T, Lassmann T, Petrovic N, Hamilton D, Gimeno R, Wahlestedt C, Baar K, Nedergaard J, Cannon B** 2007 Myogenic gene expression signature establishes that brown and white adipocytes originate from distinct cell lineages. Proceedings of the National Academy of Sciences of the United States of America 104:4401-4406

74. **Wu J, Cohen P, Spiegelman B** 2013 Adaptive thermogenesis in adipocytes: is beige the new brown? Genes & development 27:234-250

75. **Wu J, Boström P, Sparks L, Ye L, Choi J, Giang A-H, Khandekar M, Virtanen K, Nuutila P, Schaart G, Huang K, Tu H, van Marken Lichtenbelt W, Hoeks J, Enerbäck S, Schrauwen P, Spiegelman B** 2012 Beige adipocytes are a distinct type of thermogenic fat cell in mouse and human. Cell 150:366-376

76. **Harms M, Seale P** 2013 Brown and beige fat: development, function and therapeutic potential. Nature medicine 19:1252-1263

77. **Bianco AC, Kim BW** 2006 Deiodinases: implications of the local control of thyroid hormone action. J Clin Invest 116:2571-2579

78. **Gereben B, Zavacki AM, Ribich S, Kim BW, Huang SA, Simonides WS, Zeold A, Bianco AC** 2008 Cellular and molecular basis of deiodinase-regulated thyroid hormone signaling. Endocr Rev 29:898-938

79. **Brent GA** 2012 Mechanisms of thyroid hormone action. J Clin Invest 122:3035-3043

80. **Bianco AC, Salvatore D, Gereben B, Berry MJ, Larsen PR** 2002 Biochemistry, cellular and molecular biology, and physiological roles of the iodothyronine selenodeiodinases. Endocr Rev 23:38-89

81. **Moore JM, Guy RK** 2005 Coregulator interactions with the thyroid hormone receptor. Mol Cell Proteomics 4:475-482

82. **Sjogren M, Alkemade A, Mittag J, Nordstrom K, Katz A, Rozell B, Westerblad H, Arner A, Vennstrom B** 2007 Hypermetabolism in mice caused by the central action of an unliganded thyroid hormone receptor alpha1. The EMBO journal 26:4535-4545

83. **Yen P, Ando S, Feng X, Liu Y, Maruvada P, Xia X** 2006 Thyroid hormone action at the cellular, genomic and target gene levels. Molecular and cellular endocrinology 246:121-127

84. **Gereben B, Zeold A, Dentice M, Salvatore D, Bianco AC** 2007 Activation and inactivation of thyroid hormone by deiodinases: Local action with general consequences. Cell Mol Life Sci

85. **Silva JE, Larsen PR** 1983 Adrenergic activation of triiodothyronine production in brown adipose tissue. Nature 305:712-713

86. **Croteau W, Davey JC, Galton VA, St Germain DL** 1996 Cloning of the mammalian type II iodothyronine deiodinase. A selenoprotein differentially expressed and regulated in human and rat brain and other tissues. J Clin Invest 98:405-417

87. **Callebaut I, Curcio-Morelli C, Mornon JP, Gereben B, Buettner C, Huang S, Castro B, Fonseca TL, Harney JW, Larsen PR, Bianco AC** 2003 The iodothyronine selenodeiodinases are thioredoxin-fold family proteins containing a glycoside hydrolase clan GH-A-like structure. J Biol Chem 278:36887-36896

88. **Sagar GD, Gereben B, Callebaut I, Mornon JP, Zeold A, da Silva WS, Luongo C, Dentice M, Tente SM, Freitas BC, Harney JW, Zavacki AM, Bianco AC** 2007 Ubiquitination-induced conformational change within the deiodinase dimer is a switch regulating enzyme activity. Mol Cell Biol 27:4774-4783

89. **Silva J, Dick T, Larsen P** 1978 The contribution of local tissue thyroxine monodeiodination to the nuclear 3,5,3'-triiodothyronine in pituitary, liver, and kidney of euthyroid rats. Endocrinology 103:1196-1207

90. **Arrojo E Drigo R, Fonseca T, Werneck-de-Castro J, Bianco A** 2013 Role of the type 2 iodothyronine deiodinase (D2) in the control of thyroid hormone signaling. Biochimica et biophysica acta 1830:3956-3964

91. **Hernández A, Obregón M** 2000 Triiodothyronine amplifies the adrenergic stimulation of uncoupling protein expression in rat brown adipocytes. American journal of physiology Endocrinology and metabolism 278:77

92. **St Germain D** 1988 The effects and interactions of substrates, inhibitors, and the cellular thiol-disulfide balance on the regulation of type II iodothyronine 5'-deiodinase. Endocrinology 122:1860-1868

93. **Steinsapir J, Bianco AC, Buettner C, Harney J, Larsen PR** 2000 Substrate-induced down-regulation of human type 2 deiodinase (hD2) is mediated through proteasomal degradation and requires interaction with the enzyme's active center. Endocrinology 141:1127-1135

94. **Bianco AC, Silva JE** 1987 Intracellular conversion of thyroxine to triiodothyronine is required for the optimal thermogenic function of brown adipose tissue. J Clin Invest 79:295-300

95. **Bianco AC, Silva JE** 1988 Cold exposure rapidly induces virtual saturation of brown adipose tissue nuclear T3 receptors. Am J Physiol 255:E496-503

96. **Schneider MJ, Fiering SN, Pallud SE, Parlow AF, St Germain DL, Galton VA** 2001 Targeted disruption of the type 2 selenodeiodinase gene (DIO2) results in a phenotype of pituitary resistance to T4. Mol Endocrinol 15:2137-2148

97. **de Jesus LA, Carvalho SD, Ribeiro MO, Schneider M, Kim SW, Harney JW, Larsen PR, Bianco AC** 2001 The type 2 iodothyronine deiodinase is essential for adaptive thermogenesis in brown adipose tissue. J Clin Invest 108:1379-1385

98. **Christoffolete MA, Linardi CC, de Jesus L, Ebina KN, Carvalho SD, Ribeiro MO, Rabelo R, Curcio C, Martins L, Kimura ET, Bianco AC** 2004 Mice with targeted disruption of the Dio2 gene have cold-induced overexpression of the uncoupling protein 1 gene but fail to increase brown adipose tissue lipogenesis and adaptive thermogenesis. Diabetes 53:577-584

99. **Watanabe M, Houten SM, Mataki C, Christoffolete MA, Kim BW, Sato H, Messaddeq N, Harney JW, Ezaki O, Kodama T, Schoonjans K, Bianco AC, Auwerx J** 2006 Bile acids induce energy expenditure by promoting intracellular thyroid hormone activation. Nature 439:484-489

100. **Marsh-Armstrong N, Huang H, Remo BF, Liu TT, Brown DD** 1999 Asymmetric growth and development of the Xenopus laevis retina during metamorphosis is controlled by type III deiodinase. Neuron 24:871-878

101. **Dentice M, Bandyopadhyay A, Gereben B, Callebaut I, Christoffolete MA, Kim BW, Nissim S, Mornon JP, Zavacki AM, Zeold A, Capelo LP, Curcio-Morelli C, Ribeiro R, Harney JW, Tabin CJ, Bianco AC** 2005 The Hedgehog-inducible ubiquitin ligase subunit WSB-1 modulates thyroid hormone activation and PTHrP secretion in the developing growth plate. Nat Cell Biol 7:698-705

102. **Campos-Barros A, Amma LL, Faris JS, Shailam R, Kelley MW, Forrest D** 2000 Type 2 iodothyronine deiodinase expression in the cochlea before the onset of hearing. Proceedings of the National Academy of Sciences of the United States of America 97:1287-1292

103. **Ng L, Goodyear RJ, Woods CA, Schneider MJ, Diamond E, Richardson GP, Kelley MW, Germain DL, Galton VA, Forrest D** 2004 Hearing loss and retarded cochlear development in mice lacking type 2 iodothyronine deiodinase. Proceedings of the National Academy of Sciences of the United States of America 101:3474-3479

104. **Dentice M, Luongo C, Huang S, Ambrosio R, Elefante A, Mirebeau-Prunier D, Zavacki AM, Fenzi G, Grachtchouk M, Hutchin M, Dlugosz AA, Bianco AC, Missero C, Larsen PR, Salvatore D** 2007 Sonic hedgehog-induced type 3 deiodinase blocks thyroid hormone action enhancing proliferation of normal and malignant keratinocytes. Proc Natl Acad Sci U S A 104:14466-14471

105. **Darimont C, Gaillard D, Ailhaud G, Negrel R** 1993 Terminal differentiation of mouse preadipocyte cells: adipogenic and antimitogenic role of triiodothyronine. Mol Cell Endocrinol 98:67-73

106. **Ailhaud G, Dani C, Amri EZ, Djian P, Vannier C, Doglio A, Forest C, Gaillard D, Negrel R, Grimaldi P** 1989 Coupling growth arrest and adipocyte differentiation. Environmental health perspectives 80:17-23

107. **Ying H, Araki O, Furuya F, Kato Y, Cheng SY** 2007 Impaired adipogenesis caused by a mutated thyroid hormone alpha1 receptor. Molecular and cellular biology 27:2359-2371

108. **Hernandez A, Garcia B, Obregon MJ** 2007 Gene expression from the imprinted Dio3 locus is associated with cell proliferation of cultured brown adipocytes. Endocrinology 148:3968-3976

109. **Lin S-P, Youngson N, Takada S, Seitz H, Reik W, Paulsen M, Cavaille J, Ferguson-Smith A** 2003 Asymmetric regulation of imprinting on the maternal and paternal chromosomes at the Dlk1-Gtl2 imprinted cluster on mouse chromosome 12. Nature genetics 35:97-102

110. **Tuca A, Giralt M, Villarroya F, Viñas O, Mampel T, Iglesias R** 1993 Ontogeny of thyroid hormone receptors and c-erbA expression during brown adipose tissue development: evidence of fetal acquisition of the mature thyroid status. Endocrinology 132:1913-1920

111. **Obregon MJ, Ruiz de Ona C, Hernandez A, Calvo R, Escobar del Rey F, Morreale de Escobar G** 1989 Thyroid hormones and 5'-deiodinase in rat brown adipose tissue during fetal life. Am J Physiol 257:E625-631

112. **Iglesias R, Fernandez J, Mampel T, Obregón M, Villarroya F** 1987 Iodothyronine 5'-deiodinase activity in rat brown adipose tissue during development. Biochimica et biophysica acta 923:233-240

113. **Carmona M, Iglesias R, Obregón M-J, Darlington G, Villarroya F, Giralt M** 2002 Mitochondrial biogenesis and thyroid status maturation in brown fat require CCAAT/enhancer-binding protein alpha. The Journal of biological chemistry 277:21489-21498

114. **Boden G** 1997 Role of fatty acids in the pathogenesis of insulin resistance and NIDDM. Diabetes 46:3-10

115. **Shaw JE, Sicree RA, Zimmet PZ** 2010 Global estimates of the prevalence of diabetes for 2010 and 2030. Diabetes Res Clin Pract 87:4-14

116. **American Diabetes A** 2014 Diagnosis and classification of diabetes mellitus. Diabetes Care 37 Suppl 1:S81-90

117. **Newgard CB** 2004 Regulation of glucose metabolism in the liver. In: DeFronzo RA, Ferrannini E, Keen H, Zimmet P eds. International Textbook of Diabetes, Third Edition. Chichester, UK: John Wiley & Sons; 253-275

118. **Magnusson I, Rothman DL, Katz LD, Shulman RG, Shulman GI** 1992 Increased rate of gluconeogenesis in type II diabetes mellitus. A 13C nuclear magnetic resonance study. J Clin Invest 90:1323-1327

119. **Hundal RS, Krssak M, Dufour S, Laurent D, Lebon V, Chandramouli V, Inzucchi SE, Schumann WC, Petersen KF, Landau BR, Shulman GI** 2000 Mechanism by which metformin reduces glucose production in type 2 diabetes. Diabetes 49:2063-2069

120. **Herzig S, Long F, Jhala US, Hedrick S, Quinn R, Bauer A, Rudolph D, Schutz G, Yoon C, Puigserver P, Spiegelman B, Montminy M** 2001 CREB regulates hepatic gluconeogenesis through the coactivator PGC-1. Nature 413:179-183

121. **Quinn PG, Granner DK** 1990 Cyclic AMP-dependent protein kinase regulates transcription of the phosphoenolpyruvate carboxykinase gene but not binding of nuclear factors to the cyclic AMP regulatory element. Mol Cell Biol 10:3357-3364

122. **Liu JS, Park EA, Gurney AL, Roesler WJ, Hanson RW** 1991 Cyclic AMP induction of phosphoenolpyruvate carboxykinase (GTP) gene transcription is mediated by multiple promoter elements. J Biol Chem 266:19095-19102

123. **Koo SH, Flechner L, Qi L, Zhang X, Screaton RA, Jeffries S, Hedrick S, Xu W, Boussouar F, Brindle P, Takemori H, Montminy M** 2005 The CREB coactivator TORC2 is a key regulator of fasting glucose metabolism. Nature 437:1109-1111

124. **Yoon JC, Puigserver P, Chen G, Donovan J, Wu Z, Rhee J, Adelmant G, Stafford J, Kahn CR, Granner DK, Newgard CB, Spiegelman BM** 2001 Control of hepatic gluconeogenesis through the transcriptional coactivator PGC-1. Nature 413:131-138

125. **Puigserver P, Rhee J, Donovan J, Walkey CJ, Yoon JC, Oriente F, Kitamura Y, Altomonte J, Dong H, Accili D, Spiegelman BM** 2003 Insulin-regulated hepatic gluconeogenesis through FOXO1-PGC-1alpha interaction. Nature 423:550-555

126. **Rhee J, Inoue Y, Yoon JC, Puigserver P, Fan M, Gonzalez FJ, Spiegelman BM** 2003 Regulation of hepatic fasting response by PPARgamma coactivator-1alpha (PGC-1): requirement for hepatocyte nuclear factor 4alpha in gluconeogenesis. Proc Natl Acad Sci U S A 100:4012-4017

127. **Nakae J, Park BC, Accili D** 1999 Insulin stimulates phosphorylation of the forkhead transcription factor FKHR on serine 253 through a Wortmannin-sensitive pathway. J Biol Chem 274:15982-15985

128. **Guo S, Rena G, Cichy S, He X, Cohen P, Unterman T** 1999 Phosphorylation of serine 256 by protein kinase B disrupts transactivation by FKHR and mediates effects of insulin on insulin-like growth factor-binding protein-1 promoter activity through a conserved insulin response sequence. J Biol Chem 274:17184-17192

129. **Goswami R, Lacson R, Yang E, Sam R, Unterman T** 1994 Functional analysis of glucocorticoid and insulin response sequences in the rat insulin-like growth factor-binding protein-1 promoter. Endocrinology 134:736-743

130. **Ayala JE, Streeper RS, Desgrosellier JS, Durham SK, Suwanichkul A, Svitek CA, Goldman JK, Barr FG, Powell DR, O'Brien RM** 1999 Conservation of an insulin response unit between mouse and human glucose-6-phosphatase catalytic subunit gene promoters: transcription factor FKHR binds the insulin response sequence. Diabetes 48:1885-1889

131. **Onuma H, Vander Kooi BT, Boustead JN, Oeser JK, O'Brien RM** 2006 Correlation between FOXO1a (FKHR) and FOXO3a (FKHRL1) binding and the inhibition of basal glucose-6-phosphatase catalytic subunit gene transcription by insulin. Mol Endocrinol 20:2831-2847

132. **O'Brien RM, Lucas PC, Forest CD, Magnuson MA, Granner DK** 1990 Identification of a sequence in the PEPCK gene that mediates a negative effect of insulin on transcription. Science 249:533-537

133. **Liao J, Barthel A, Nakatani K, Roth RA** 1998 Activation of protein kinase B/Akt is sufficient to repress the glucocorticoid and cAMP induction of phosphoenolpyruvate carboxykinase gene. J Biol Chem 273:27320-27324

134. **Schmoll D, Walker KS, Alessi DR, Grempler R, Burchell A, Guo S, Walther R, Unterman TG** 2000 Regulation of glucose-6-phosphatase gene expression by protein kinase Balpha and the forkhead transcription factor FKHR. Evidence for insulin response unit-dependent and -independent effects of insulin on promoter activity. J Biol Chem 275:36324-36333

135. **Nakae J, Kitamura T, Silver DL, Accili D** 2001 The forkhead transcription factor Foxo1 (Fkhr) confers insulin sensitivity onto glucose-6-phosphatase expression. J Clin Invest 108:1359-1367

136. **Rena G, Guo S, Cichy SC, Unterman TG, Cohen P** 1999 Phosphorylation of the transcription factor forkhead family member FKHR by protein kinase B. J Biol Chem 274:17179-17183

137. **Li X, Monks B, Ge Q, Birnbaum MJ** 2007 Akt/PKB regulates hepatic metabolism by directly inhibiting PGC-1alpha transcription coactivator. Nature 447:1012-1016

138. **Brunet A, Bonni A, Zigmond MJ, Lin MZ, Juo P, Hu LS, Anderson MJ, Arden KC, Blenis J, Greenberg ME** 1999 Akt promotes cell survival by phosphorylating and inhibiting a Forkhead transcription factor. Cell 96:857-868

139. **Matsuzaki H, Daitoku H, Hatta M, Tanaka K, Fukamizu A** 2003 Insulin-induced phosphorylation of FKHR (Foxo1) targets to proteasomal degradation. Proc Natl Acad Sci U S A 100:11285-11290

140. **Matsumoto M, Pocai A, Rossetti L, Depinho RA, Accili D** 2007 Impaired regulation of hepatic glucose production in mice lacking the forkhead transcription factor Foxo1 in liver. Cell Metab 6:208-216

141. **Altomonte J, Richter A, Harbaran S, Suriawinata J, Nakae J, Thung SN, Meseck M, Accili D, Dong H** 2003 Inhibition of Foxo1 function is associated with improved fasting glycemia in diabetic mice. Am J Physiol Endocrinol Metab 285:E718-728

142. **Dong XC, Copps KD, Guo S, Li Y, Kollipara R, DePinho RA, White MF** 2008 Inactivation of hepatic Foxo1 by insulin signaling is required for adaptive nutrient homeostasis and endocrine growth regulation. Cell Metab 8:65-76

143. **Lu M, Wan M, Leavens KF, Chu Q, Monks BR, Fernandez S, Ahima RS, Ueki K, Kahn CR, Birnbaum MJ** 2012 Insulin regulates liver metabolism in vivo in the absence of hepatic Akt and Foxo1. Nat Med 18:388-395

144. **Gross DN, Wan M, Birnbaum MJ** 2009 The role of FOXO in the regulation of metabolism. Current diabetes reports 9:208-214

145. **Biggs WH, 3rd, Cavenee WK, Arden KC** 2001 Identification and characterization of members of the FKHR (FOX O) subclass of winged-helix transcription factors in the mouse. Mammalian genome : official journal of the International Mammalian Genome Society 12:416-425

146. **Jacobs FM, van der Heide LP, Wijchers PJ, Burbach JP, Hoekman MF, Smidt MP** 2003 FoxO6, a novel member of the FoxO class of transcription factors with distinct shuttling dynamics. J Biol Chem 278:35959-35967

147. **Eijkelenboom A, Burgering BM** 2013 FOXOs: signalling integrators for homeostasis maintenance. Nat Rev Mol Cell Biol 14:83-97

148. **Furuyama T, Nakazawa T, Nakano I, Mori N** 2000 Identification of the differential distribution patterns of mRNAs and consensus binding sequences for mouse DAF-16 homologues. Biochem J 349:629-634

149. **Kops GJ, de Ruiter ND, De Vries-Smits AM, Powell DR, Bos JL, Burgering BM** 1999 Direct control of the Forkhead transcription factor AFX by protein kinase B. Nature 398:630-634

150. **Zhang K, Li L, Qi Y, Zhu X, Gan B, DePinho RA, Averitt T, Guo S** 2012 Hepatic suppression of Foxo1 and Foxo3 causes hypoglycemia and hyperlipidemia in mice. Endocrinology 153:631-646

151. **Arden KC** 2008 FOXO animal models reveal a variety of diverse roles for FOXO transcription factors. Oncogene 27:2345-2350

152. **Hosaka T, Biggs WH, 3rd, Tieu D, Boyer AD, Varki NM, Cavenee WK, Arden KC** 2004 Disruption of forkhead transcription factor (FOXO) family members in mice reveals their functional diversification. Proc Natl Acad Sci U S A 101:2975-2980

153. **van der Horst A, Burgering BM** 2007 Stressing the role of FoxO proteins in lifespan and disease. Nat Rev Mol Cell Biol 8:440-450

154. **Woods YL, Rena G, Morrice N, Barthel A, Becker W, Guo S, Unterman TG, Cohen P** 2001 The kinase DYRK1A phosphorylates the transcription factor FKHR at Ser329 in vitro, a novel in vivo phosphorylation site. Biochem J 355:597-607

155. **Rena G, Woods YL, Prescott AR, Peggie M, Unterman TG, Williams MR, Cohen P** 2002 Two novel phosphorylation sites on FKHR that are critical for its nuclear exclusion. EMBO J 21:2263-2271

156. **Housley MP, Rodgers JT, Udeshi ND, Kelly TJ, Shabanowitz J, Hunt DF, Puigserver P, Hart GW** 2008 O-GlcNAc regulates FoxO activation in response to glucose. J Biol Chem 283:16283-16292

157. **Zhao Y, Wang Y, Zhu WG** 2011 Applications of post-translational modifications of FoxO family proteins in biological functions. J Mol Cell Biol 3:276-282

158. **Lehtinen MK, Yuan Z, Boag PR, Yang Y, Villen J, Becker EB, DiBacco S, de la Iglesia N, Gygi S, Blackwell TK, Bonni A** 2006 A conserved MST-FOXO signaling pathway mediates oxidative-stress responses and extends life span. Cell 125:987-1001

159. **Yamagata K, Daitoku H, Takahashi Y, Namiki K, Hisatake K, Kako K, Mukai H, Kasuya Y, Fukamizu A** 2008 Arginine methylation of FOXO transcription factors inhibits their phosphorylation by Akt. Mol Cell 32:221-231

160. **Daitoku H, Sakamaki J, Fukamizu A** 2011 Regulation of FoxO transcription factors by acetylation and protein-protein interactions. Biochim Biophys Acta 1813:1954-1960

161. **Brunet A, Sweeney LB, Sturgill JF, Chua KF, Greer PL, Lin Y, Tran H, Ross SE, Mostoslavsky R, Cohen HY, Hu LS, Cheng HL, Jedrychowski MP, Gygi SP, Sinclair DA, Alt FW, Greenberg ME** 2004 Stress-dependent regulation of FOXO transcription factors by the SIRT1 deacetylase. Science 303:2011-2015

162. **Daitoku H, Hatta M, Matsuzaki H, Aratani S, Ohshima T, Miyagishi M, Nakajima T, Fukamizu A** 2004 Silent information regulator 2 potentiates Foxo1-mediated transcription through its deacetylase activity. Proc Natl Acad Sci U S A 101:10042-10047

163. **van der Horst A, Tertoolen LG, de Vries-Smits LM, Frye RA, Medema RH, Burgering BM** 2004 FOXO4 is acetylated upon peroxide stress and deacetylated by the longevity protein hSir2(SIRT1). J Biol Chem 279:28873-28879

164. **Plas DR, Thompson CB** 2003 Akt activation promotes degradation of tuberin and FOXO3a via the proteasome. J Biol Chem 278:12361-12366

165. **Huang H, Regan KM, Wang F, Wang D, Smith DI, van Deursen JM, Tindall DJ** 2005 Skp2 inhibits FOXO1 in tumor suppression through ubiquitin-mediated degradation. Proc Natl Acad Sci U S A 102:1649-1654

166. **Yang JY, Zong CS, Xia W, Yamaguchi H, Ding Q, Xie X, Lang JY, Lai CC, Chang CJ, Huang WC, Huang H, Kuo HP, Lee DF, Li LY, Lien HC, Cheng X, Chang KJ, Hsiao CD, Tsai FJ, Tsai CH, Sahin AA, Muller WJ, Mills GB, Yu D, Hortobagyi GN, Hung MC** 2008 ERK promotes tumorigenesis by inhibiting FOXO3a via MDM2-mediated degradation. Nat Cell Biol 10:138-148

167. **Fu W, Ma Q, Chen L, Li P, Zhang M, Ramamoorthy S, Nawaz Z, Shimojima T, Wang H, Yang Y, Shen Z, Zhang Y, Zhang X, Nicosia SV, Zhang Y, Pledger JW, Chen J, Bai W** 2009 MDM2 acts downstream of p53 as an E3 ligase to promote FOXO ubiquitination and degradation. J Biol Chem 284:13987-14000

168. **Kato S, Ding J, Pisck E, Jhala US, Du K** 2008 COP1 functions as a FoxO1 ubiquitin E3 ligase to regulate FoxO1-mediated gene expression. J Biol Chem 283:35464-35473

169. **Li F, Xie P, Fan Y, Zhang H, Zheng L, Gu D, Patterson C, Li H** 2009 C terminus of Hsc70-interacting protein promotes smooth muscle cell proliferation and survival through ubiquitin-mediated degradation of FoxO1. J Biol Chem 284:20090-20098

170. **van der Horst A, de Vries-Smits AM, Brenkman AB, van Triest MH, van den Broek N, Colland F, Maurice MM, Burgering BM** 2006 FOXO4 transcriptional activity is regulated by monoubiquitination and USP7/HAUSP. Nat Cell Biol 8:1064-1073

171. **Brenkman AB, de Keizer PL, van den Broek NJ, van der Groep P, van Diest PJ, van der Horst A, Smits AM, Burgering BM** 2008 The peptidyl-isomerase Pin1 regulates p27kip1 expression through inhibition of Forkhead box O tumor suppressors. Cancer Res 68:7597-7605

172. **Brenkman AB, de Keizer PL, van den Broek NJ, Jochemsen AG, Burgering BM** 2008 Mdm2 induces mono-ubiquitination of FOXO4. PLoS One 3:e2819

173. **Welchman R, Gordon C, Mayer R** 2005 Ubiquitin and ubiquitin-like proteins as multifunctional signals. Nature reviews Molecular cell biology 6:599-609

174. **Komander D** 2009 The emerging complexity of protein ubiquitination. Biochemical Society transactions 37:937-953

175. **Xu P, Duong DM, Seyfried NT, Cheng D, Xie Y, Robert J, Rush J, Hochstrasser M, Finley D, Peng J** 2009 Quantitative proteomics reveals the function of unconventional ubiquitin chains in proteasomal degradation. Cell 137:133-145

176. **Dammer EB, Na CH, Xu P, Seyfried NT, Duong DM, Cheng D, Gearing M, Rees H, Lah JJ, Levey AI, Rush J, Peng J** 2011 Polyubiquitin linkage profiles in three models of proteolytic stress suggest the etiology of Alzheimer disease. J Biol Chem 286:10457-10465

177. **Peng J, Schwartz D, Elias J, Thoreen C, Cheng D, Marsischky G, Roelofs J, Finley D, Gygi S** 2003 A proteomics approach to understanding protein ubiquitination. Nature biotechnology 21:921-926

178. **Kulathu Y, Komander D** 2012 Atypical ubiquitylation - the unexplored world of polyubiquitin beyond Lys48 and Lys63 linkages. Nat Rev Mol Cell Biol 13:508-523

179. **Kerscher O, Felberbaum R, Hochstrasser M** 2006 Modification of proteins by ubiquitin and ubiquitin-like proteins. Annual review of cell and developmental biology 22:159-180

180. **Rotin D, Kumar S** 2009 Physiological functions of the HECT family of ubiquitin ligases. Nat Rev Mol Cell Biol 10:398-409

181. **Deshaies RJ, Joazeiro CA** 2009 RING domain E3 ubiquitin ligases. Annu Rev Biochem 78:399-434

182. **Reyes-Turcu FE, Ventii KH, Wilkinson KD** 2009 Regulation and cellular roles of ubiquitin-specific deubiquitinating enzymes. Annu Rev Biochem 78:363-397

183. **Nijman SM, Luna-Vargas MP, Velds A, Brummelkamp TR, Dirac AM, Sixma TK, Bernards R** 2005 A genomic and functional inventory of deubiquitinating enzymes. Cell 123:773-786

184. **Ventii KH, Wilkinson KD** 2008 Protein partners of deubiquitinating enzymes. Biochem J 414:161-175

185. **Everett RD, Meredith M, Orr A, Cross A, Kathoria M, Parkinson J** 1997 A novel ubiquitin-specific protease is dynamically associated with the PML nuclear domain and binds to a herpesvirus regulatory protein. EMBO J 16:1519-1530

186. **Li M, Chen D, Shiloh A, Luo J, Nikolaev AY, Qin J, Gu W** 2002 Deubiquitination of p53 by HAUSP is an important pathway for p53 stabilization. Nature 416:648-653

187. **Nicholson B, Suresh Kumar KG** 2011 The Multifaceted Roles of USP7: New Therapeutic Opportunities. Cell Biochem Biophys 60:61-68

188. **Cummins JM, Vogelstein B** 2004 HAUSP is required for p53 destabilization. Cell Cycle 3:689-692

189. **Sowa ME, Bennett EJ, Gygi SP, Harper JW** 2009 Defining the human deubiquitinating enzyme interaction landscape. Cell 138:389-403

190. **Kessler BM, Fortunati E, Melis M, Pals CE, Clevers H, Maurice MM** 2007 Proteome changes induced by knock-down of the deubiquitylating enzyme HAUSP/USP7. J Proteome Res 6:4163-4172

191. **Song MS, Salmena L, Carracedo A, Egia A, Lo-Coco F, Teruya-Feldstein J, Pandolfi PP** 2008 The deubiquitinylation and localization of PTEN are regulated by a HAUSP-PML network. Nature 455:813-817

192. **Hussain S, Zhang Y, Galardy PJ** 2009 DUBs and cancer: the role of deubiquitinating enzymes as oncogenes, non-oncogenes and tumor suppressors. Cell Cycle 8:1688-1697

193. **Nicholson B, Kumar S, Agarwal S, Eddins M, Marblestone JG, Wu J, Kodrasov MP, Larocque JP, Sterner DE, Mattern MR** 2014 Discovery of Therapeutic Deubiquitylase Effector Molecules: Current Perspectives. Journal of biomolecular screening

Chapter 2

Absence of thyroid hormone activation during development underlies a permanent defect in adaptive thermogenesis

AUTHOR CONTRIBUTIONS

I conceptualized and performed all *in vivo* experiments on the role of type 2 deiodinase in brown adipose tissue development. This included maintenance of mouse breeding colonies, determination of timed-pregnancies, and tissue harvests. I also conducted the deiodinase activity assays, sample preparation for histology, gene expression analyses, and lipid peroxidation studies that went along with the embryo studies. I determined plasma hormone levels from embryos with assistance from Mayrin Correa-Medina. Gordana Simovic assisted with quantification of deiodination products by Ultra Performance Liquid Chromatography.

The *in vitro* brown preadipocyte differentiation experiments were largely a collaborative effort. Marcelo Christoffolete performed the gene expression time course analyses on differentiating brown adipocytes. He also analyzed oxygen consumption and determined reactive oxygen species (ROS) of day 10 differentiated brown adipocytes. I performed the complementary ROS determination of brown preadipocyte cultures. Scott Ribich performed all insulin signaling experiments and microscopy/cell counting experiments. I wrote the manuscript with Antonio Bianco. Mary Elizabeth Patti contributed to discussion and edited the manuscript.

Absence of Thyroid Hormone Activation during Development Underlies a Permanent Defect in Adaptive Thermogenesis

Jessica A. Hall[1†], Scott Ribich[2†], Marcelo A. Christoffolete[2], Gordana Simovic[4], Mayrin Correa-Medina[4], Mary Elizabeth Patti[3], and Antonio C. Bianco[2,4]

A similar version of this work has been published

Endocrinology 151(9), September 2010, pp4573–4582

[1]Biological and Biomedical Sciences Program, [2]Division of Endocrinology, Diabetes and Hypertension, Brigham and Women's Hospital, and [3]Research Division, Joslin Diabetes Center, Harvard Medical School, Boston, MA 02215; and [4]Division of Endocrinology, Diabetes and Metabolism, University of Miami Miller School of Medicine, Miami, FL 33136.

[†]These authors contributed equally to this work.

ABSTRACT

Type 2 deiodinase (D2), which is highly expressed in brown adipose tissue (BAT), is an enzyme that amplifies thyroid hormone signaling in individual cells. Mice with inactivation of the D2 pathway (D2KO) exhibit dramatically impaired thermogenesis in BAT, leading to hypothermia during cold exposure and a greater susceptibility to diet-induced obesity. This was interpreted as a result of defective acute activation of BAT D2. Here we report that the adult D2KO BAT has a permanent thermogenic defect that stems from impaired embryonic BAT development. D2KO embryos have normal serum T3 but due to lack of D2-generated T3 in BAT, this tissue exhibits decreased expression of genes defining BAT identity [i.e. *UCP1*, *PGC-1α* and *Dio2* (nonfunctional)], which results in impaired differentiation and oxidative capacity. Coinciding with a reduction of these T3-responsive genes, there is oxidative stress that in a cell model of brown adipogenesis can be linked to decreased insulin signaling and decreased adipogenesis. This discovery highlights the importance of deiodinase-controlled thyroid hormone signaling in BAT development, where it has important metabolic repercussions for energy homeostasis in adulthood.

INTRODUCTION

Brown adipose tissue (BAT) is a major site of adaptive thermogenesis, having gained recent appreciation for presence and activity in adult humans (1). Its capacity to convert chemical energy into heat is used to preserve thermal and caloric homeostasis. Both pathways rely on uncoupling protein 1 (UCP1), a thyroid hormone-responsive gene (2). While small mammals use BAT activation to defend core temperature in the cold, hypothyroid animals succumb within hours because of insufficient BAT thermogenesis (3, 4).

Thyroid hormone signaling can be controlled in individual cells through the selective activation or inactivation of thyroid hormone via the deiodinases (5). Although thyroid hormone primarily exists as the minimally active prohormone T4 (thyroxine), extrathyroidal tissues can convert T4 to the biologically active T3 (3,5,3′-triiodothyronine), which binds thyroid hormone receptor (TR) to regulate transcription of T3-responsive genes. This reaction is catalyzed by the type 2 deiodinase (D2), while both T4 and T3 can be inactivated by the type 3 deiodinase (D3) (Figure 2.1, A and B, respectively). As a result, D2-expressing cells have a higher T3 concentration and TR activation. Correspondingly, D3-expressing cells can inactivate incoming T3, thereby reducing TR activation, such as during myocardium hypoxia (6).

While the serum concentration of T3 is normal in mice with targeted deletion of D2 gene (D2KO) (7), BAT thermogenesis is severely impaired (8). Freshly isolated D2KO brown adipocytes have impaired lipogenesis, generate less cAMP, and fail to increase metabolic rate in response to adrenergic stimulation (8, 9). D2KO animals can only survive in the cold due to an increase in BAT sympathetic activity and shivering, a behavior not normally observed in cold-exposed mice. In addition, D2KO mice are more susceptible to obesity when placed on a high-fat diet (Castillo & Hall *et al*., unpublished).

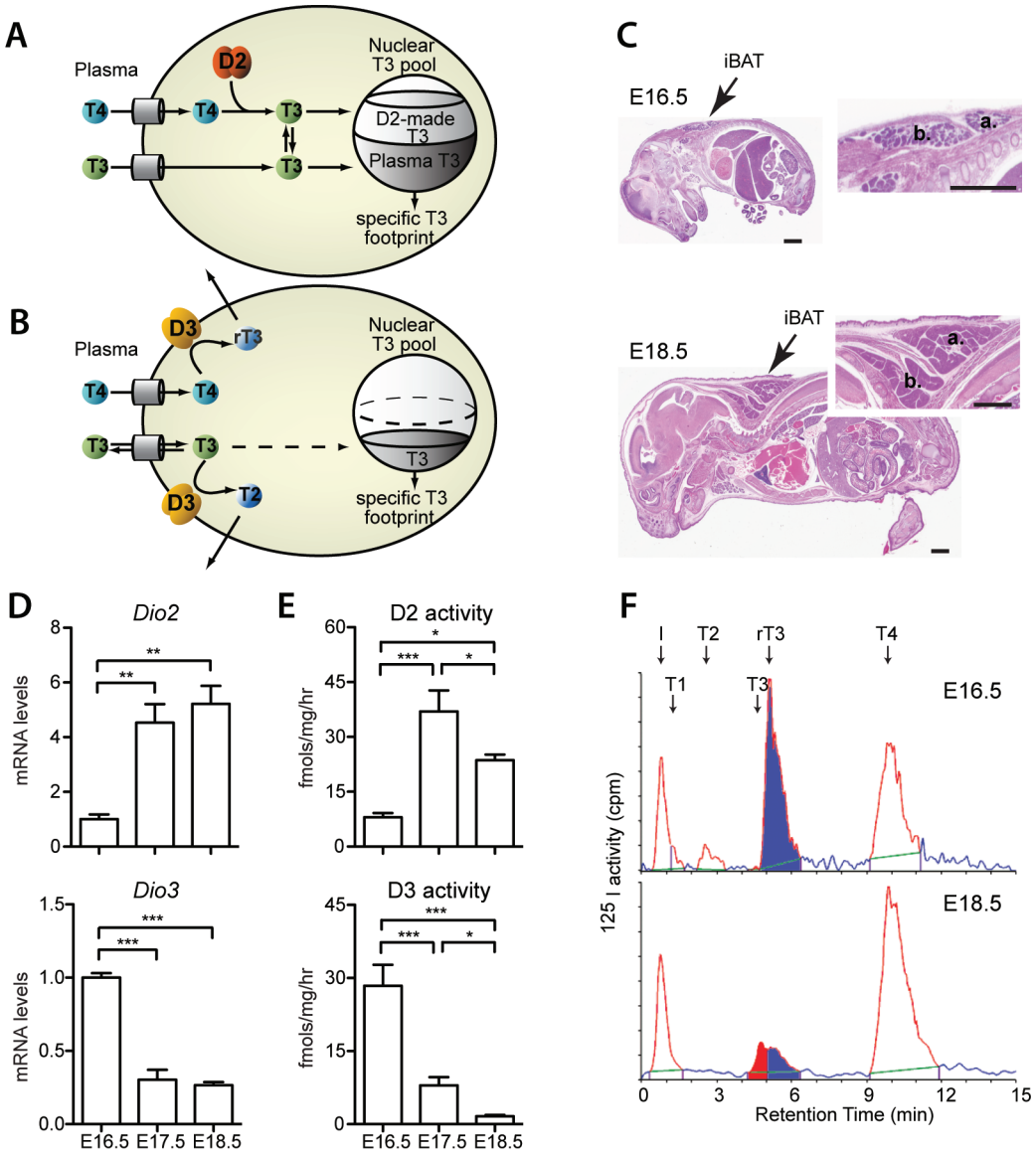

Figure 2.1. Deiodinase expression during BAT development. (**A and B**) Schematic of D2 and D3 modulation of thyroid hormone signal. D2 converts T4 to T3 (**A**), increasing nuclear T3 levels, while D3 can inactivate T3 and T4 (**B**), decreasing thyroid hormone signal. (**C**) Image of H&E section of wildtype mouse embryo at E16.5 (*top*) and E18.5 (*bottom*) with arrow indicating interscapular BAT (iBAT). *Inset* shows enlarged iBAT, where a. is section of BAT dissected for subsequent analyses. *Bars*, 1 mm. (**D**) *Dio2* and *Dio3* mRNA levels of embryonic BAT graphed relative to E16.5 expression. (**E**) D2 and D3 activity of BAT sonicates from E16.5, E17.5, and E18.5 embryos. *, $p < 0.05$; **, $p < 0.01$; and ***, $p < 0.001$ by one-way ANOVA with Newman-Keuls Multiple comparison. (**F**) Chromatogram of T4-fate, as resolved by UPLC, when E16.5 (*top*) and E18.5 (*bottom*) BAT sonicates are incubated with ^{125}I-T4. Deiodination products are labeled by arrow according to retention time. Area depicting T3 peak is colored in *red*; rT3 peak in *blue*.

Here we investigated whether insufficient D2KO BAT thermogenesis stems from impaired BAT development or results primarily from defective activation of the mature tissue. We have found that absence of D2-mediated thyroid hormone signaling in embryonic BAT contributes to a decrease of T3-responsive genes, such as *PGC-1α*, *UCP1*, and *Dio2*. Furthermore, in D2KO embryonic BAT there is oxidative stress, which in a cell model of brown adipogenesis can lead to decreased insulin signaling and impaired differentiation. These data illustrate the critical role played by D2 in BAT development, the absence of which results in a defective mature brown adipocyte.

MATERIALS AND METHODS

Materials

Unless otherwise specified, reagents were purchased from Sigma-Aldrich (St. Louis, MO). BODIPY 493/503, Fungizone, Trizol, Oil Red O, and SlowFade Gold with DAPI were from Invitrogen (Carlsbad, CA). Anion exchange resin AG1-X8 was obtained from Bio-Rad (Richmond, CA). Anti-Phospho-Akt (Ser473), anti-Akt, anti-Phospho-IRS-1 (Ser307), anti-IRS1 antibody, anti-PDK1, and anti-Phospho-IκBα (Ser32) antibodies were obtained from Cell Signaling (Danvers, MA). Anti-IRβ antibody was from Santa Cruz Biotechnology (Santa Cruz, CA). The anti-rabbit Alexa647, anti-rabbit Alexa488, and anti-rabbit Alexa593 antibodies were from Invitrogen. Outer-ring labeled ^{125}I-T4 and -T3 were purchased from PerkinElmer (Boston, MA) and purified on LH-20 columns (Sigma) before use. Dithiothreitol (DTT) was from Calbiochem (San Diego, CA).

Animals

All studies were performed according to protocols approved by the Animal Care and Use Committees of Harvard Medical School and University of Miami Miller School of Medicine. Mice with targeted disruption of the *Dio2* gene (D2KO) were backcrossed into a C57BL/6J background for 10 generations. Genotyping of D2KO mice was as previously described (9). C57BL/6J mice (wildtype, WT) were purchased from Jackson Laboratories (Bar Harbor, MA). For the embryo studies, WT mice were mated with D2KO mice to generate mice heterozygous for the D2KO allele (D2Het mice). Timed-pregnant dams of D2Het pairs were used to obtain littermate embryos of WT, D2Het and D2KO genotypes. Pregnancy was determined by presence of a vaginal plug (embryonic day 0.5, E0.5). All mice were maintained on normal chow and housed under a 12-hour light, 12-hour dark cycle at 22°C.

Histology

Hematoxylin and eosin staining was performed on paraffin-embedded sections of embryos that had been fixed in 10% neutral buffered formalin.

Deiodination assays

D2 and D3 activity was determined as previously described (10). D2 activity was measured on 30–40 μg protein of BAT homogenates in the presence of outer-ring labeled ^{125}I-T4, 0.1 nM T4 substrate, and 20 mM DTT for 4 hours at 37°C and ^{125}I release quantified with a γ counter (2470 WIZARD^2, PerkinElmer Life Sciences, Boston, MA). Samples treated with 100 nM T4 (saturating) were used for background measurements. D3 activity was assayed by quantification of deiodination products on UPLC (ACQUITY, Waters Corporation, Milford,

MA) after 1-hour incubation at 37°C with outer-ring labeled ^{125}I-T3, 0.1 nM T3 substrate, 1 mM PTU, and 10 mM DTT. For determination of T4-fate, deiodination products were resolved by Ultra Performance Liquid Chromatography (UPLC) after incubation for 2 hours with outer-ring labeled ^{125}I-T4, 1 mM PTU, and 10 mM DTT.

Plasma hormone levels

Plasma levels of TSH, T4, and T3 were determined using a MILLIPLEX rat thyroid hormone panel kit as described by the manufacturer (Millipore, Billerica, MA) and read on a BioPlex (Bio-Rad, Hercules, CA). Plasma from hypo- and hyperthyroid mice (treated for 10 days with Sodium Perchlorate and Methimazole or 80 mg/kg T4, respectively) was used to prepare mouse TSH standards. Both rat and mouse curves were parallel and separated by a factor of 5. Mouse embryo serum samples were diluted 1:2.5 for analysis, and settings for the BioPlex included a modified specification of 100 events per bead.

Brown preadipocyte tissue culture

Interscapular brown adipose tissue (iBAT) was dissected from male and female mice from 4–8 weeks of age and processed as previously described (11). Unless indicated, cells were grown in DMEM + 10% fetal bovine serum, supplemented with 10 mM HEPES, 10^{-7} M sodium selenite, 3 nM insulin, 25 mg/L tetracycline, 25 mg/L streptomycin, 25 mg/L ampicillin, and 1 mg/L fungizone. The preadipocytes were propagated and plated at confluence (20,000 cells/cm^2), corresponding to day 0 of differentiation. Cells were differentiated for 10 days in this media unless noted. T3-responsiveness was performed with thyroid hormone-depleted serum (AG1-X8 resin/charcoal-stripped) as previously described (11). An adipogenic cocktail of indomethacin

(125 μM), IBMX (0.5 mM), and dexamethasone (0.5 μM) was used with or without insulin in indicated experiments. Other treatments included Ascorbic Acid (1 mM), rT3 (200 nM), and T3 (50 nM or 100 nM).

Microscopy and cell counting

For the cell counting experiments, day 0 cultures were differentiated on LabTek permanox slides (Nalge Nunc International, Rochester, NY). Cells were fixed in 4% PFA, and immunocytochemistry performed as suggested by antibody manufacturers (Abcam and Invitrogen). Slides were imaged on a Nikon Eclipse 90i microscope (Melville, NY), with a total of 15 fields in three different wells acquired for each sample at each time point. The location of individual fields was kept consistent between slides with a reference guide on the microscope stage. Nuclei or cells were counted using the Nikon NIS-Elements imaging software (for DAPI), or manually (for BODIPY 493/503). Identical thresholds for fluorescent intensity were used for WT and D2KO fields. Percent differentiation was determined as fraction of cells staining for BODIPY 493/503.

Flow cytometry

WT and D2KO cells differentiated for 10 days were treated with trypsin, resuspended in growth media, centrifuged briefly and both the upper layer of supernatant (containing adipocytes) and the cell pellet (containing preadipocytes) mixed together with BODIPY 493/503 (6 ng/mL in PBS) for 5 min at room temperature. These cells were then centrifuged again and the upper layer of supernatant and the cell pellet resuspended together again in PBS. Cells were sorted in DakoCytomation MoFlo (Dako North America, Inc., Carpinteria, CA) using the FL1

channel (488 nm excitation and 515 nm emission) at the Dana-Farber Cancer Institute Flow Cytometry Core Facility (Boston, MA) and separated as positive and negative for BOPIDY staining. In each individual preparation, two cell populations were obtained based on the fluorescence intensity (FL): a preadipocyte population in which BODIPY staining was about 30 FL units, close to that seen for the negative controls HEK293 and COS-7 cell lines (~20 FL units), and a differentiated brown adipocyte population containing fat droplets in which fluorescence intensity averaged 85 and 88 FL units for WT and D2KO cells.

Cellular O_2 consumption

Ten-day differentiated WT and D2KO brown adipocyte cultures were seeded in 24-well microplates and assayed in the XF24 instrument from Seahorse Bioscience (Billerica, MA), as described previously (12).

Quantitative RT–PCR

For expression analyses of embryonic BAT, total RNA was extracted using RNeasy® Lipid Tissue Mini kit (Qiagen Sciences) and contaminating DNA removed with TURBO DNA-free (Ambion), followed by cDNA preparation from 0.3–1 μg of total RNA with Applied Biosystem's High Capacity cDNA RT kit. For cell culture samples, total RNA was extracted using the Trizol method, and 1.5–10 μg of total RNA was used in the SuperScript First-Strand Synthesis System for RT-PCR (Invitrogen) on a Robocycler (Stratagene, La Rolla, CA). For mitochondrial DNA content, DNA was recovered during the Trizol RNA isolation, and 18 ng of total DNA used for amplification. cDNA products were quantified by real-time PCR using the SYBR Green FastMix (Quanta) on a MyiQ iCycler (Bio-Rad) under conditions as previously

described (9). Primer sequences available upon request. Gene expression was determined by generation of a standard curve and normalized for the expression of *Cyclophilin B*. For the qRT-PCR analysis of insulin signaling components, WT and D2KO preadipocytes were cultured in media without supplemental insulin to minimize secondary transcriptional effects of insulin resistance.

Insulin signaling and Western blotting

For insulin signaling experiments, brown preadipocyte cultures were serum starved for 20 hours. Cells were stimulated with varying insulin concentrations (0–7.5 nM) for 5 min, and then lysed in 50 mM HEPES (pH 7.4), 137 mM NaCl, 1 mM $MgCl_2$, 1 mM $CaCl_2$, 10 mM sodium pyrophosphate, 10 mM NaF, 2 mM EGTA, 2 mM Na_3VO_4, 2 mM phenylmethylsulfonylfluoride, 1% NP-40, and 10% Glycerol. Extracts were sonicated, total lysates separated on a pre-cast gel (Bio-Rad), transferred to Immobilon-P transfer membranes (Millipore, Bedford, MA), and blotted as directed by manufacturer. Western blots were stripped using Restore PLUS Western Blot Stripping Buffer (Thermo Scientific, Rockford, IL) as directed. Scanned images were processed in Adobe Photoshop Elements 2.0 software and auto levels used to increase brightness for publication.

Reactive oxygen species (ROS) detection by flow cytometry

WT and D2KO preadipocyte cultures were pretreated for 30 min with 5 mm CM-H_2DCFDA (Invitrogen) and subsequently harvested and washed with PBS. Cell suspensions were immediately sorted at the Dana-Farber Cancer Institute Flow Cytometry Core Facility

(Boston, MA) Core. Data analysis was performed with the FlowJo Flow Cytometry Analysis Software (Ashland, OR), with a lower cutoff of 1000 FL intensity for the CM-H_2DCFDA dye.

ROS detection by confocal microscopy

Intracellular ROS production was determined by confocal microscopy after incubation of day 10 WT and D2KO brown adipocyte cultures with CM-H_2DCFDA using previously described methods (13).

Detection of lipid peroxidation

Embryonic BAT was frozen in liquid nitrogen upon dissection and stored at -80°C until analysis. For homogenization, tissue was resuspended in cell lysis buffer (Cell Signaling) containing a complete protease inhibitor cocktail from Roche (Basel, Switzerland) and sonicated. Protein concentration was determined using the Bradford method (Bio-Rad). Lipid peroxidation was detected on 20 μg of BAT protein lysate with the OxiSelect Malondialdehyde (MDA) Immunoblot kit (Cell Biolabs) using a rabbit anti-MDA antibody according to the manufacturer's instructions.

Oil Red O staining and analysis

Oil Red O Staining was performed as described (14). Pictures were taken in a CKX41 Culture microscope (Olympus, Melvile, NY) and analyzed in Adobe Photoshop Elements 2.0 (Adobe, San Jose, CA). Oil Red O in the plates was eluted in DMSO and absorbance performed in a Smartspec spectrophotometer (BioRad, Richmond CA) at 535 nM.

Microarray analysis

Total RNA (8 μg) was extracted from day 0 brown preadipocyte cultures using Trizol, digested with DNase I (Invitrogen), either re-extracted with Trizol or purified with the Rneasy MinElute Cleanup Kit (Qiagen, Valencia, CA), and submitted for microarray analysis at the Dana-Farber Cancer Institute Microarray Core Facility, Boston, MA, using Affimatrix chip MOE430 2.0. This was done in duplicate with cultures grown and processed independently, as a control for consistency. Data was initially processed and clustering analysis performed using the dCHIP software (http://biosun1.harvard.edu/complab/dchip/manual.htm) according to the developer's manual (15). Comparison between WT and D2KO samples was performed and genes statistically different (fold difference > 1.05 and $P < 0.05$) selected. A further restriction was placed on genes requiring a P call > 20%. This analysis allows a wide approach to spot trends of alterations in different pathways while keeping False Detection Rate (FDR) low at 7.9%. Hierarchical clustering of genes was done using dCHIP with restrictions of pathway $p < 0.05$ and gene $p < 0.005$. Further expression analysis was also done using GenMAPP2 (http://www.genmapp.org) (16).

Statistical analysis

Data were analyzed using PRISM software (GraphPad Software, Inc, San Diego, CA) and expressed as mean ± SEM. Western blot signal was analyzed with ImageJ software (National Institutes of Health, Bethesda, MD) and normalized to α-Tubulin signal on each blot. A two-tailed Student's *t* test or one-way ANOVA with Newman-Keuls Multiple Comparison test (or Dunnett's Multiple Comparison test, where indicated) was used to compare means between groups.

RESULTS

Local thyroid hormone signaling increases during brown adipogenesis

It is not known whether D2 plays its critical role during development of BAT or exclusively during acute activation of mature BAT. To address this question, we focused on BAT development during embryonic life, where embryos are held *in utero* at thermoneutrality, allowing for capture of D2-mediated events of an adipogenic nature. In rodents, BAT develops late during the prenatal period, such that at birth the BAT is equipped with its full thermogenic potential (17). Using a mouse model of BAT development, an interscapular BAT depot became evident at embryonic day (E)16.5, reaching a substantial size by E18.5 (~5 mm) (Figure 2.1C). With this 3-day developmental snapshot to study *in vivo* adipogenesis, we then analyzed the mRNA transcripts of D2 and D3 (*Dio2* and *Dio3*, respectively). *Dio2* expression increased considerably from E16.5 to E18.5, reaching levels over 5-fold greater by E18.5 (Figure 2.1D). This corresponded with a decrease in *Dio3*, from its highest expression level at E16.5 to 27% by E18.5. Deiodinase activity correlated with mRNA levels for D3, where its highest activity was observed at E16.5. On the other hand, D2 activity increased from E16.5 to E18.5, with peak D2 activity at E17.5 (Figure 2.1E).

We verified that these reciprocal changes in deiodinase activity modify thyroid hormone signaling in the developing brown adipocyte by following the fate of the prohormone T4 during incubation with E16.5 or E18.5 BAT sonicates (Figure 2.1F). At E16.5, almost all T4 exposed to BAT sonicates was inactivated to rT3 (via D3), and no T3 was detected, as it was rapidly inactivated to T2 (via D3). This indicates that early during brown adipogenesis thyroid hormone signaling is kept at a minimum as both T4 and T3 are inactivated by high levels of D3. On the other hand, at E18.5, there was an identifiable peak of T3, resulting from T4 activation by D2. At

the same time, rT3 production decreased dramatically, and T3 inactivation to T2 was undetected. Thus, coordinated changes in deiodinase behavior mediate an increase in thyroid hormone signaling during BAT development. These patterns of deiodinase expression were also found by comparing *in vitro* proliferating brown preadipocytes with isolated mature brown adipocytes (Figure 2.2).

Impaired expression of T3-dependent genes disrupts D2KO brown adipogenesis

To test the hypothesis that D2-generated T3 plays a role during BAT development, we studied D2KO embryos from E16.5–E18.5. By breeding mice heterozygous for the D2KO allele (D2Het), we could compare D2KO and D2Het embryos with WT littermates. Importantly, we determined that E18.5 D2KO and D2Het embryos are systemically euthyroid with normal concentrations of T3 in plasma (Figure 2.3A), which is a phenotype that persists into adulthood (7). This is further supported by an analysis of 81 E18.5 WT, D2Het, and D2KO embryos, which had similar body weight and length (Table 2.1). Thus, differences between WT and D2KO BAT should reflect effects based on a local (tissue-specific) decrease in thyroid hormone signaling.

Although we were unable to find gross differences in BAT pad appearance or size between E18.5 WT and D2KO littermates (data not shown), we sought to detect changes at the transcript level that would shed light on BAT integrity. First, we looked at the expression of genes common to both white and brown adipogenesis, including the anti-adipogenic preadipocyte factor-1 (*Pref1*; also known as *DLK1*) and *Dio3* (both genes are in the same locus) (18-20), and the master transcriptional regulators of adipogenesis CCAAT/enhancer-binding protein-α (*C/EBPα*) and peroxisome proliferator-activated receptor-γ (*PPARγ*) (21). Notably,

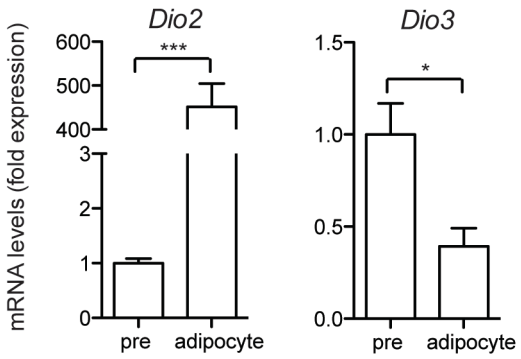

Figure 2.2. Reciprocal changes in deiodinase expression *in vitro*. Expression of *Dio2* and *Dio3* in proliferating brown preadipocytes (pre) and primary adipocytes isolated from BAT (adipocyte), as determined by qRT-PCR. *, $P < 0.05$; and ***, $P < 0.001$ *vs*. preadipocytes by Student's *t* test.

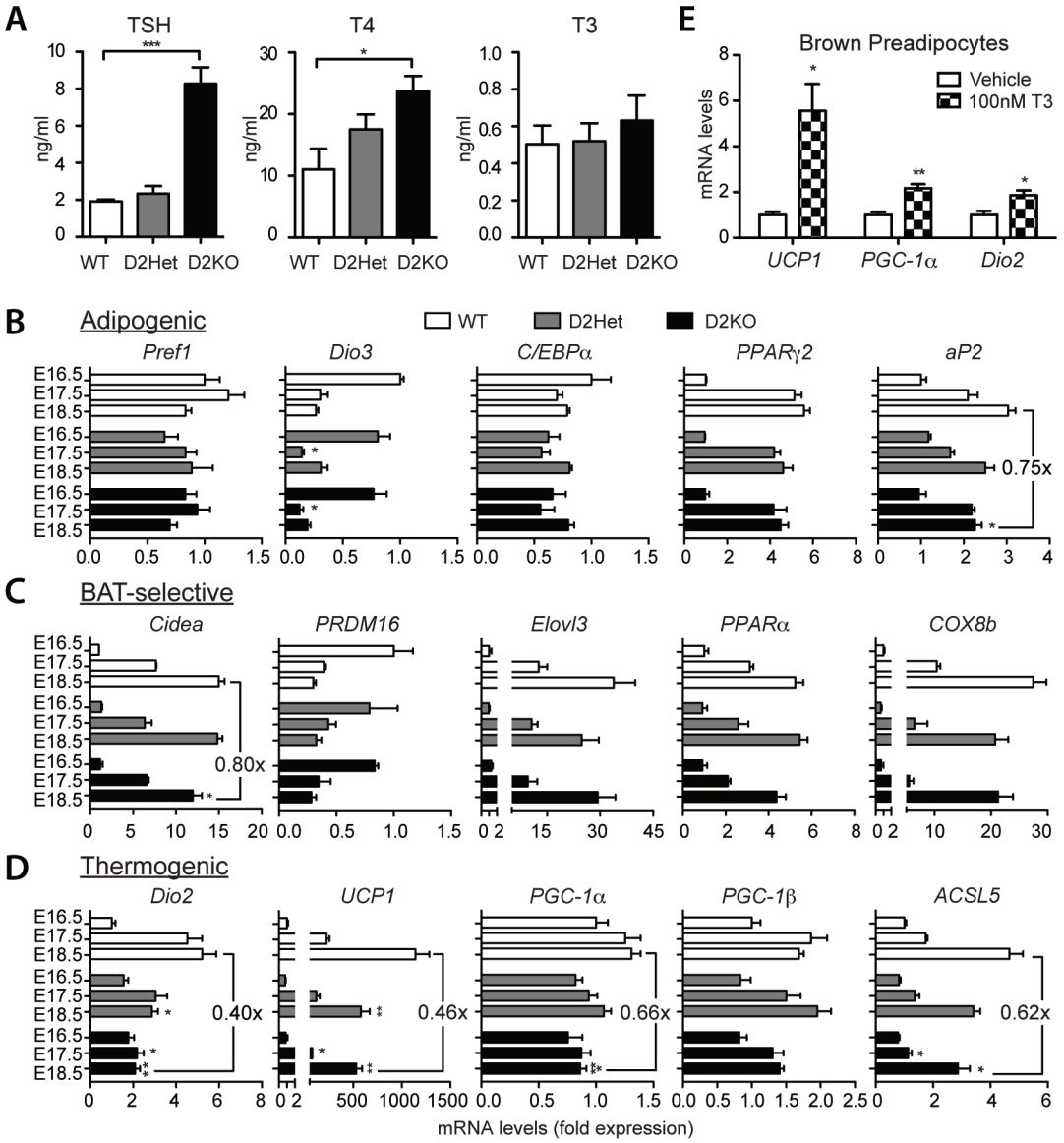

Figure 2.3. D2-generated T3 contributes to brown fat identity. (**A**) Plasma TSH, T4, and T3 concentrations of E18.5 WT (n = 3), D2Het (n = 8), and D2KO (n = 5) E18.5 embryos from 5 litters. (**B–D**) Expression of selective genes in iBAT from WT, D2Het, and D2KO embryos at embryonic day E16.5, E17.5, and E18.5. mRNA levels were determined by qRT-PCR and are graphed relative to E16.5 WT expression. Genes are grouped into (**B**) genes common to both white and brown adipogenesis, (**C**) genes that are specific to BAT, and (**D**) genes that are involved in thermogenesis. *, $P < 0.05$; **, $P < 0.01$; and ***, $p < 0.001$ *vs*. WT of respective day by one-way ANOVA with Dunnett's Multiple Comparison test. (**E**) Gene expression in confluent brown preadipocytes after 24 hours in stripped serum plus vehicle or 100 nM T3. *, $P < 0.05$; and **, $P < 0.01$ by Student's *t* test.

Table 2.1. No gross morphological changes between WT, D2Het, and D2KO embryos.

BODY WEIGHT						
	WT		D2Het		D2KO	
Embryonic Age	Mean ± SEM	n	Mean ± SEM	n	Mean ± SEM	n
E16.5	0.54 ± 0.01	3	0.56 ± 0.02	4	0.54 ± 0.03	3
E17.5	0.99 ± 0.04	4	0.92 ± 0.03	5	1.01 ± 0.03	3
E18.5	1.20 ± 0.03	21	1.20 ± 0.01	39	1.17 ± 0.03	21

CROWN-RUMP LENGTH						
	WT		D2Het		D2KO	
Embryonic Age	Mean ± SEM	n	Mean ± SEM	n	Mean ± SEM	n
E16.5	1.53 ± 0.03	3	1.55 ± 0.04	4	1.53 ± 0.07	3
E17.5	2.00 ± 0.04	4	1.93 ± 0.05	5	1.97 ± 0.03	3
E18.5	2.21 ± 0.03	21	2.23 ± 0.06	39	2.22 ± 0.03	21

Body weight (g) and crown-rump length (cm) measurements made on embryos from several litters that resulted from D2Het matings. Appropriate genotypes were determined post-measurement. Data are expressed as mean ± SEM. Measurement differences between genotypes did not reach significance ($P > 0.05$) by one-way ANOVA with Newman-Keuls Multiple comparison.

while there was a trend for lower expression of *PPARγ2* in the D2KO BAT, the expression of the terminal differentiation marker, *aP2*, which is a target of *PPARγ*, was significantly decreased by E18.5 in D2KO BAT (25% lower than WT) (Figure 2.3B). Second, we looked at genes selective for the molecular signature of brown adipocytes, where we found *Cidea,* which can modulate UCP1 activity (22), to be reduced 20% in D2KO E18.5 BAT, but other genes preferentially expressed in brown *vs*. white adipocytes (*PRDM16*, *Elovl3*, *PPARα*, and *Cox8b*) to be unaffected (Figure 2.3C). Third, we examined the expression of several genes important for the thermogenic function of BAT. *UCP1* increased dramatically during the course of development, but 54% of this induction was lost by E18.5 in D2KO BAT (Figure 2.3D). D2KO mice still express a nonfunctional mRNA of *Dio2* (7), and without D2 activity, the developmental induction of *Dio2* and *PGC-1α* were also significantly blunted (60% and 34% decreased, respectively). *PGC-1β* was slightly decreased in late prenatal D2KO BAT, but this difference did not reach statistical significance. Long-chain acyl-CoA synthetase (*ACSL5*), which plays a role in β-oxidation, was also significantly decreased in D2KO E18.5 BAT (38%). Moreover, BAT from D2Het embryos tended to have an intermediate phenotype, at times behaving more like WT BAT (i.e. expression of *Cidea*), and at other times like D2KO BAT (i.e. expression of *UCP1*), suggesting that BAT impairment is related to dose of the *Dio2* gene. In fact, whereas embryonic D2KO BAT has no D2 activity, heterozygotes have ~50% less D2 activity in BAT compared with WT (data not shown).

Thus, targeted disruption of *Dio2* selectively impairs the expression of key molecules in brown adipogenesis involved in fatty acid metabolism (aP2, Cidea, and ACSL5) and mitochondrial respiration (UCP1, PGC-1α, and D2). To test the hypothesis that these are T3-responsive pathways, we turned to an *in vitro* primary culture model of differentiating brown

preadipocytes, in which differentiation is induced in 10 days driven only by low levels (3 nM) of insulin (Figure 2.4, A–C). These cells are propagated in 10% fetal bovine serum (FBS), which provides physiological levels of thyroid hormone (23). In this setting, induction of *aP2*, *Cidea*, *UCP1*, and *PGC-1α* in D2KO brown adipocytes were progressively less than WT cultures (Figure 2.4D and data not shown). Additionally, *C/EBPα* and *PPARγ2* reached levels lower than 50% of WT by day 10. An expanded search of several downstream targets of *C/EBPα* and *PPARγ2* led to the detection of 13 additional genes with known roles in brown adipocyte function that were insufficiently induced in D2KO cells (Figure 2.4D). Lastly, gene responsiveness to T3 was tested in confluent WT brown preadipocytes exposed to T3 for 24 hours, which resulted in a 5.5-fold induction of *UCP1*, and about 2-fold induction of *PGC-1α* and *Dio2*, confirming direct responsiveness to T3 (Figure 2.3E). On the other hand, prolonged T3 exposure (6 days) caused the additional stimulation of *PPARγ2* and *CEBPα* (data not shown). Taken together, these data indicate a role for D2-generated T3 in BAT development, where the enhanced thyroid hormone signaling provided by intracellular T3 production primes the mature tissue with molecular aspects required for adaptive thermogenesis.

Confirming that these reductions in the expression of T3-responsive genes were detrimentally affecting the differentiation process, the phenotype of the D2KO cells included a delay in the maturation process as assessed by lipid accumulation via immunofluorescence after staining with the lipid-specific dye BODIPY 493/503 (Figure 2.5A). D2KO adipocyte cultures contained a lower fractional number of lipid-containing cells (37% lower at day 10), indicating that fewer D2KO cells terminally differentiate into brown adipocytes at each time-point analyzed (Figure 2.5A). This was verified by flow cytometry (Figure 2.6A) and Oil Red O staining intensity (Figure 2.6B). Notably, these changes are connected with a decrease in thyroid

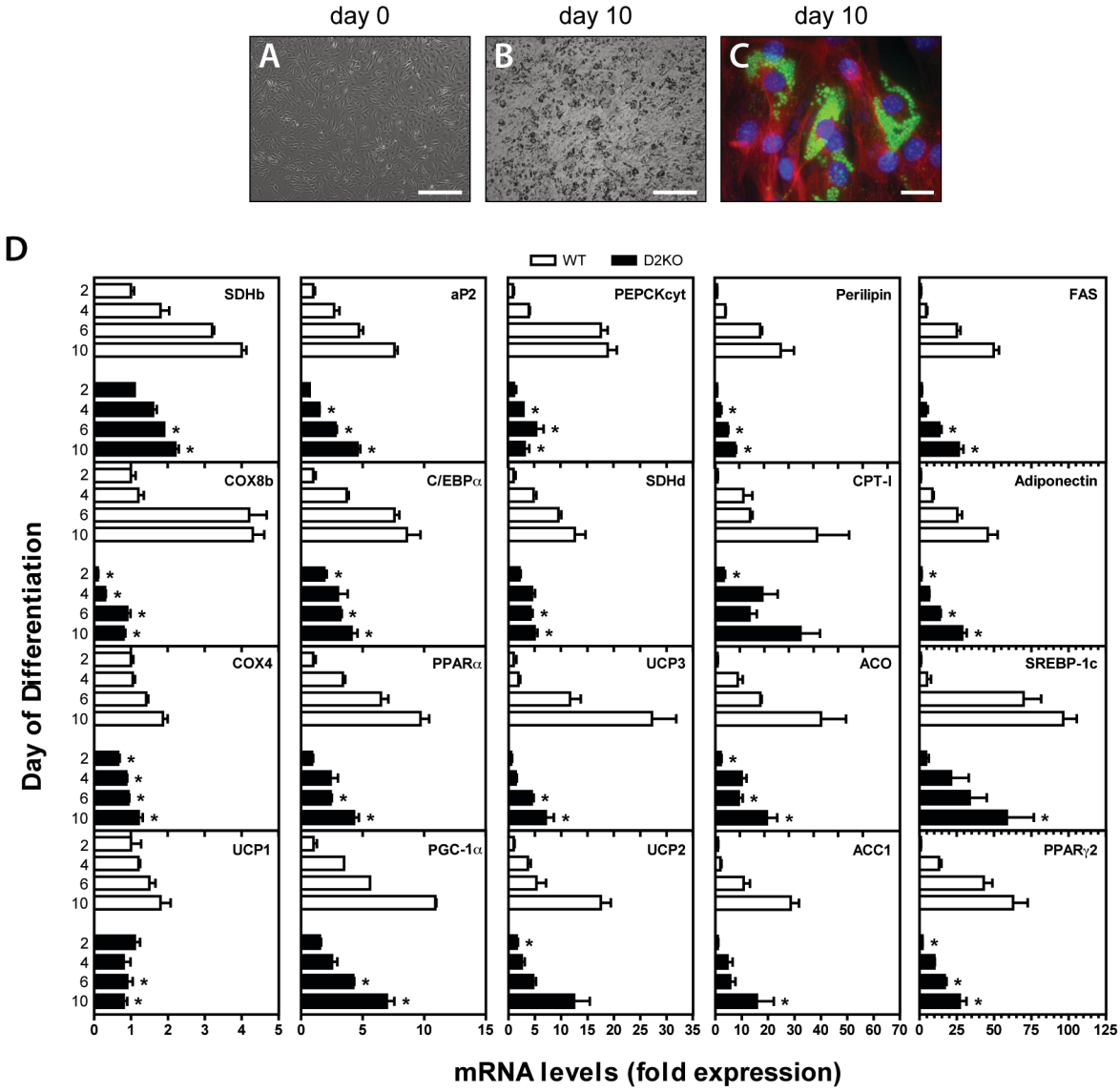

Figure 2.4. Impaired expression during differentiation of D2KO brown adipocyte cultures. (**A**) Bright field imaging of day 0 undifferentiated WT preadipocytes (grayscale image). 10X magnification; bars are 200 μm. (**B**) Oil Red O staining of WT brown adipocytes cultures at day 10 (grayscale image). 60X magnification; bars are 25 μm. (**C**) High magnification immunofluorescent imaging of differentiated adipocytes. Blue: DAPI. Green: BODIPY 493/503. Red: anti-α-Tubulin antibody. (**D**) Relative mRNA levels as quantified by qRT-PCR for the indicated genes during differentiation in WT and D2KO brown adipocyte cultures. All entries were normalized to the respective WT value at day 2. Gene profile at day 10 was similar in another 4 independent experiments. Gene expression was determined by ΔCt method. *, $P < 0.05$ as compared to WT value by Student's *t* test.

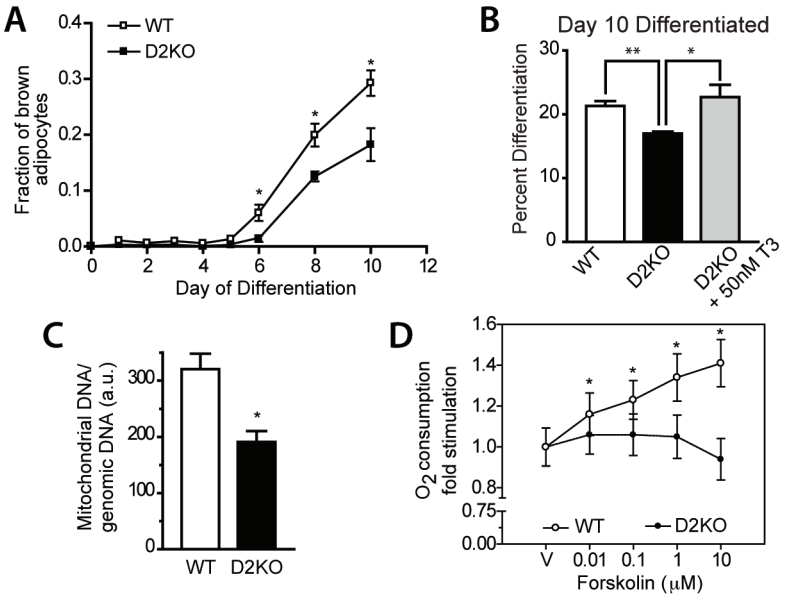

Figure 2.5. Impaired D2KO brown adipocyte differentiation. (**A**) Brown preadipocytes were isolated from iBAT of WT and D2KO mice and differentiated in culture. Percentage of differentiated brown adipocytes determined by immunocytochemistry after staining with BODIPY 493/503. (**B**) Treatment of D2KO preadipocyte cultures with 50 nM T3 during the early stages of differentiation (days 0–4) restores the WT percentage differentiation at day 10. (**C**) Mitochondrial content in WT and D2KO day 10 brown adipocytes by quantification of Cox1/2 and Cox8 gDNA by qRT-PCR, expressed as mitochondrial/genomic DNA ratio. (**D**) O_2 consumption of WT and D2KO day 10 brown adipocyte cultures in response to increasing concentrations of forskolin. (**A–D**) Values are mean ± SEM of 3–30 data points unless otherwise indicated. *, $P < 0.05$; and **, $P < 0.01$ *vs*. WT (or as indicated) by Student's *t* test.

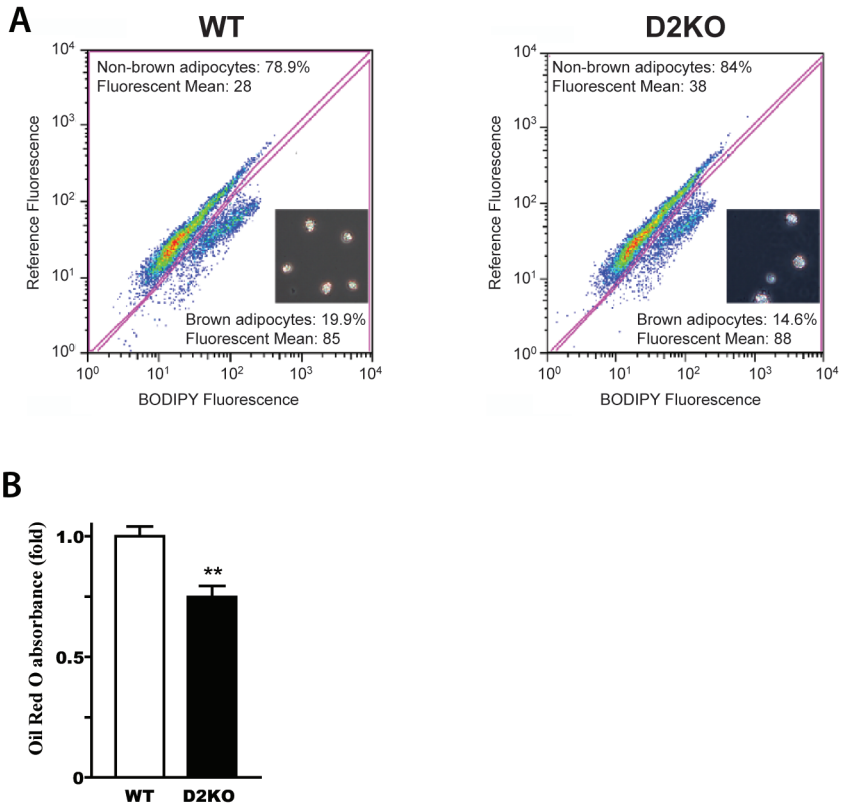

Figure 2.6. Decreased adipogenesis in D2KO brown adipocyte cultures. (**A**) Flow cytometry of WT and D2KO brown adipocytes. Frequency distribution of approximately $3x10^6$ WT or D2KO brown adipocytes as sorted by fluorescence activated cell sorting (FACS) using BODIPY 493/503, a neutral lipid fluorescent dye. Fluorescence intensity is given in arbitrary units. Viability was about 50% for both cell genotypes. D2KO cultures contained approximately 27% fewer mature brown adipocytes. (**B**) Determination of lipid content in day 10 WT and D2KO brown adipocyte cultures. Cultures were stained with Oil Red O and then eluted for measurement of Oil Red O absorbance. **, $P < 0.01$, as measured by Student's *t*-test.

hormone signaling, given the complete rescue of the D2KO phenotype by treatment with 50 nM T3 (Figure 2.5B). If not rescued, the D2KO brown adipocytes have approximately 40% fewer mitochondria (Figure 2.5C) and impaired cAMP-induced oxidative capacity (Figure 2.5D). Using a XF24 instrument that monitors oxygen (O_2) consumption, D2KO brown adipocyte cultures failed to increase O_2 consumption in a wide range of forskolin concentrations (Figure 2.5D). Collectively, these findings indicate a defect in differentiation that results in a substantial impairment in the mature adipocyte function, such as lipid accumulation and oxidative capacity.

D2KO BAT has decreased antioxidant defenses and is susceptible to oxidative stress

As an unbiased approach to elucidate additional transcriptional pathways that underlie the D2KO BAT phenotype, we used microarray analysis of E18.5 BAT from WT and D2KO littermates. This approach confirmed our previous observations (Figure 2.3 and data not shown) and led to additional genes with reported roles in regulation of ROS formation and damage, including *GPx3*, *Mb*, *Msrb2*, and *PKD1*. The expression of these genes (with the exception of *PKD1*) was greatly increased throughout the course of BAT development (Figure 2.7A). Glutathione peroxidase 3 (*GPx3*), which is an antioxidant that is highly expressed in BAT (24), was significantly less (38%) in BAT pads of D2KO mice. Also, reductions of approximately 30% were seen in expression of methionine sulfoxide reductase B2 (*MsrB2*), an enzyme that repairs oxidized proteins and protects against oxidative stress (25), and protein kinase D1 (*PKD1*), which regulates protective signaling in response to ROS (26). Most dramatically, expression of myoglobin (*Mb*) was reduced by 72% in E18.5 D2KO BAT compared with WT. Mb, which is known to increase in BAT during cold exposure (27), plays roles in oxygen

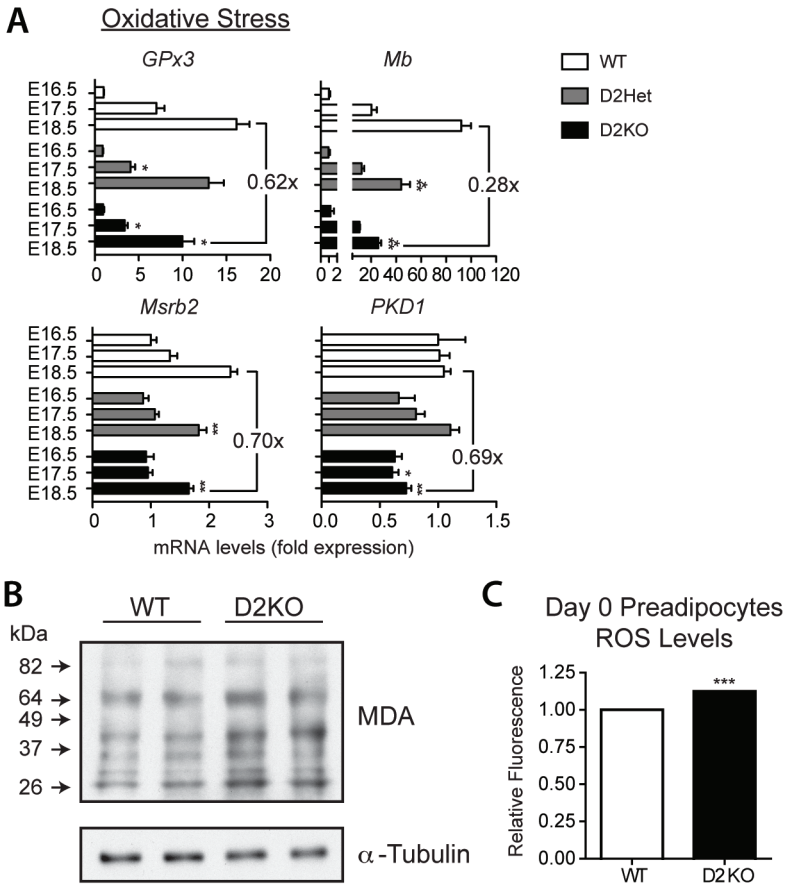

Figure 2.7. Oxidative stress in D2KO embryonic BAT. (**A**) Expression of genes related to oxidative stress response processes in iBAT from WT, D2Het, and D2KO embryos at embryonic day E16.5, E17.5, and E18.5. mRNA levels determined by qRT-PCR are graphed relative to E16.5 WT expression. *, $P < 0.05$; **, $p < 0.01$; and ***, $P < 0.001$ *vs*. WT of respective day by one-way ANOVA with Dunnet's Multiple correction. (**B**) Lipid peroxidation in iBAT lysates from E18.5 WT and D2KO littermates as indicated by immunoblotting for malonaldehyde (MDA). α-Tubulin shown as loading control. (**C**) Average CM-H_2DCFDA fluorescence in day 0 brown preadipocytes after quantification with flow cytometry. ***, $P < 0.001$ by Student's *t* test.

transport and scavenging of ROS (28). Importantly, this decrease in ROS defense coincided with oxidative damage, as evidenced by increased lipid peroxidation end products (as observed by immunoblotting for malondialdehyde) in E18.5 D2KO BAT (Figure 2.7B). These data indicate that the absence of D2 modifies the developing BAT transcriptome, limiting defenses against ROS accumulation and oxidative stress.

To confirm that these changes in gene expression were leading to accumulation of ROS, we incubated *in vitro* differentiated D2KO brown adipocytes with the ROS sensitive dye CM-H_2DCFDA to quantify signal intensity. Indeed, day 10 D2KO brown adipocytes exhibited higher levels of ROS (Figure 2.8). Elevated ROS levels were observed even in D2KO preadipocytes at day 0, a time at which differences based solely on decreased fat cell number could be avoided. Notably, ROS levels in D2KO preadipocytes are already 12.5% higher than WT, suggesting that defects in gene expression are present at early stages of differentiation (Figure 2.7C). In fact, microarray analysis of these preadipocytes identified decreases in genes involved in ROS metabolic processes (Tabe 2.2), which was determined by GeneMAPP2 evaluation to be one of the most significantly altered biological pathways in D2KO brown preadipocytes (Z scores >10, $P < 0.05$; Table 2.2). Collectively, these patterns of altered gene expression indicate that D2KO preadipocytes are at higher risk of developing oxidative stress due to ROS accumulation.

Next, we looked for potential metabolic perturbations downstream of oxidative stress. Specifically, we examined insulin signaling via the PI3K/Akt pathway in D2KO brown preadipocytes, because oxidative stress has been reported to trigger insulin resistance in adipocytes (29). Remarkably, insulin signaling, as determined by an active phosphorylated form of Akt (Ser473), was much lower in D2KO preadipocytes, when exposed to varying levels of insulin (Figure 2.9, A and B). A link between D2 activity and insulin signaling was confirmed by

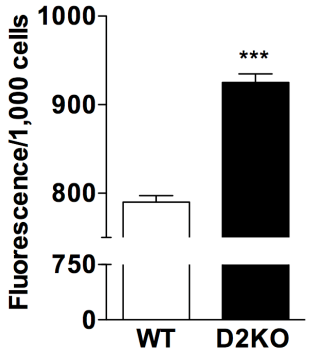

Figure 2.8. Elevated ROS levels in day 10 D2KO brown adipocyte cultures. ROS levels in day 10 differentiated WT and D2KO brown adipocyte cultures were determined by CM-H_2DCFDA fluorescence using confocal microscopy. ***, $P < 0.001$, as measured by Student's *t* test.

Table 2.2. Altered expression of oxygen and ROS metabolic pathways in day 0 D2KO brown preadipocyte cultures.

Gene	WT	D2KO	D2KO/WT Ratio	*P* value
Scd2: stearoyl-Coenzyme A desaturase 2	2926.46	2336.21	-1.25	0.023
Scd1: stearoyl-Coenzyme A desaturase 1	889.52	568.11	-1.57	0.046
Sod3: superoxide dismutase 3, extracellular	1078.11	789.61	-1.37	0.018
Gpx3: glutathione peroxidase 3	10533.44	9247.7	-1.14	0.028

Gene list was generated by use of the dCHIP microarray analysis and GeneMAPP programs, using only genes that had greater than 1.05 fold difference, a P call of > 20%, and were statistically significant. These conditions yielded a false discovery rate (FDR) of 7.9%.

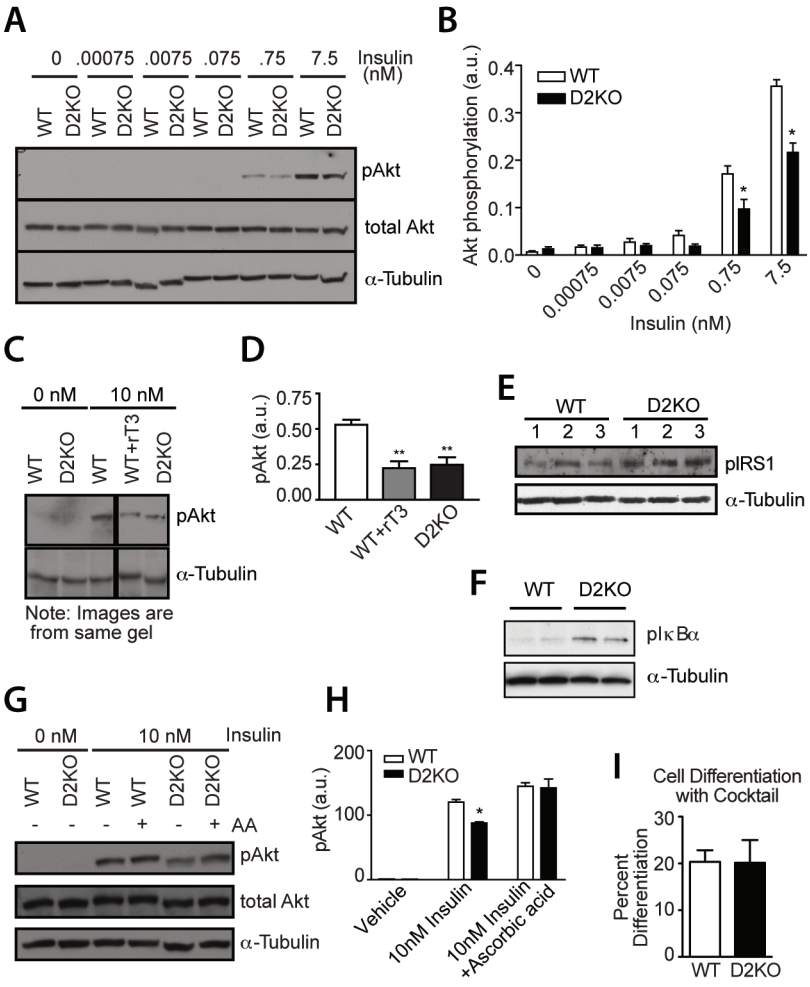

Figure 2.9. ROS causes decreased insulin signaling. (**A–B**) WT and D2KO day 0 brown preadipocytes were serum starved for 20 hours, treated for 5 min with varying doses of insulin, and levels of pAkt (Ser473), total Akt, and α-Tubulin determined by immunoblotting. (**C–D**) Immunoblotting of pAkt (S473) and α-Tubulin in vehicle-treated WT and D2KO preadipocytes, as well as WT preadipocytes treated with rT3 since differentiation. Images are from different regions of same gel. (**E**) Immunoblot analysis of day 0 serum starved WT and D2KO brown preadipocytes for phospho-IRS1 (S307) and α-Tubulin. (**F**) Immunoblot of phosphorylated IκBα in extracts from day 2 WT and D2KO brown preadipocytes. (**G–H**) Treatment with the anti-oxidant ascorbic acid restores phosporylation of pAkt (S473) in D2KO brown preadipocytes to WT levels. (**I**) Analysis of WT and D2KO preadipocytes differentiated with adipogenic cocktail, as described in text. Fractional number of brown adipocytes quantified by immunocytochemistry as previously described. Values are mean ± SEM of 2–4 data points. (**B, D, and H**) Quantification of Akt (Ser473) phosphorylation by normalization to α-Tubulin levels and total signal on each Western blot. Values are mean ± SEM of 3–5 data points. *, $P < 0.05$ by Student's *t* test (**B and H**). **, $P < 0.01$ by one-way ANOVA with Newman-Keuls Multiple Comparison (**D**).

chemically inactivating D2 with rT3 in WT preadipocytes, which produced similar defects in Akt phosphorylation (Figure 2.9, C and D). Oxidative stress can induce insulin resistance through inhibitory phosphorylation of IRS1 by IKK (30, 31). Thus, increased IRS1 Ser307 phosphorylation in D2KO preadipocytes (Figure 2.9E) without changing expression of key insulin signaling components (Figure 2.10, A and B) suggests that oxidative stress leads to the decreased insulin signaling. This is corroborated by increased IκBα phosphorylation (Figure 2.9F), which is a downstream effector of IKK and consistent with NFκB activation upon cellular stress. Finally, we treated WT and D2KO cells with the anti-oxidant ascorbic acid, which rescued insulin signaling in the D2KO to WT levels, indicating that elevated levels of ROS lead to decreased insulin signaling in these cells (Figure 2.9, G and H).

Supplemental insulin (3 nM) is the predominant force driving adipogenesis in our *in vitro* model, so we hypothesized that the defective differentiation phenotype that is observed in the D2KO cells could be due to disruption of insulin signaling. In fact, this is confirmed by experiments in which differentiation was carried out in the absence of supplemental insulin, but rather with an adipogenic cocktail (IBMX, dexamethasone, and indomethacin) for two days. In this setting, differences in the relative number of mature brown adipocytes between WT and D2KO cells were dissipated (Figure 2.9I). These findings suggest that other stimuli present during BAT development may bypass a more severe defect in brown adipogenesis, such as the differentiation phenomenon that is observed when insulin alone is pushing the conversion of preadipocytes to brown adipocytes.

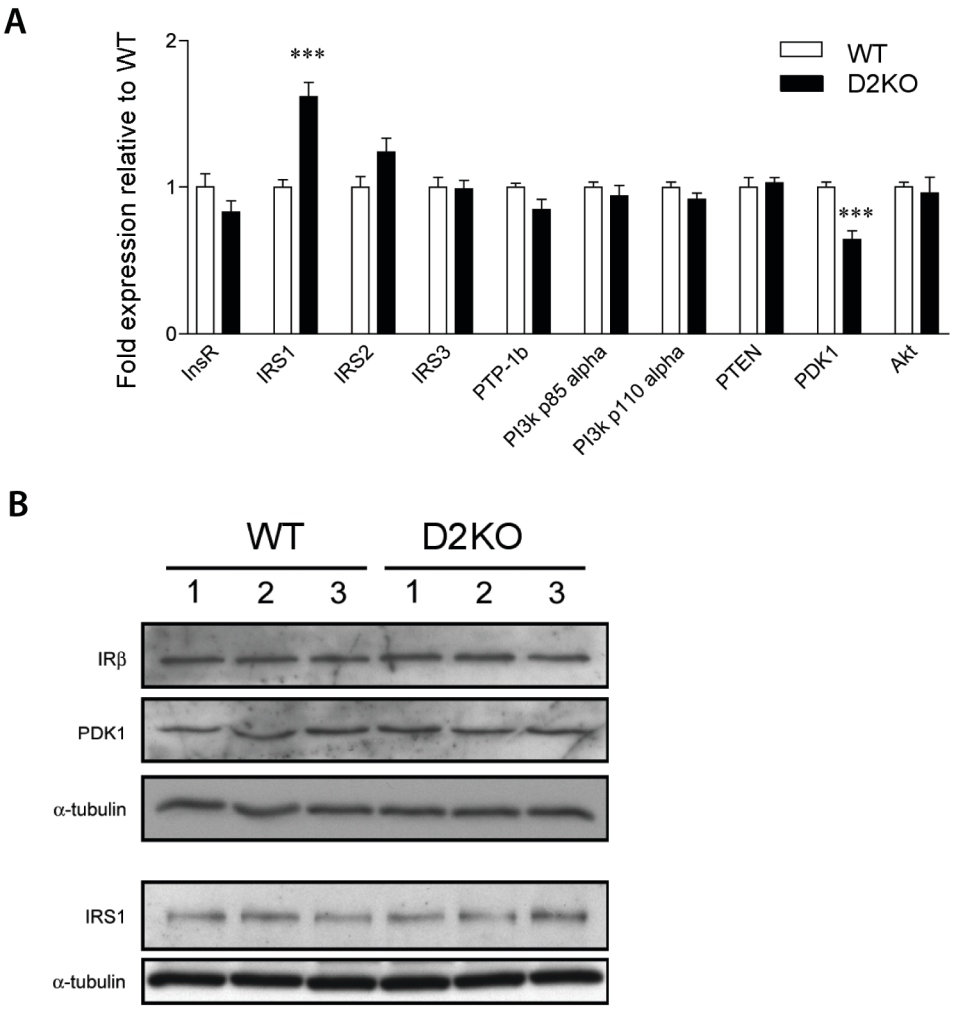

Figure 2.10. Insulin signaling components unchanged in D2KO brown preadipocytes. (**A**) Expression of insulin signaling genes in D2KO brown preadipocytes. Relative mRNA levels as quantified by qRT-PCR for the major indicated insulin signaling components at day 0 of the differentiation process. All entries were normalized to the respective WT value. Values are mean ± SEM of at least 4 data points. ***, $P < 0.001$ as compared to WT value by Student's *t* test. (**B**) Protein levels of insulin signaling genes in D2KO brown preadipocytes. Immunoblotting of insulin signaling components whose expression was different in D2KO brown preadipocytes according to qRT-PCR in A, as well as the insulin receptor β. No difference in protein levels was observed.

DISCUSSION

The present study demonstrates that impaired BAT thermogenesis in the D2KO mouse stems from an embryologic defect due to a role played by D2-generated T3 in enhancing the expression of BAT-selective genes. Notably, these changes in gene expression are observed *in utero*, without a thermogenic challenge, which highlights the relevance of D2 and its ability to amplify thyroid hormone signaling in a developmental setting. As BAT develops, coordinated changes in deiodinase expression (*Dio2* induction and *Dio3* suppression) enhance thyroid hormone signaling (Figure 2.1, C–F), which can be linked to peak T3 concentration in developing BAT (32). A similar mechanism has been shown in other developing tissues, including the coordinated expression of D2 and D3 at a critical period of cochlear development in mammals, where absence of either deiodinase leads to inappropriate exposure to T3 and results in deafness (10, 33, 34). Our data indicate that this deiodinase-based mechanism plays a hitherto under-appreciated role in the developing BAT.

The process of brown adipocyte differentiation involves molecular pathways that are common to both white and brown adipocyte lineages and pathways that are BAT-specific, including transcriptional changes that confer its thermogenic function (35). It is well established that thyroid hormone plays a role in adipogenesis *per se*. T3 is frequently used in adipogenic cocktails and is absolutely required for terminal differentiation, possibly through regulation of PPARγ (36, 37). What is remarkable and evidenced by our data are that the deiodinases, by increasing thyroid hormone signaling, can affect BAT development without changing the extracellular levels of thyroid hormone. The inactivation of a single component of this mechanism (i.e. D2) results in embryonic BAT with decreased expression of key thermogenic genes, without gross impairments in the adipogenic process (Figure 2.3, B–D). Only with *in vitro*

differentiated D2KO brown preadipocytes do we find defective differentiation, suggesting the existence of potent *in vivo* compensatory mechanisms. The key aspect here is that D2 is necessary for coordinating the expression of genes that contribute to the identity of BAT *in vivo*, and, thus, plays a role in its thermogenic capacity. In fact, when fetal D2 activity is blocked by iopanoic acid treatment of pregnant mothers, newborn rats show a blunted response to thermal stress upon birth (17).

Given that T3-TR modifies gene expression, we show that brown preadipocytes exposed to T3 have increased expression of *UCP1*, *Dio2*, and *PGC-1α*, transcripts found to be decreased in D2KO embryonic BAT (Figure 2.3, D and E). In a variety of settings, *UCP1*, *Dio2*, and *PGC-1α* have been shown to be T3-responsive genes (2, 11, 38, 39) and have been independently linked to BAT function. Additionally, PGC-1α is a partner of PPARγ and TRβ in coactivating the *UCP1* promoter (40) and is necessary for the increased expression of *UCP1* and *Dio2* after stimulation with a cyclic AMP agonist (41). The novelty of our findings is that the expression of these three genes is interconnected during BAT development, with D2 generating T3 that will further enhance its own production and induce PGC-1α and UCP1 in a positive feedback loop (Figure. 2.11). Notably, brown adipocytes deficient in PGC-1α exhibit a relatively normal transcriptome with defects lying primarily in thermogenic activation by cAMP (41). This is a milder phenotype than that of D2KO cells, emphasizing a predominant role for D2 in BAT development.

Embryonic BAT lacking D2-generated T3 is more susceptible to oxidative damage, which results from uncontrolled oxidative stress by a decrease in anti-ROS defenses (Figure 2.7, A and B). However, acute T3-responsiveness was not found in the subset of ROS-detoxifying genes perturbed in the D2KO BAT (data not shown). PGC-1α has been shown to be a critical

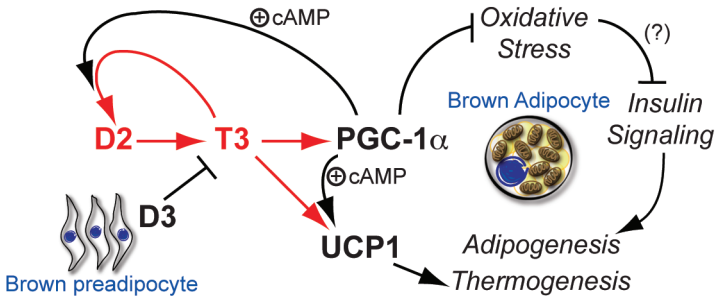

Figure 2.11. Proposed model of positive feedback involving *Dio2*, *PGC-1α*, and *UCP1* expression during BAT development. Schematic representation of the proposed role of D2 and D2-generated T3 in the development of brown adipocytes. D3, which decreases thyroid hormone signaling, is highest in the undeveloped brown preadipocyte. As the brown preadipocyte matures, D2, by enhancing thyroid hormone signaling, increases expression of *PGC-1α*, which coactivates TR, leading to enhanced *UCP1* expression. Notably, *Dio2* is also upregulated by increased T3-signaling. These changes provide the mature brown adipocyte with its thermogenic function and also limit oxidative stress. If oxidative stress goes unchecked, then insulin signaling and adipogenesis may be altered.

regulator of ROS detoxification through induction of ROS-scavenging enzymes (42). Thus, D2 could play a role upstream of PGC-1α, where D2 generating T3 induces PGC-1α, turning on an anti-ROS gene program. While it is not possible yet to conclude whether oxidative damage in D2KO E18.5 BAT contributes toward decreased insulin signaling *in vivo*, our *in vitro* D2KO brown preadipocyte data strongly suggest that under the appropriate conditions ROS leads to decreased insulin signaling and impaired differentiation. It is interesting to speculate that such mechanisms could also play a role in other settings in which *Dio2* and *PGC-1α* are highly expressed, such as the brain.

Our analysis of the mechanisms underlying impaired thermogenic function of D2KO BAT has led us to the identification of a critical deiodinase-mediated pathway in BAT development. This explains the hypothermic and obesity phenotype observed in adult D2KO mice. It is clear that D2 acts on an important aspect of brown adipocyte biology (i.e. BAT identity) but other pathways might also be involved (i.e. protection from oxidative damage). Here we identified a developmental relationship between D2-generated T3, UCP1, and PGC-1α in the absence of a thermogenic stimulus (Figure 2.11). Uncovering this connection illustrates how such a pathway is critical for maintenance of energy homeostasis in adulthood.

ACKNOWLEDGEMENTS

We are grateful for the technical assistance of Matthew Rosene and Kevin Johnson (Diabetes Research Institute Immunohistochemistry Core). We would also like to acknowledge Jack Y. Lee and Christine Knoblauch for assistance in cell preparation for FACS analysis. This work was supported in part by National Institutes of Health Grant DK65055 and by Dana-Farber Microarray Core Facility.

REFERENCES

1. **Nedergaard J, Cannon B** 2010 The Changed Metabolic World with Human Brown Adipose Tissue: Therapeutic Visions. Cell Metabolism 11:268-272

2. **Bianco AC, Sheng XY, Silva JE** 1988 Triiodothyronine amplifies norepinephrine stimulation of uncoupling protein gene transcription by a mechanism not requiring protein synthesis. J Biol Chem 263:18168-18175

3. **Sellers EA, You SS** 1950 Role of the thyroid in metabolic responses to a cold environment. Am J Physiol 163:81-91

4. **Bianco AC, Silva JE** 1987 Intracellular conversion of thyroxine to triiodothyronine is required for the optimal thermogenic function of brown adipose tissue. J Clin Invest 79:295-300

5. **Gereben B, Zavacki AM, Ribich S, Kim BW, Huang SA, Simonides WS, Zeold A, Bianco AC** 2008 Cellular and molecular basis of deiodinase-regulated thyroid hormone signaling. Endocr Rev 29:898-938

6. **Simonides WS, Mulcahey MA, Redout EM, Muller A, Zuidwijk MJ, Visser TJ, Wassen FW, Crescenzi A, da-Silva WS, Harney J, Engel FB, Obregon MJ, Larsen PR, Bianco AC, Huang SA** 2008 Hypoxia-inducible factor induces local thyroid hormone inactivation during hypoxic-ischemic disease in rats. J Clin Invest 118:975-983

7. **Schneider MJ, Fiering SN, Pallud SE, Parlow AF, St Germain DL, Galton VA** 2001 Targeted disruption of the type 2 selenodeiodinase gene (DIO2) results in a phenotype of pituitary resistance to T4. Mol Endocrinol 15:2137-2148

8. **de Jesus LA, Carvalho SD, Ribeiro MO, Schneider M, Kim SW, Harney JW, Larsen PR, Bianco AC** 2001 The type 2 iodothyronine deiodinase is essential for adaptive thermogenesis in brown adipose tissue. J Clin Invest 108:1379-1385

9. **Christoffolete MA, Linardi CC, de Jesus L, Ebina KN, Carvalho SD, Ribeiro MO, Rabelo R, Curcio C, Martins L, Kimura ET, Bianco AC** 2004 Mice with targeted disruption of the Dio2 gene have cold-induced overexpression of the uncoupling protein 1 gene but fail to increase brown adipose tissue lipogenesis and adaptive thermogenesis. Diabetes 53:577-584

10. **Ng L, Hernandez A, He W, Ren T, Srinivas M, Ma M, Galton VA, St Germain DL, Forrest D** 2009 A protective role for type 3 deiodinase, a thyroid hormone-inactivating enzyme, in cochlear development and auditory function. Endocrinology 150:1952-1960

11. **Martinez-deMena R, Hernandez A, Obregon MJ** 2002 Triiodothyronine is required for the stimulation of type II 5'-deiodinase mRNA in rat brown adipocytes. Am J Physiol Endocrinol Metab 282:E1119-1127

12. **Watanabe M, Houten SM, Mataki C, Christoffolete MA, Kim BW, Sato H, Messaddeq N, Harney JW, Ezaki O, Kodama T, Schoonjans K, Bianco AC, Auwerx J** 2006 Bile acids induce energy expenditure by promoting intracellular thyroid hormone activation. Nature 439:484-489

13. **Bae YS, Kang SW, Seo MS, Baines IC, Tekle E, Chock PB, Rhee SG** 1997 Epidermal growth factor (EGF)-induced generation of hydrogen peroxide. Role in EGF receptor-mediated tyrosine phosphorylation. J Biol Chem 272:217-221

14. **Koopman R, Schaart G, Hesselink MK** 2001 Optimisation of oil red O staining permits combination with immunofluorescence and automated quantification of lipids. Histochemistry & Cell Biology 116:63-68

15. **Li C, Wong WH** 2001 Model-based analysis of oligonucleotide arrays: expression index computation and outlier detection. Proc Natl Acad Sci U S A 98:31-36

16. **Salomonis N, Hanspers K, Zambon AC, Vranizan K, Lawlor SC, Dahlquist KD, Doniger SW, Stuart J, Conklin BR, Pico AR** 2007 GenMAPP 2: new features and resources for pathway analysis. BMC Bioinformatics 8:217

17. **Giralt M, Martin I, Iglesias R, Vinas O, Villarroya F, Mampel T** 1990 Ontogeny and perinatal modulation of gene expression in rat brown adipose tissue. Unaltered iodothyronine 5'-deiodinase activity is necessary for the response to environmental temperature at birth. Eur J Biochem 193:297-302

18. **Smas CM, Sul HS** 1993 Pref-1, a protein containing EGF-like repeats, inhibits adipocyte differentiation. Cell 73:725-734

19. **Lin SP, Youngson N, Takada S, Seitz H, Reik W, Paulsen M, Cavaille J, Ferguson-Smith AC** 2003 Asymmetric regulation of imprinting on the maternal and paternal chromosomes at the Dlk1-Gtl2 imprinted cluster on mouse chromosome 12. Nat Genet 35:97-102

20. **Hernandez A, Garcia B, Obregon MJ** 2007 Gene expression from the imprinted Dio3 locus is associated with cell proliferation of cultured brown adipocytes. Endocrinology 148:3968-3976

21. **Farmer SR** 2006 Transcriptional control of adipocyte formation. Cell Metab 4:263-273

22. **Zhou Z, Yon Toh S, Chen Z, Guo K, Ng CP, Ponniah S, Lin SC, Hong W, Li P** 2003 Cidea-deficient mice have lean phenotype and are resistant to obesity. Nat Genet 35:49-56

23. **Samuels HH, Tsai JS** 1973 Thyroid hormone action in cell culture: domonstration of nuclear receptors in intact cells and isolated nuclei. Proc Natl Acad Sci U S A 70:3488-3492

24. **Lee YS, Kim AY, Choi JW, Kim M, Yasue S, Son HJ, Masuzaki H, Park KS, Kim JB** 2008 Dysregulation of adipose glutathione peroxidase 3 in obesity contributes to local and systemic oxidative stress. Mol Endocrinol 22:2176-2189

25. **Cabreiro F, Picot CR, Perichon M, Castel J, Friguet B, Petropoulos I** 2008 Overexpression of mitochondrial methionine sulfoxide reductase B2 protects leukemia cells from oxidative stress-induced cell death and protein damage. J Biol Chem 283:16673-16681

26. **Storz P** 2007 Mitochondrial ROS--radical detoxification, mediated by protein kinase D. Trends Cell Biol 17:13-18

27. **Watanabe M, Yamamoto T, Kakuhata R, Okada N, Kajimoto K, Yamazaki N, Kataoka M, Baba Y, Tamaki T, Shinohara Y** 2008 Synchronized changes in transcript levels of genes activating cold exposure-induced thermogenesis in brown adipose tissue of experimental animals. Biochim Biophys Acta 1777:104-112

28. **Ordway GA, Garry DJ** 2004 Myoglobin: an essential hemoprotein in striated muscle. J Exp Biol 207:3441-3446

29. **Houstis N, Rosen ED, Lander ES** 2006 Reactive oxygen species have a causal role in multiple forms of insulin resistance. Nature 440:944-948

30. **Bloch-Damti A, Potashnik R, Gual P, Le Marchand-Brustel Y, Tanti JF, Rudich A, Bashan N** 2006 Differential effects of IRS1 phosphorylated on Ser307 or Ser632 in the induction of insulin resistance by oxidative stress. Diabetologia 49:2463-2473

31. **Gao Z, Hwang D, Bataille F, Lefevre M, York D, Quon MJ, Ye J** 2002 Serine phosphorylation of insulin receptor substrate 1 by inhibitor kappa B kinase complex. J Biol Chem 277:48115-48121

32. **Carmona MC, Iglesias R, Obregon MJ, Darlington GJ, Villarroya F, Giralt M** 2002 Mitochondrial biogenesis and thyroid status maturation in brown fat require CCAAT/enhancer-binding protein alpha. J Biol Chem 277:21489-21498

33. **Campos-Barros A, Amma LL, Faris JS, Shailam R, Kelley MW, Forrest D** 2000 Type 2 iodothyronine deiodinase expression in the cochlea before the onset of hearing. Proceedings of the National Academy of Sciences of the United States of America 97:1287-1292

34. **Ng L, Goodyear RJ, Woods CA, Schneider MJ, Diamond E, Richardson GP, Kelley MW, Germain DL, Galton VA, Forrest D** 2004 Hearing loss and retarded cochlear development in mice lacking type 2 iodothyronine deiodinase. Proceedings of the National Academy of Sciences of the United States of America 101:3474-3479

35. **Kajimura S, Seale P, Spiegelman BM** 2010 Transcriptional control of brown fat development. Cell Metab 11:257-262

36. **Ying H, Araki O, Furuya F, Kato Y, Cheng SY** 2007 Impaired adipogenesis caused by a mutated thyroid hormone alpha1 receptor. Mol Cell Biol 27:2359-2371

37. **Ailhaud G, Dani C, Amri EZ, Djian P, Vannier C, Doglio A, Forest C, Gaillard D, Negrel R, Grimaldi P** 1989 Coupling growth arrest and adipocyte differentiation. Environ Health Perspect 80:17-23

38. **Irrcher I, Adhihetty PJ, Sheehan T, Joseph AM, Hood DA** 2003 PPARgamma coactivator-1alpha expression during thyroid hormone- and contractile activity-induced mitochondrial adaptations. Am J Physiol Cell Physiol 284:C1669-1677

39. **Weitzel JM, Radtke C, Seitz HJ** 2001 Two thyroid hormone-mediated gene expression patterns in vivo identified by cDNA expression arrays in rat. Nucleic Acids Res 29:5148-5155

40. **Puigserver P, Wu Z, Park CW, Graves R, Wright M, Spiegelman BM** 1998 A cold-inducible coactivator of nuclear receptors linked to adaptive thermogenesis. Cell 92:829-839

41. **Uldry M, Yang W, St-Pierre J, Lin J, Seale P, Spiegelman BM** 2006 Complementary action of the PGC-1 coactivators in mitochondrial biogenesis and brown fat differentiation. Cell Metab 3:333-341

42. **St-Pierre J, Drori S, Uldry M, Silvaggi JM, Rhee J, Jager S, Handschin C, Zheng K, Lin J, Yang W, Simon DK, Bachoo R, Spiegelman BM** 2006 Suppression of reactive oxygen species and neurodegeneration by the PGC-1 transcriptional coactivators. Cell 127:397-408

Chapter 3

Disruption of thyroid hormone activation in type 2 deiodinase knockout mice causes obesity with glucose intolerance and liver steatosis only at thermoneutrality

AUTHOR CONTRIBUTIONS

The data in this chapter resulted from a collaborative effort. I played a large role in conceptualizing the experiments for this chapter with help from Antonio Bianco. I conceived the indirect calorimetry studies and the high-fat diet at thermoneutrality experiments. Cintia Ueta and I assisted Melany Castillo with the bulk of these experiments. I performed all body composition analyses by dual-energy X-ray absorptiometry. Also, I analyzed the biochemical data of liver triglycerides from mice on chow diet at room temperature with Hye Won Kang of David Cohen's laboratory. Melany Castillo and Cintia Ueta performed the remaining biochemical analyses under my guidance and direction. Hye Won Kang and David Cohen helped to interpret the liver triglyceride data. Mayrin Correa-Medina conducted the glucose tolerance tests and performed Oil Red O staining of liver sections. Melany Castillo, Antonio Bianco, and I completed data interpretation and wrote the manuscript with editorial suggestions from all authors.

Disruption of Thyroid Hormone Activation in Type 2 Deiodinase Knockout Mice Causes Obesity with Glucose Intolerance and Liver Steatosis Only at Thermoneutrality

Melany Castillo[1†], Jessica A. Hall[2†], Mayrin Correa-Medina[1], Cintia Ueta[1], Hye Won Kang[3], David E. Cohen[3], and Antonio C. Bianco[1]

A similar version of this work has been published

Diabetes 60(4), April 2011, pp1082–1089

[1]Division of Endocrinology, Diabetes and Metabolism, University of Miami Miller School of Medicine, Miami, FL 33136; [2]Biological and Biomedical Sciences Program, Harvard Medical School, Boston, MA 02115; and [3]Department of Medicine, Division of Gastroenterology, Brigham and Women's Hospital, Harvard Medical School, Boston, MA 02115.

[†]These authors contributed equally to this work.

ABSTRACT

Objective: Thyroid hormone accelerates energy expenditure; thus, hypothyroidism is intuitively associated with obesity. However, studies failed to establish such a connection. In brown adipose tissue (BAT), thyroid hormone activation via type 2 deiodinase (D2) is necessary for adaptive thermogenesis, such that mice lacking D2 (D2KO) exhibit an impaired thermogenic response to cold. Here we investigate whether the impaired thermogenesis of D2KO mice increases their susceptibility to obesity when placed on a high-fat diet.

Research design and methods: To test this, D2KO mice were admitted to a comprehensive monitoring system acclimatized to room temperature (22°C) or thermoneutrality (30°C) and kept either on chow or high-fat diet for 60 days.

Results: At 22°C, D2KO mice preferentially oxidize fat, have a similar sensitivity to diet-induced obesity, and are supertolerant to glucose. However, when thermal stress is eliminated at thermoneutrality (30°C), an opposite phenotype is encountered, one that includes obesity, glucose intolerance, and exacerbated hepatic steatosis. We suggest that a compensatory increase in BAT sympathetic activation of the D2KO mice masks metabolic repercussions that they would otherwise exhibit.

Conclusions: Thus, upon minimization of thermal stress, high-fat feeding reveals the defective capacity of D2KO mice for diet-induced thermogenesis, provoking a paradigm shift in the understanding of the role of the thyroid hormone in metabolism.

INTRODUCTION

Obesity results as the consequence of a positive energy balance, where energy intake is greater than energy expended. One of the key molecules in this balance is thyroid hormone, which potently accelerates the resting energy expenditure (1, 2). The adaptive (cold-induced) energy expenditure is controlled by the sympathetic nervous system and is also accelerated by thyroid hormone. In response to cold exposure, the sympathetic nervous system stimulates brown adipose tissue (BAT) and activates uncoupling protein 1 (UCP1) (3), which is transcriptionally upregulated by thyroid hormone (4). In addition, the sympathetic nervous system also stimulates the cAMP-inducible type 2 deiodinase (D2) that amplifies thyroid hormone signaling in BAT by locally converting the prohormone T4 to the active form of thyroid hormone, T3 (5). Disruption of this pathway, as in mice with targeted inactivation of D2 [D2 knockout (D2KO) mice], leads to impaired BAT thermogenesis and hypothermia during cold exposure (6, 7).

Sympathetic activity to BAT is also augmented by high-fat feeding (8), leading to diet-induced thermogenesis, but the role played by thyroid hormone in this process is largely unclear. Although there is an intuitive assumption that hypothyroid individuals/animals tend to be obese, the compilation of a vast array of data from individuals transitioning from hypo- to hyperthyroidism and vice versa exhibits only minor changes in body composition (9-11). In fact, we have reported earlier that hypothyroid rats living at room temperature placed on a high-fat diet do not accumulate more fat than euthyroid controls (12), questioning a role for thyroid hormone in this pathway.

However, it is conceivable that compensatory mechanisms activated during hypothyroidism may obscure the relevance (if any) of thyroid hormone on diet-induced thermogenesis. In this case, such mechanisms are likely to stem from the sympathetic nervous

system, given that sympathetic activity fluctuates in an opposite direction as thyroid hormone signaling (13-15). In fact, the BAT-specific decrease in thyroid hormone signaling seen in the D2KO mouse is sufficient to trigger a compensatory increase in BAT sympathetic activity during cold exposure, upregulating a series of T3-responsive metabolic parameters in the tissue, including UCP1 mRNA levels (7).

Here, we report that even at room temperature there is a chronic increase in BAT sympathetic activity. We suggest that this activity compensates for the decreased thyroid hormone signaling, thus masking profound metabolic alterations in D2KO mice. If reared at 22°C, D2KO mice have increased tolerance to glucose and gain the same weight as controls on a high-fat diet. However, when the increase in BAT sympathetic activity is minimized by rearing animals at 30°C, D2KO mice develop intolerance to glucose and become more susceptible to diet-induced obesity. Remarkably, a consistent feature of the D2KO mice, independent of ambient temperature, is liver steatosis, which becomes most severe under high-fat feeding after acclimatization to thermoneutrality. Thus, these results provoke a paradigm shift in the understanding of the role of the thyroid hormone in metabolism, uncovering a hitherto unrecognized function for thyroid hormone in prevention of obesity and its metabolic complications.

MATERIALS AND METHODS

Animals

All studies were performed under a protocol approved by the local Institutional Animal Care and Use Committee. C57BL/6J and D2KO (7) mice approximately 3 months old were used from our established colonies, kept at room temperature (22°C) or at thermoneutrality (30°C;

Columbus Instruments, Columbus, OH), with a 12-hour dark/light cycle starting at 0600 hours, and housed in standard plastic cages with four male mice per cage. Animals were kept on standard chow diet (3.5 kcal/g; 28.8% protein, 58.5% carbohydrate, 12.7% fat) (5010 LabDiet laboratory autoclavable rodent diet; PMI Nutrition, Richmond, IN) or a high-fat diet (4.5 kcal/g; 15.3% protein, 42.7% carbohydrate, 42% fat) (TD 95121; Harlan Teklad, Indianapolis, IN) as indicated. Twenty-four-hour caloric intake was measured at the indicated times using the Oxymax Feed Scale device (Columbus Instruments). At the appropriate times, animals were killed with carbon dioxide. Tissue samples were obtained and immediately snap-frozen for further analyses.

Body composition

Lean body mass (LBM) and fat mass were determined by dual-energy X-ray absorptiometry (DEXA; Lunar Pixi, Janesville, WI). For the procedure, mice were anesthetized with ketamine-xylazine (200 mg/kg and 7–20 mg/kg) before imaging.

Indirect calorimetry

Oxygen consumption (VO_2) and respiratory exchange ratio (RER) were continuously measured using the Oxymax System 4.93 (C.L.A.M.S.; Columbus Instruments). The animals were placed in the C.L.A.M.S. with free access to food and water, allowing them to acclimatize in individual metabolic cages for 48 hours before any measurements. Subsequently, 24-hour metabolic profiles were generated in successive 14-min cycles. VO_2 was expressed as milliliters per kilogram LBM per minute. Studies were performed at 30°C or 22°C for the indicated times. The sensor was calibrated against a standard gas mix containing defined quantities of O_2 and

CO_2. All analyses for VO_2 and RQ were made considering the area under the curve (i.e. VO_2 vs. time; respiratory quotient [RQ] *vs*. time) for each individual animal.

Glucose tolerance test

Tolerance to a glucose load was studied in overnight fasted live mice following intraperitoneal injection of 1 g/kg glucose. Blood samples were obtained from the tail vein and measured with Glucometer Elite (Bayer Tarrytown, NY) at different time points.

mRNA analysis

Total RNA was extracted using the RNeasy kit (Qiagen, Valencia, CA) according to the manufacturer's instructions, quantified with a Nano-Drop spectrophotometer and 2.5 μg reverse-transcribed into cDNA by using a high capacity cDNA reverse transcription kit (Applied Biosystems, Foster City, CA). Genes of interest were measured by quantitative RT-PCR (Bio-Rad iCycler iQ Real-Time PCR Detection System; Bio-Rad Laboratories Hercules, CA) using the iQ SYBR Green Supermix (Bio-Rad Laboratories) with the following conditions: 15 min at 94°C (Hot Start), 30–50 sec at 94°C, 30–50 sec at 55–60°C, and 45–60 sec at 72°C for 40 cycles. A final extension at 72°C for 5 min was performed as well as the melting curve protocol to verify the specificity of the amplicon generation. Standard curves consisting of four to five points of serial dilution of mixed experimental and control groups cDNA were prepared for each assay. *Cyclophilin A* was used as a housekeeping internal control gene. The coefficient of correlation (r^2) was >0.98 for all standard curves, and the amplification efficiency varied between 80 and 110%. Results are expressed as ratios of test mRNA to *Cyclophilin A* mRNA.

Interscapular BAT norepinephrine turnover

Interscapular BAT (IBAT) norepinephrine (NE) turnover was measured in mice acclimatized at 22°C or at 30°C. Mice were anesthetized with urethane (1.2 g/kg i.p.) and given 300 mg/kg α-methyl parathyrosine (α-MT) to block NE synthesis as described (7). Mice were killed at 0, 1, 2, 3, or 4 hours after the α-MT injection, and the IBAT was processed for NE measurement by radioimmunoassay (Alpco Diagnostics, Windham, NH).

Biochemical analyses

Immediately after mice were killed, liver fragments were obtained and fixed in 4% paraformaldehyde in 0.1 mL PBS for 24 hours at 4°C, frozen, sectioned, stained with Oil Red O, and counterstained with Meyer's hematoxylin. Frozen liver fragments (~200 mg) were homogenized, and lipids were extracted using chloroform/methanol (2:1) and 0.05% sulfuric acid as described (16). An aliquot of the organic phase was collected and mixed with chloroform containing 1% Triton X-100, dried under nitrogen stream, and resuspended in water. Triglycerides were determined using a commercially available kit (Sigma-Aldrich, St. Louis, MO).

Statistical analysis

All data were analyzed using Prism software (GraphPad Software, Inc., San Diego, CA) and are expressed as means ± SE. One-way ANOVA was used to compare more than two groups, followed by the Newman-Keuls multiple comparison test to detect differences between groups. The Student's *t* test was used to compare the differences between two groups. $P < 0.05$ was used to reject the null hypothesis.

RESULTS

D2KO mouse metabolic profile depends on ambient temperature

Under the mild thermal stress conditions of room temperature (22°C) and on a chow diet (12.7% fat), D2KO mice have similar caloric intake (Figure 3.1A) and percent composition of lean and fat masses as age-matched wildtype (WT) controls (Figure 3.2A). Even after 2 weeks of acclimatization at 30°C, percent body composition remains unchanged in chow-fed D2KO and WT mice (Figure 3.2A).

We next analyzed parameters of energy homeostasis using indirect calorimetry. At 22°C, despite having a similar rate of oxygen consumption (VO_2; Figure 3.2B), D2KO mice had a relatively higher percentage of fatty acid oxidation compared with WT, as reflected by a significantly lower respiratory exchange ratio (RQ; Figure 3.2C). These findings led us to analyze the BAT NE turnover rate as an index of sympathetic stimulation of this tissue. Remarkably, although WT controls had a NE turnover rate of about 9.5 ± 0.6%/hour, D2KO animals maintained a rate of ~15 ± 1.1%/hour (Figure 3.2D; $P < 0.01$).

Thus, to examine whether this difference in sympathetic activity depends on ambient temperature, D2KO and WT mice were acclimatized at 30°C. In this setting, the BAT NE turnover rate was reduced in both groups to ~5%/hour, with no differences between WT and D2KO mice (Figure 3.2D). This was paralleled by a decrease in VO_2 as compared with the rates at 22°C, with D2KO mice maintaining similar values as WT mice (Figure 3.2B). Of interest, thermoneutrality dissipated the differences in RQ between WT and D2KO mice (Figure 3.2C), with RQ increasing significantly from 22°C values in both groups of mice (~0.9). In addition, at 30°C, no differences in food consumption between D2KO and WT mice were noted (Figure 3.1).

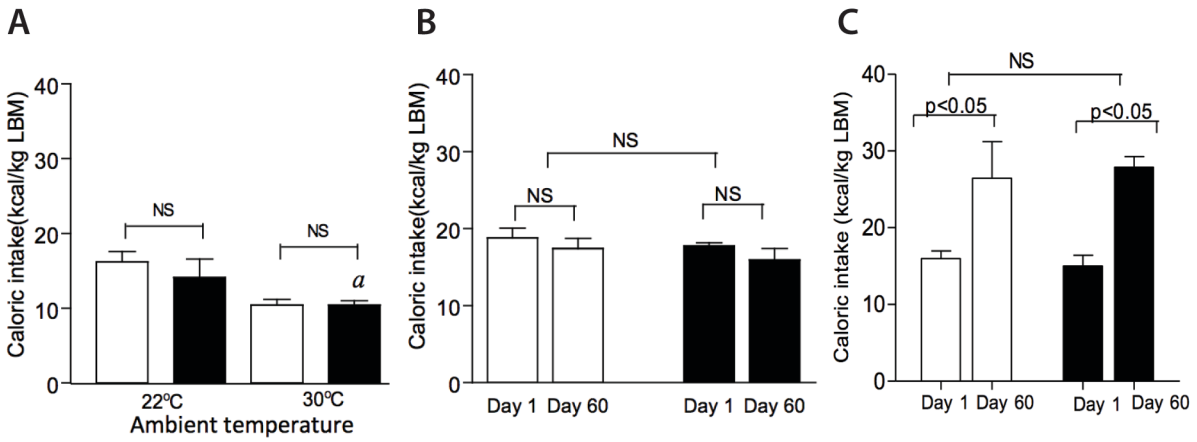

Figure 3.1. Caloric intake in WT and D2KO. (**A**) Caloric intake in WT and D2KO mice acclimatized at the indicated ambient temperature. (**B**) Caloric intake in WT and D2KO at day 1 and at day 60 of feeding with high-fat diet acclimatized to 22°C. (**C**) Same as B, except that the acclimatization temperature is 30°C. Entries are mean ± SEM of 3 animals.

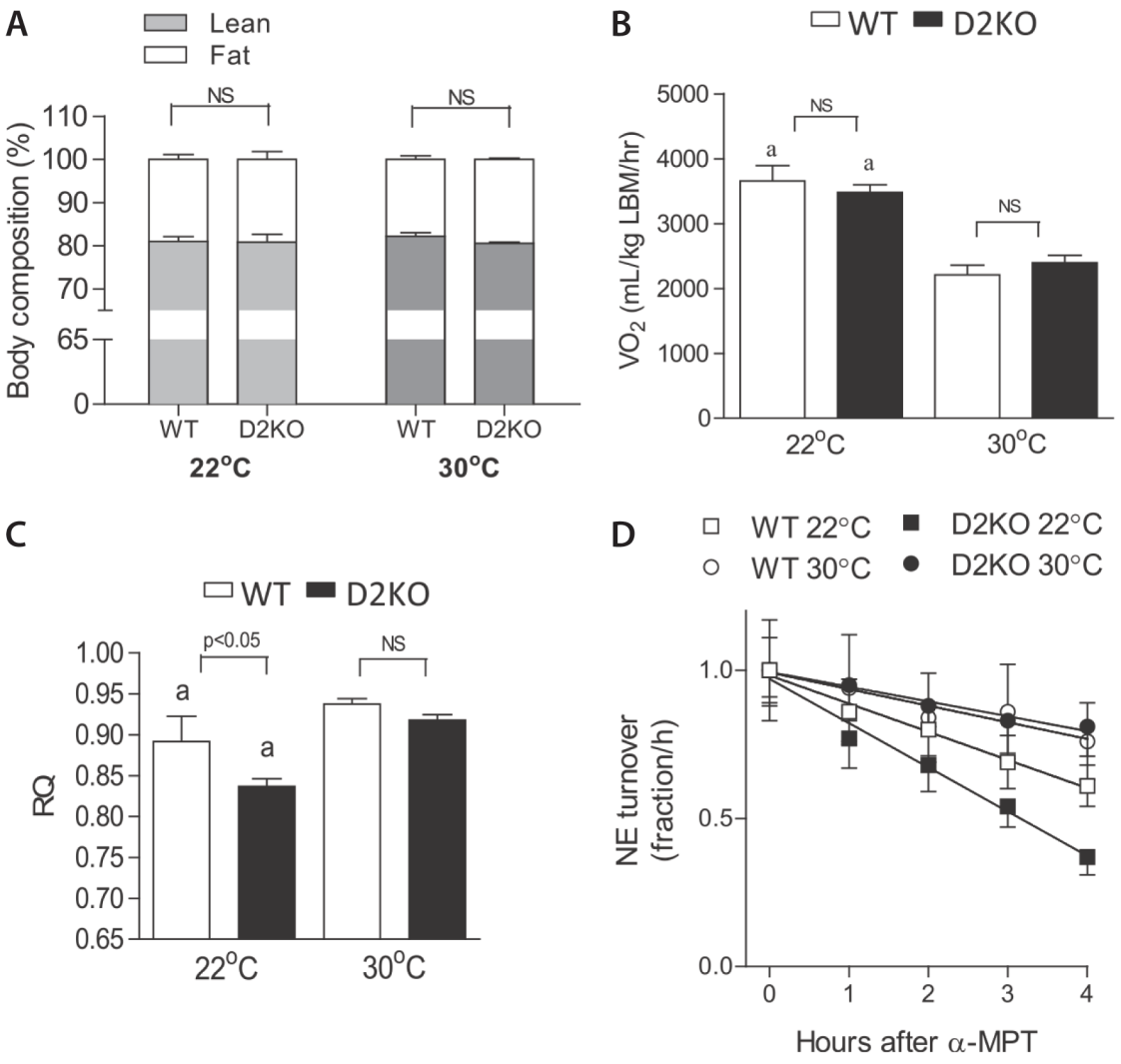

Figure 3.2. Effect of ambient temperature on body composition, indirect calorimetry, and NE turnover of D2KO mice. (**A**) Body composition as measured by DEXA in WT and D2KO mice acclimatized at the indicated ambient temperatures; body weights were as follows: D2KO, 21.55 ± 0.46 and WT, 25.4 ± 0.6 g at 22°C; D2KO, 22.4 ± 0.45 and WT, 23.9 ± 0.6 g at 30°C. (**B**) Same as in A, except that what is shown is VO_2. (**C**) Same as in B, except that what is shown is RQ. (**D**) Interscapular BAT NE turnover at the indicated time points. All animals were kept on chow diet. Measurements were made during the light cycle. Entries are means ± SE of four to five animals; *a* is $P < 0.01$ *vs*. animals of the same genotype. NS, not significant.

D2KO mice have similar weight gain on high-fat diet at room temperature

To test the sensitivity of D2KO mice to diet-induced obesity, groups of age-matched WT and D2KO mice maintained at 22°C were placed on a high-fat diet (42% fat). No major differences were found between WT and D2KO mice (Figure 3.3). After 60 days of ad libitum high-fat diet feeding, both groups experienced a similar increase in body fat (from about 20–33%; $P < 0.01$) as reflected in the body composition analyses (Figure 3.2A *vs*. Figure 3.3A). After 60 days, there was a minimal decrease in VO_2 in both groups (Figure 3.3B), with RQ remaining slightly lower in D2KO animals (Figure 3.3C; $P < 0.05$). Despite similar caloric intake in both groups (Figure 3.1B), D2KO mice gained slightly less body weight as compared with WT (30 *vs*. 37%), although differences did not reach statistical significance (Figure 3.3D; $P = 0.2$).

Thermoneutrality reveals sensitivity to diet-induced obesity in D2KO mice

To test the hypothesis that the increased metabolism at 22°C overrules the effect of hypothyroidism, we next repeated the 60-day feeding period with high-fat diet in WT and D2KO mice that were maintained at 30°C. This time, major differences were indeed found between WT and D2KO mice (Figure 3.4). After 60 days of ad libitum high-fat diet feeding, D2KO animals experienced a much greater increase in body fat (~20–45%; $P < 0.01$) compared with WT animals (~20–35%; $P < 0.01$) as reflected in the body composition analyses (Figure 3.2A *vs*. Figure 3.4A). There was a small but significant increase in VO_2 in both groups (Figure 3.4B), but, most importantly, the difference in RQ was dissipated on the very day 1 of high-fat feeding (Figure 3.4C). Although no differences in caloric intake were observed between D2KO and WT animals under these conditions (Figure 3.1C), D2KO mice had a 66% increase in body weight,

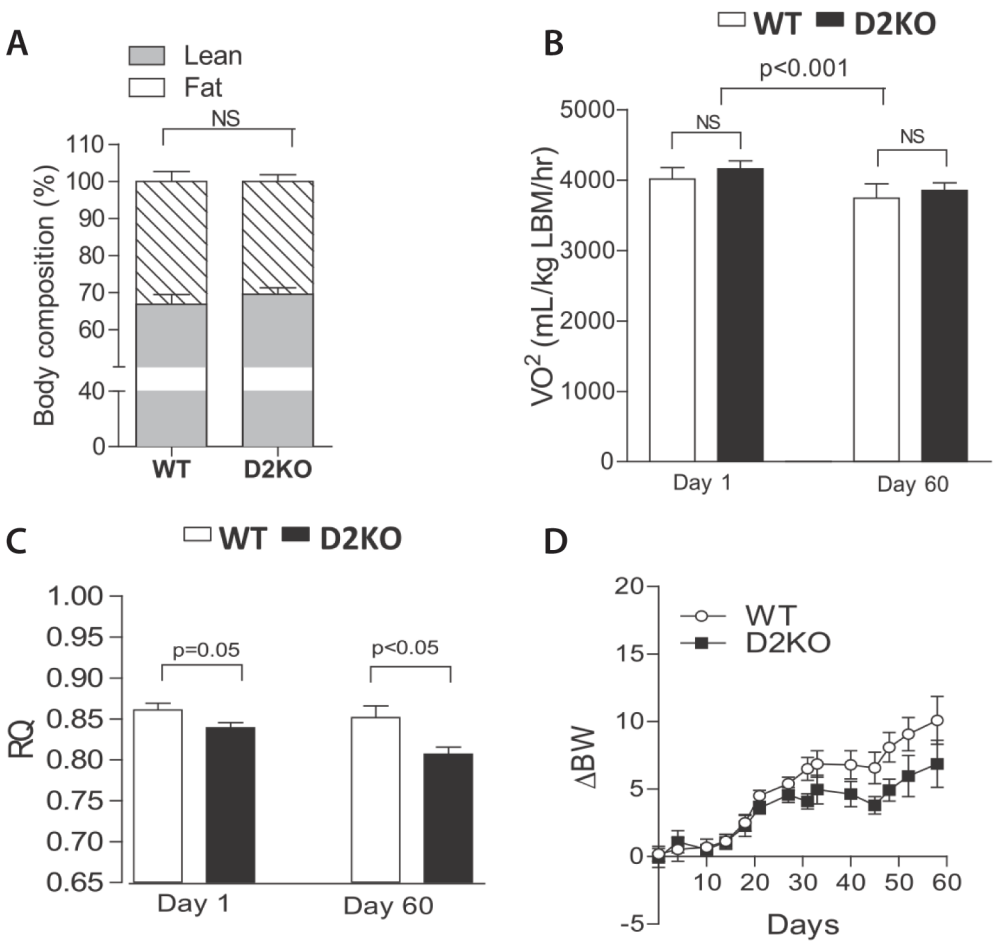

Figure 3.3. Effect of high-fat feeding at room temperature on body composition and indirect calorimetry. D2KO and WT mice were fed with high-fat diet for 8 weeks and kept at 22°C (A–D). (**A**) Body composition as measured by DEXA in WT and D2KO mice at the end of the experiment; body weights were D2KO, 26.9 ± 2.68 and WT, 36.3 ± 2.5 g. (**B**) VO_2 was measured at day 1 and day 60 in WT and D2KO, after the animals started on the high-fat feeding. (**C**) Same as B, except that what is shown is RQ. (**D**) Body weight gain in WT and D2KO mice. Entries are means ± SE of four to five animals; *a* is $P < 0.05$ *vs*. animals of the same genotype.

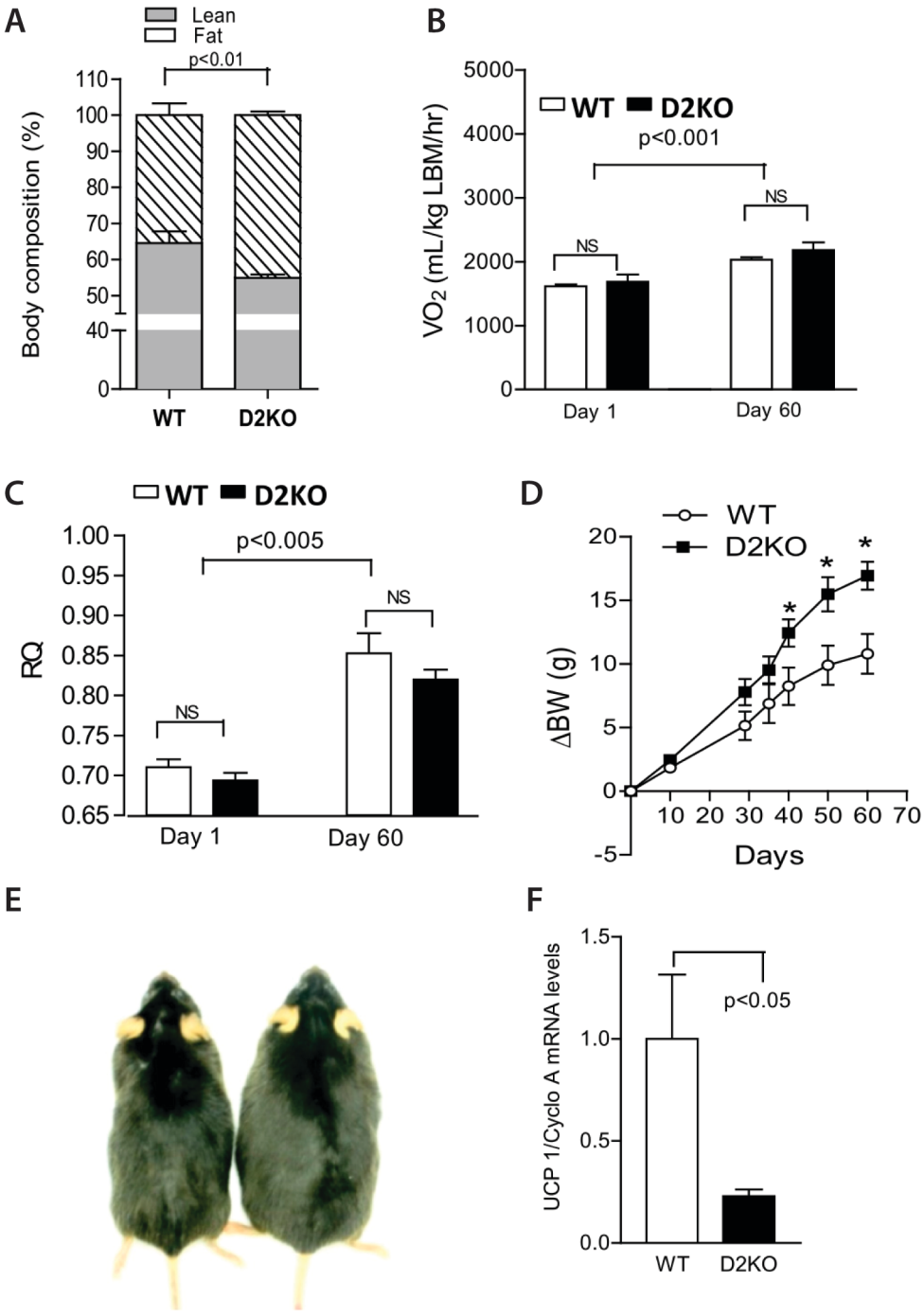

Figure 3.4. Effect of high-fat feeding at thermoneutrality on body composition and indirect calorimetry. D2KO and WT mice were acclimatized at 30°C for 2 weeks and subsequently fed with high-fat diet for 8 weeks while at 30°C (A–F). (**A**) Body composition as measured by DEXA in WT and D2KO mice at the end of the experiment; body weights were D2KO, 41.6 ± 1.23 and WT, 39.45 ± 1.8 g. (**B**) VO_2 was measured at day 1 and day 60 in WT and D2KO. (**C**) Same as B, except that what is shown is RQ. (**D**) Body weight gain in WT and D2KO mice. At day 1 body weights were D2KO, 25.5 ± 0.57 and WT, 28.43 ± 1.12 g. (**E**) Image of

Figure 3.4 (Continued). representative WT and D2KO mice at the end of the experiment. (**F**) UCP1/Cyclophilin A mRNA levels in the BAT at the end of the experiment. Entries are means ± SE of four to five animals; **P* < 0.01 *vs*. WT.

which was nearly twice that of the 37% increase seen in WT mice (Figure 3.4D; $P < 0.01$). The increased susceptibility of the D2KO mouse to obesity at 30°C could also be noted upon visual inspection (Figure 3.4E). That the increased fat gain was attributable to defective diet-induced thermogenesis was supported by a ~80% lower *UCP1* expression in the BAT of D2KO mice (Figure 3.4F).

D2KO exhibit liver steatosis and glucose intolerance

Histological and biochemical liver analysis revealed increased triglyceride deposits in D2KO mice that were kept on a chow diet at 22°C (~30%; Table 3.1; Figure 3.5, A and E). Acclimatization to 30°C did not significantly change fat deposition in liver of both groups of animals (Table 3.1; Figure 3.5, B and F), and the differences between WT and D2KO were minimized (~22%; $P = 0.06$; Table 3.1; Figure 3.5, B and F). High-fat feeding for 60 days increased fat deposition in the WT liver by ~3.7-fold at 22°C and ~5.0-fold at 30°C (Table 3.1; Figure 3.5, C and D). In the D2KO livers, the increase in fat content reached ~3.6-fold at 22°C and, remarkably, 10-fold at 30°C (Table 3.1 and Figure 3.5, G and H). Although the differences of liver triglyceride content between WT and D2KO animals kept on a high-fat diet remained relatively stable at 22°C (~28%; Table 3.1 and Figure 3.5, C and D), moving the animals to 30°C dramatically increased this difference to ~2.7-fold (Table 3.1 and Figure 3.5, D and H).
The more extensive fat deposition in the liver of D2KO animals and its sensitivity to acclimatization temperature suggested that lipolysis and/or the level of serum fatty acids (nonesterified fatty acids [NEFA]) was playing a role. However, regardless of the diet, NEFA serum levels were not different between WT and D2KO animals at 22°C (Table 3.1). Of note, high-fat feeding did increase NEFA levels in both groups (Table 3.1).

Table 3.1. Liver triglycerides content (mg/g) and serum NEFA levels (mEq/L) in WT and D2KO mice kept on chow or high-fat diet: effect of environment temperature.

	LIVER TRIGLYCERIDES				SERUM NEFA			
	Chow diet		High-fat Diet		Chow diet		High-fat Diet	
	22°C	30°C	22°C	30°C	22°C	30°C	22°C	30°C
Genotype								
WT	25±0.7	47±2.3	93±2[b]	126±42[c]	0.62±0.06	0.3±0.05[b]	0.9±0.06[b]	0.66±0.12[g]
D2KO	33±0.9*	58±4.7[a]	119±5**[e]	339±92*[d,f]	0.49±0.06	0.6±0.13*	0.9±0.05[h]	0.99±0.04*[i]

All values in the table are means ± SEM of four to five animals. *$P < 0.05$; **$P < 0.005$; [a]$P = 0.057$ *vs*. WT on the same temperature and diet; [b]$P < 0.05$ *vs*. 22°C on chow diet; [c]$P < 0.01$ vs. 30°C on chow diet; [d]$P < 0.001$ *vs*. 22°C on high-fat diet; [e]$P < 0.001$ *vs*. 22°C on chow diet; [f]$P < 0.001$ *vs*. 30°C on high-fat diet; [g]$P < 0.05$ *vs*. 30°C on chow diet; [h]$P < 0.01$ *vs*. 22°C on chow diet; [i]$P < 0.01$ *vs*. 30°C on chow diet by one-way ANOVA.

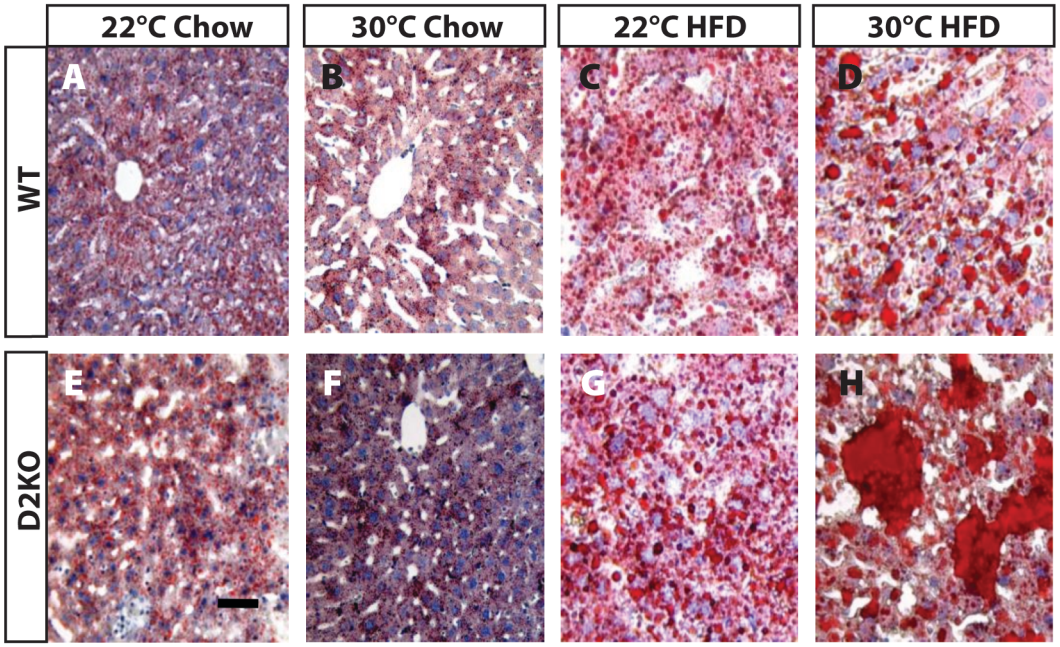

Figure 3.5. Effect of acclimatization temperature and/or diet on lipid deposition in the liver. Oil Red O staining of liver sections obtained from D2KO and WT fed with chow or high-fat diet (HFD) for 8 weeks, acclimatized to 22°C or 30°C, as indicated (A–H) is shown. (**A and B**) D2KO and WT fed with chow diet, acclimatized to 22°C. (**C and D**) Same as A and B, except acclimatization was at 30°C. (**E and F**) D2KO and WT fed with high-fat diet for 8 weeks, acclimatized to 22°C. (**G and H**) Same as E and F, except acclimatization was at 30°C. Scale bar is 50 μm.

In addition, only WT animals experienced decreased NEFA serum levels when maintained at 30°C, which also does not correlate with our findings of fat deposition in the liver (Table 3.1). Thus, it does not seem that differences in serum NEFA levels contribute to liver steatosis in the D2KO animals.

Remarkably, the D2KO animals acclimatized at 22°C are substantially more tolerant to a glucose load than WT (Figure 3.6A). Acclimatization to 30°C dissipated this difference in glucose handling (Figure 3.6B), suggesting that chronic sympathetic BAT stimulation observed in D2KO mice at 22°C could make the animals more tolerant to glucose. This is supported by studies in rats, where cold exposure enhanced disposal of circulating glucose as a result of BAT activation (17). It is noteworthy that during high-fat feeding at 22°C, there were no differences between D2KO and WT animals in terms of glucose tolerance (Figure 3.6C). During acclimatization at 30°C, feeding with a high-fat diet promoted glucose intolerance in D2KO mice, which were less capable of disposing of a glucose load (Figure 3.6D).

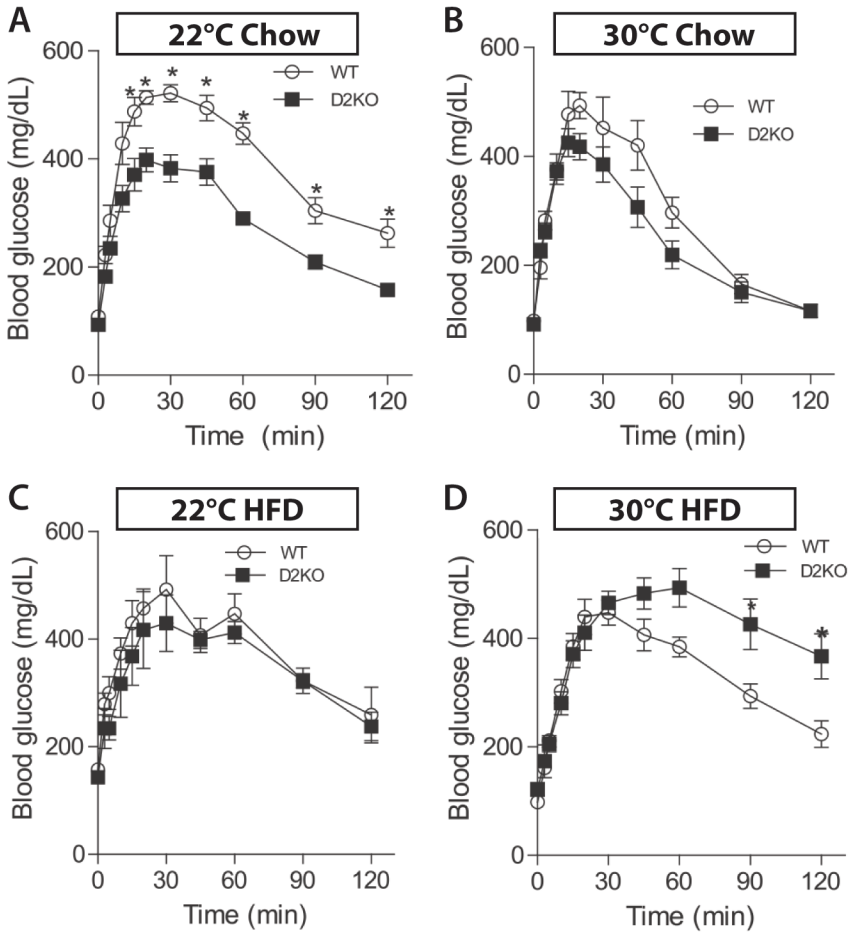

Figure 3.6. Effect of temperature and/or diet on glucose tolerance. Blood glucose concentrations at the indicated time points following intraperitoneal injection of 1 g/kg glucose in D2KO and WT animals fed with chow or high-fat diet, acclimatized to 22°C or 30°C, as indicated are shown. (**A**) D2KO and WT fed with chow diet, acclimatized to 22°C. (**B**) Same as A, except acclimatization was at 30°C. (**C**) D2KO and WT fed with high-fat diet for 8 weeks, acclimatized to 22°C. (**D**) Same as C, except acclimatization was at 30°C. Entries are means ± SE of four to five animals; **P* < 0.01 *vs*. WT.

DISCUSSION

Thyroid hormone and the sympathetic nervous system share a number of common target systems, including cellular pathways involved in metabolic control (1). BAT capitalizes on the synergistic relationship between the sympathetic and thyroid hormone systems for activation of adaptive thermogenesis. BAT expresses D2, which itself is a cAMP-responsive gene, increasing local T3 concentration four- to fivefold during sympathetic stimulation without significant alteration of systemic T3 levels (18); the end result being upregulation of T3-dependent genes such as *UCP1*, which is both cAMP- and T3-sensitive (5, 19). Here, we show that when D2-mediated T3 production is prevented, as with the D2KO mouse, there is a compensatory increase in BAT sympathetic activity to offset the tissue-level hypothyroidism (Figure 3.2D). We suggest that this compensatory sympathetic response neutralizes much of the phenotype that D2KO mice would otherwise exhibit as a result of the disruption in thyroid hormone signaling (Figures 3.2 and 3.3). At 22°C, the D2KO mouse preferentially oxidizes fat (Figure 3.2C), has a similar sensitivity to diet-induced obesity (Figure 3.3), and is supertolerant to a glucose load (Figure 3.6A). However, by eliminating thermal stress and rearing these animals at thermoneutrality (30°C), an opposite phenotype is encountered, one that includes obesity (Figure 3.4) and glucose intolerance (Figure 3.6D). These results define a critical role played by D2 in adaptive thermogenesis, revealing a novel aspect of the thyroid-adrenergic synergism.

Uncoupling substrate oxidation from ATP synthesis is an important pathway for maintaining body temperature when small mammals are exposed to cold. Given recruitment of BAT and increased adrenergic responsiveness in mice fed a cafeteria diet (20), a similar pathway may be harnessed to activate BAT and dissipate excess calories as a form of diet-induced thermogenesis. In fact, activation of the adrenergic system has been used to counteract obesity

(21). However, similar to our present findings, studies performed with high-fat feeding of *UCP1*$^{-/-}$ mice, which were expected to become obese, yielded drastically different phenotypes that were dependent on whether ambient temperature prevented or promoted thermal stress. Although *UCP1*$^{-/-}$ mice reared at 30°C are prone to diet-induced obesity, under subthermoneutral temperatures, *UCP1*$^{-/-}$ mice are lean with elevated D2 in inguinal fat (22, 23). It has been suggested that in the absence of the UCP1 pathway, alternative mechanisms are triggered to maintain body temperature, such as an increase in thyroid hormone signaling. Consequently, when both UCP1 and a thyroid hormone-responsive mechanism, glycerol phosphate cycling, are inactivated, mice accumulate even less fat mass at 22°C (24). Our current findings support and confirm this notion of the importance of thyroid hormone (and its activation by D2) as an efficient means for maintenance of thermal homeostasis, where compromising the action of thyroid hormone leads to obesity only when without a thermal challenge.

So far, the link between thyroid hormone and body weight has been anecdotal. Although patients and lay individuals almost immediately associate hypothyroidism with obesity, the incidence of hypothyroidism in obese individuals is not increased, and changes in body composition during the transition from severe hypothyroidism to mild thyrotoxicosis are meager (9-11). Given our data, the mild apparent impact of thyroid dysfunction on metabolism is likely the result of the effectiveness of the sympathetic-mediated compensatory mechanisms, whereby an inverse relationship exists between T3 and sympathetic signaling. By inactivating the sympathetic system through acclimatization to 30°C, we could better appreciate the importance for thyroid hormone activation on metabolic control, i.e. weight gain, tolerance to glucose load, and liver steatosis (Figure 3.4). Thus, if this hypothesis proves to be correct, it is likely that a failure to trigger these strong compensatory mechanisms would result in symptoms and signs

that would be more in line with our intuitive reasoning and prove clinically relevant. This is particularly pertinent given the finding of substantial amounts of functional BAT in adult humans (25).

Liver steatosis is a novel aspect of the D2KO phenotype (Figure 3.5), which could be explained by increased NEFA uptake, impaired β-oxidation, and/or decreased secretion of VLDL. The lower RQ in the D2KO suggests that increased NEFA is a contributing factor, but no correlation could be found in the WT or D2KO animals between NEFA levels and liver steatosis (Table 3.1). Thyroid hormone is known to induce peroxisome proliferator–activated receptor (PPAR) (26) and β-oxidation in the liver (27) and, in BAT, D2 is a downstream target of FGF21 through a PPAR-mediated mechanism (28). In addition, liver delivers triglycerides to peripheral tissues by production of VLDL, of which apolipoprotein B, which is positively regulated by thyroid hormone (in HepG2 cells), is a major component (29). Given that serum T3 levels are normal in the D2KO mouse (30), it is conceivable that the D2 pathway is locally controlling thyroid hormone activation in liver and loss of which is directly contributing to the liver phenotype in the D2KO mouse. Although liver is known as a D1-expressing tissue, we have found measurable liver D2 activity and mRNA that are induced many fold and play a role in the double LXR KO mouse phenotype (31). It is noteworthy that hypoxia, a known inducer of the type 3 deiodinase (D3), which inactivates thyroid hormone and creates local hypothyroidism, aggravates liver steatosis and inhibits PPAR expression (32). Thus, it is conceivable that an active D2 pathway in liver upregulates genes involved in fatty acid economy. In addition, given the wealth of information about cross-talk between the sympathetic nervous system and the liver (33), it is also conceivable that brain D2 plays an indirect metabolic role in the liver via its expression in the medial basal hypothalamus and/or other brain regions.

Although it can be debated whether diet-induced thermogenesis exists and whether it exists outside of UCP1 and BAT, undoubtedly, adrenergic signaling plays a key role in the development of or protection from obesity upon disruption of thyroid hormone signaling. It is possible that variations in adrenergic signaling and not BAT itself could explain the energy balance in D2KO mice. Increased susceptibility to obesity at 30°C may be because of decreased adrenergic signaling and not the role of D2 in diet-induced thermogenesis *per se*, as has been suggested for *UCP1*$^{-/-}$ mice (34). It also has been recently suggested that diet-induced thermogenesis takes place in tissues other than BAT, such as muscle (35). D2 is highly expressed in BAT, and, thus, it is logical to assume that the present results are directly related to the action of D2 in this tissue. However, we have not looked directly at oxygen consumption of BAT, so diet-induced thermogenesis could stem from elsewhere. D2 is expressed in a number of other tissues, including skeletal muscle (36), and the contribution of D2 in these tissues to metabolic control remains to be elucidated. Finally, it could be argued that it is the mere fact that the D2KO mice are at 22°C (and thus have an increased metabolism) that hides the true phenotype observable at 30°C. In this case, there would be no compensatory mechanisms, i.e. the increased metabolism at 22°C would simply override any other effects.

ACKNOWLEDGMENTS

The authors are grateful to Monica Murillo from University of Miami for technical assistance. These studies were supported by the National Institutes of Health grants DK-65055, DK-56625, and DK-48873.

REFERENCES

1. **Silva JE** 2006 Thermogenic mechanisms and their hormonal regulation. Physiol Rev 86:435-464

2. **Bianco AC, Maia AL, da Silva WS, Christoffolete MA** 2005 Adaptive activation of thyroid hormone and energy expenditure. Biosci Rep 25:191-208

3. **Lowell BB, Spiegelman BM** 2000 Towards a molecular understanding of adaptive thermogenesis. Nature 404:652-660

4. **Bianco AC, Sheng XY, Silva JE** 1988 Triiodothyronine amplifies norepinephrine stimulation of uncoupling protein gene transcription by a mechanism not requiring protein synthesis. J Biol Chem 263:18168-18175

5. **Bianco AC, Silva JE** 1987 Intracellular conversion of thyroxine to triiodothyronine is required for the optimal thermogenic function of brown adipose tissue. J Clin Invest 79:295-300

6. **de Jesus LA, Carvalho SD, Ribeiro MO, Schneider M, Kim SW, Harney JW, Larsen PR, Bianco AC** 2001 The type 2 iodothyronine deiodinase is essential for adaptive thermogenesis in brown adipose tissue. J Clin Invest 108:1379-1385

7. **Christoffolete MA, Linardi CC, de Jesus L, Ebina KN, Carvalho SD, Ribeiro MO, Rabelo R, Curcio C, Martins L, Kimura ET, Bianco AC** 2004 Mice with targeted disruption of the Dio2 gene have cold-induced overexpression of the uncoupling protein 1 gene but fail to increase brown adipose tissue lipogenesis and adaptive thermogenesis. Diabetes 53:577-584

8. **Young JB, Saville E, Rothwell NJ, Stock MJ, Landsberg L** 1982 Effect of diet and cold exposure on norepinephrine turnover in brown adipose tissue of the rat. J Clin Invest 69:1061-1071

9. **Wolf M, Weigert A, Kreymann G** 1996 Body composition and energy expenditure in thyroidectomized patients during short-term hypothyroidism and thyrotropin-suppressive thyroxine therapy. Eur J Endocrinol 134:168-173

10. **Lonn L, Stenlof K, Ottosson M, Lindroos AK, Nystrom E, Sjostrom L** 1998 Body weight and body composition changes after treatment of hyperthyroidism. J Clin Endocrinol Metab 83:4269-4273

11. **Kyle LH, Ball MF, Doolan PD** 1966 Effect of thyroid hormone on body composition in myxedema and obesity. N Engl J Med 275:12-17

12. **Curcio C, Lopes AM, Ribeiro MO, Francoso OA, Jr., Carvalho SD, Lima FB, Bicudo JE, Bianco AC** 1999 Development of compensatory thermogenesis in response to overfeeding in hypothyroid rats. Endocrinology 140:3438-3443

13. **Landsberg L, Axelrod J** 1968 Influence of pituitary, thyroid, and adrenal hormones on norepinephrine turnover and metabolism in the rat heart. Circ Res 22:559-571

14. **Matsukawa T, Mano T, Gotoh E, Minamisawa K, Ishii M** 1993 Altered muscle sympathetic nerve activity in hyperthyroidism and hypothyroidism. Journal of the autonomic nervous system 42:171-175

15. **Tu T, Nash CW** 1975 The influence of prolonged hyper- and hypothyroid states on the noradrenaline content of rat tissues and on the accumulation and efflux rates of tritiated noradrenaline. Canadian journal of physiology and pharmacology 53:74-80

16. **Hyogo H, Roy S, Paigen B, Cohen DE** 2002 Leptin promotes biliary cholesterol elimination during weight loss in ob/ob mice by regulating the enterohepatic circulation of bile salts. J Biol Chem 277:34117-34124

17. **Vallerand AL, Lupien J, Bukowiecki LJ** 1986 Cold exposure reverses the diabetogenic effects of high-fat feeding. Diabetes 35:329-334

18. **Gereben B, Zavacki AM, Ribich S, Kim BW, Huang SA, Simonides WS, Zeold A, Bianco AC** 2008 Cellular and molecular basis of deiodinase-regulated thyroid hormone signaling. Endocr Rev 29:898-938

19. **Branco M, Ribeiro M, Negrao N, Bianco AC** 1999 3,5,3'-Triiodothyronine actively stimulates UCP in brown fat under minimal sympathetic activity. Am J Physiol 276:E179-187

20. **Rothwell NJ, Stock MJ** 1979 A role for brown adipose tissue in diet-induced thermogenesis. Nature 281:31-35

21. **Collins S, Cao W, Robidoux J** 2004 Learning new tricks from old dogs: beta-adrenergic receptors teach new lessons on firing up adipose tissue metabolism. Mol Endocrinol 18:2123-2131

22. **Feldmann HM, Golozoubova V, Cannon B, Nedergaard J** 2009 UCP1 ablation induces obesity and abolishes diet-induced thermogenesis in mice exempt from thermal stress by living at thermoneutrality. Cell Metab 9:203-209

23. **Liu X, Rossmeisl M, McClaine J, Riachi M, Harper ME, Kozak LP** 2003 Paradoxical resistance to diet-induced obesity in UCP1-deficient mice. J Clin Invest 111:399-407

24. **Anunciado-Koza R, Ukropec J, Koza RA, Kozak LP** 2008 Inactivation of UCP1 and the glycerol phosphate cycle synergistically increases energy expenditure to resist diet-induced obesity. J Biol Chem 283:27688-27697

25. **Nedergaard J, Bengtsson T, Cannon B** 2007 Unexpected evidence for active brown adipose tissue in adult humans. Am J Physiol Endocrinol Metab 293:E444-452

26. **Adams AC, Astapova I, Fisher FM, Badman MK, Kurgansky KE, Flier JS, Hollenberg AN, Maratos-Flier E** 2010 Thyroid hormone regulates hepatic expression of fibroblast growth factor 21 in a PPARalpha-dependent manner. J Biol Chem 285:14078-14082

27. **Araki O, Ying H, Zhu XG, Willingham MC, Cheng SY** 2009 Distinct dysregulation of lipid metabolism by unliganded thyroid hormone receptor isoforms. Mol Endocrinol 23:308-315

28. **Hondares E, Rosell M, Gonzalez FJ, Giralt M, Iglesias R, Villarroya F** 2010 Hepatic FGF21 expression is induced at birth via PPARalpha in response to milk intake and contributes to thermogenic activation of neonatal brown fat. Cell Metab 11:206-212

29. **Theriault A, Ogbonna G, Adeli K** 1992 Thyroid hormone modulates apolipoprotein B gene expression in HepG2 cells. Biochem Biophys Res Commun 186:617-623

30. **Schneider MJ, Fiering SN, Pallud SE, Parlow AF, St Germain DL, Galton VA** 2001 Targeted disruption of the type 2 selenodeiodinase gene (DIO2) results in a phenotype of pituitary resistance to T4. Mol Endocrinol 15:2137-2148

31. **Kalaany NY, Gauthier KC, Zavacki AM, Mammen PP, Kitazume T, Peterson JA, Horton JD, Garry DJ, Bianco AC, Mangelsdorf DJ** 2005 LXRs regulate the balance between fat storage and oxidation. Cell Metab 1:231-244

32. **Piguet AC, Stroka D, Zimmermann A, Dufour JF** 2010 Hypoxia aggravates non-alcoholic steatohepatitis in mice lacking hepatocellular PTEN. Clinical science 118:401-410

33. **Fliers E, Klieverik LP, Kalsbeek A** 2010 Novel neural pathways for metabolic effects of thyroid hormone. Trends Endocrinol Metab 21:230-236

34. **Kozak LP** 2010 Brown fat and the myth of diet-induced thermogenesis. Cell Metab 11:263-267

35. **Chen M, Chen H, Nguyen A, Gupta D, Wang J, Lai EW, Pacak K, Gavrilova O, Quon MJ, Weinstein LS** 2010 G(s)alpha deficiency in adipose tissue leads to a lean phenotype with divergent effects on cold tolerance and diet-induced thermogenesis. Cell Metab 11:320-330

36. **Grozovsky R, Ribich S, Rosene ML, Mulcahey MA, Huang SA, Patti ME, Bianco AC, Kim BW** 2009 Type 2 deiodinase expression is induced by peroxisomal proliferator-activated receptor-gamma agonists in skeletal myocytes. Endocrinology 150:1976-1983

Chapter 4

USP7 attenuates hepatic gluconeogenesis through modulation of FoxO1 gene promoter occupancy

AUTHOR CONTRIBUTIONS

I performed all experiments and data analyses described in this chapter. Joseph Rodgers and Pere Puigserver conceived the strategy of examining the role of USP7 in gluconeogenesis, though they predicted a different target substrate. Joseph Rodgers also designed the short-hairpin RNA (shRNA) constructs targeting USP7. I performed all subsequent subcloning and generation of adenoviruses expressing the shRNAs. Mitsuhisa Tabata provided assistance with adenoviral tail vein injections and pyruvate tolerance tests. I wrote the manuscript with editorial suggestions from all authors.

USP7 Attenuates Hepatic Gluconeogenesis through Modulation of FoxO1 Gene Promoter Occupancy

Jessica A. Hall, Mitsuhisa Tabata, Joseph T. Rodgers, and Pere Puigserver

A similar version of this work has been published

Molecular Endocrinology April 2014, me20131420 [Epub ahead of print]

Departments of Cancer Biology, Dana-Farber Cancer Institute and Cell Biology, Harvard Medical School, Boston, Massachusetts 02115

ABSTRACT

Hepatic forkhead protein FoxO1 is a key component of systemic glucose homeostasis via its ability to regulate the transcription of rate-limiting enzymes in gluconeogenesis. Important in the regulation of FoxO1 transcriptional activity are the modifying/de-modifying enzymes that lead to posttranslational modification. Here, we demonstrate the functional interaction and regulation of FoxO1 by USP7, a deubiquitinating enzyme. We show that USP7-mediated mono-deubiquitination of FoxO1 results in suppression of FoxO1 transcriptional activity through decreased FoxO1 occupancy on the promoters of gluconeogenic genes. Knockdown of USP7 in primary hepatocytes leads to increased expression of FoxO1-target gluconeogenic genes and elevated glucose production. Consistent with this, USP7 gain-of-function suppresses the fasting/cAMP-induced activation of gluconeogenic genes in hepatocyte cells and in mouse liver, resulting in decreased hepatic glucose production. Notably, we show that the effects of USP7 on hepatic glucose metabolism depend on FoxO1. Together, these results place FoxO1 under the intimate regulation of deubiquitination and glucose metabolic control with important implication in diseases such as diabetes.

INTRODUCTION

Glucose homeostasis is maintained by action of the opposing pancreatic hormones, glucagon and insulin. Glucagon serves, in part, to induce hepatic gluconeogenesis, the *de novo* synthesis of glucose from non-carbohydrate precursors, during states of nutrient deprivation. During feeding, insulin curtails the rise in blood glucose by increasing glucose uptake in peripheral tissues and suppressing gluconeogenesis in the liver. However, in diabetic individuals with insulin resistance, the liver functions as in the fasted state and inappropriately activates

gluconeogenesis (1). Anti-diabetic drugs, such as the widely prescribed metformin, are believed to lower blood glucose primarily through repression of hepatic gluconeogenesis (2).

Both insulin and glucagon lead to rapid changes in signaling pathways that converge on the transcriptional regulation of the rate-limiting enzymes in gluconeogenesis, glucose-6-phosphatase (*G6Pc*; G6Pase) and phosphoenolpyruvate carboxykinase (*Pck1*; PEPCK). Glucagon release in the fasted state initiates the gluconeogenic gene program via induction of the cAMP/protein kinase A (PKA) pathway and activation of transcription factors, such as cAMP-responsive element (CRE)-binding protein (CREB), hepatic nuclear factor 4α (HNF4α), and forkhead box O1 (FoxO1) (3-6). As an additional level of regulation, coactivators peroxisome proliferator-activated receptor-γ coactivator 1 α (PGC-1α) and cAMP-regulated transcriptional coactivator (CRTC2) interact with and potentiate the transcriptional activity of these gluconeogenic transcription factors (3, 7, 8). In opposition, insulin suppresses hepatic gluconeogenesis primarily through its activation of phosphatidylinositol 3-kinase (PI3K) and Akt pathways, leading to negative regulation of PGC-1α and FoxO1 (9-11).

FoxO1, a member of the FoxO subfamily of forkhead winged/helix transcription factors, is critical for the insulin-mediated suppression of gluconeogenesis (12, 13). FoxO1 interacts with an insulin responsive element (IRE) on the promoter region(s) of *G6Pc* and *Pck1* (14-17). Insulin signaling results in suppression of FoxO1 transcriptional activity through Akt-dependent phosphorylation of FoxO1 on specific conserved residues (T24, S256, and S319 in human FoxO1) (15, 18). Once phosphorylated, FoxO1 associates with 14-3-3 proteins, leading to cytoplasmic sequestration (19), followed by ubiquitination and degradation (20, 21). Consistent with the suppressive effect of insulin on FoxO1 activity, insulin resistance in diabetes leads to hyperactivation of FoxO1 with consequent elevation of FoxO1 target genes (5). Mice lacking

hepatic FoxO1 display reduced gluconeogenic gene expression, increased glucose tolerance, and reduced hepatic glucose production (13). Moreover, inhibition of hepatic FoxO1 has been shown to ameliorate fasting hyperglycemia in several diabetic animal models (5, 12, 22). Thus, the rapid repression of FoxO1, and subsequent decrease in gluconeogenic gene expression, is a key component of glucose homeostasis and may provide a strategy for intervention in the management of insulin-resistant diabetes.

FoxO family members govern a variety of cellular processes—some unique and some overlapping—and exhibit considerable levels of regulation. In general, FoxO activity is regulated by post-translational modifications that affect subcellular localization, protein stability, and DNA binding. These include phosphorylation, acetylation, methylation, glycosylation, and ubiquitination [reviewed in (23)]. Some of these modifications and the responsible kinases/enzymes are shared among family members, but the extent to which they have been characterized is by no means exhaustive. Thus, a better grasp on the effectors and their mode of regulation has the potential to reveal fresh alternatives for controlling FoxO1 activity.

Ubiquitination, the covalent addition of ubiquitin moieties to a target protein, can lead to decreased stability (through ubiquitin-targeted proteasomal degradation) or alteration of localization and/or activity of the modified protein. And the process of ubiquitin modification can be reversed by the action of deubiquitinating enzymes (24). Recently, the deubiquitinating enzyme USP7 has been identified in the negative regulation of FoxO3/4 transcriptional activity. Monoubiquitination of FoxO3/4 results in re-localization to the nucleus, which is counteracted by USP7-induced deubiquitination (25).

USP7, also known as HAUSP (herpesvirus-associated ubiquitin-specific protease), belongs to the ubiquitin-specific proteases family of deubiquitinating enzymes and contains a

characteristic cysteine motif in its catalytic domain (26). USP7 is most notable for its complex role in regulating stability of the p53 tumor suppressor, where it directly binds to and deubiquitinates both p53 and Mdm2, the E3 ubiquitin ligase responsible for p53 destabilization (27, 28). In fact, USP7 regulates several tumor suppressors, and a role for inhibition of USP7 in cancer is an active area of study (29). Indeed, FoxO proteins are considered tumor suppressors (30), making the interaction of USP7 with FoxO3/4 highly attractive to cancer research. However, it is unknown whether USP7 controls the action of FoxO proteins in other biological areas, namely, glucose metabolism.

Although the effect of polyubiquitination and ubiquitin-targeted proteasomal degradation of FoxO1 is well-appreciated, a role for monoubiquitination of FoxO1 *per se* has not been examined. We hypothesized that a similar interaction with USP7 might exist for FoxO1, which led us to interrogate a mechanistic link between USP7 and FoxO1 metabolic function. Here, we expand the list of USP7 targets to include FoxO1, showing that USP7 deubiquitinates monoubiquitinated FoxO1 to affect its association with the *G6Pc* and *Pck1* promoters. We demonstrate that knockdown of USP7 elevates gluconeogenic genes, whereas overexpression of USP7 leads to suppression of gluconeogenesis in cell culture and in the whole animal. Notably, we determine a requirement of FoxO1 activity for USP7's effects on gluconeogenic gene expression. Taken together, our findings reveal USP7 activation as a powerful inhibitor of FoxO1 activity and a potential therapeutic route in the amelioration of hyperglycemia associated with insulin-resistant malignancies.

MATERIALS AND METHODS

DNA constructs and adenoviruses

The pcDNA3 Flag-FoxO1, 3X IRS luciferase, and myristoylated Akt reporter constructs have previously been described (31). Myc-tagged USP7 was a gift from Dr. Pier Pandolfi, and pCl-neo Flag-tagged USP7 was provided by Dr. Bert Vogelstein via Addgene plasmid 16655 (32). pRK5 HA-Ubiquitin (Ub) wildtype and lysine-less KO (Addgene plasmids 17608 and 17603, respectively) were provided by Dr. Ted Dawson (33). A Flag-tagged non-insulin-sensitive FoxO1 mutant (pcDNA3 Flag-FoxO1 T24A/S256A/S319A; Addgene plasmid 13508) was provided by Dr. Kunliang Guan (31). Plasmids carrying cDNAs encoding FoxO1-GFP fusion proteins were gifts from Dr. Alexander Banks and have previously been described (34). Point mutant generation of USP7 C223S was conducted by PCR-based mutagenesis. Short-hairpin RNA (shRNA) constructs targeting USP7 (with 100% sequence complementarity to both human and mouse) were generated in a pLKO.1 backbone with the following target sequences: shUSP7#1, 5′-TGTATCTATTGACTGCCCTTT-3′; and shUSP7#2, 5′-GGCAACCTTTCAGT-TCACTGT-3′.

Adenoviruses were generated with the pAd-Track/pAd-Easy system unless otherwise noted. Flag-USP7 adenoviruses were subcloned from pCl-neo Flag-USP7 constructs and express USP7 under a CMV promoter. Adenoviruses expressing shRNAs were subcloned from pLKO.1 vectors and are driven by a U6 promoter. A non-targeting control shRNA adenovirus containing a scrambled sequence (SCR) has previously been described (35). Adenoviruses encoding FoxO1 shRNA and corresponding control shRNA were gifts from Dr. Alexander Banks and were generated as previously described (36). All adenoviruses were amplified in HEK293A cells, purified by CsCl gradient centrifugation, and dialyzed in buffer containing 10 mM Tris (pH 8.0),

2 mM $MgCl_2$, and 4% glycerol. Adenoviral titer was determined by serial dilution/infection of HEK293A cells and quantifying the number of fluorescing cells.

Cell culture and treatment

HEK293A cells were maintained in DMEM containing 10% FBS and penicillin/streptomycin. Transfections were performed with Lipofectamine 2000 transfection reagent (Invitrogen, Life Technologies) according to the manufacturer's recommendations. Where indicated, HEK293A cells were rinsed with PBS and switched to DMEM lacking serum. Live-cell visualization of FoxO1-GFP localization was imaged by fluorescence microscopy on a Leica DMI6000B microscope (Leica Microsystems). Images were processed in Adobe Photoshop CS4 software to increase brightness for publication; consistent threshold settings were maintained across images.

Mouse primary hepatocytes were isolated from male C57BL/6 mice by perfusion with liver digest medium (Gibco, Life Technologies; pH 7.4) followed by 70 μm filtration exclusion and Percoll (Sigma) gradient centrifugation. Cells were seeded in DMEM containing 10% FBS, 2 mM sodium pyruvate, 1 μM dexamethasone, 0.1 μM insulin, and penicillin/streptomycin. After cell attachment, medium was replaced with DMEM supplemented with 0.2% BSA, 2 mM sodium pyruvate, 0.1 μM dexamethasone, 1 nM insulin, and penicillin/streptomycin (maintenance medium). Adenovirus infections were performed the following day for 4 hours with 3.5×10^6 infectious particles per 4×10^5 cells. Fresh maintenance medium was replenished daily. Cells were harvested 48 hours post-infection. Where indicated, cells were serum-starved in DMEM containing 0.2% BSA, 2 mM sodium pyruvate, and penicillin/streptomycin prior to stimulation with insulin (Sigma) and/or forskolin (Fisher). For measurement of glucose

production, cells were cultured for 3 hours in 0.2% BSA, phenol red-free, glucose-free DMEM. Amount of glucose in the medium was quantified using a colorimetric glucose assay (EnzyChrom, BioAssay Systems) and normalized to total protein amount in the whole-cell lysates. Assays were conducted with or without 20 mM sodium lactate and 2 mM sodium pyruvate, and glucose production in the absence of lactate/pyruvate subtracted from that produced in the presence of lactate/pyruvate.

Transcriptional reporter assays

HEK293A cells were transfected to a fixed amount of DNA as corrected with empty vector plasmid. Cells were harvested 24 hours post-transfection with 1X Passive Lysis Buffer (Promega). Firefly luciferase reporter was determined by addition of Luciferase Assay Substrate (Dual-Luciferase Reporter Assay System, Promega) and quantification of luminescence on a FLUOstar Omega plate reader (BMG Labtech). Of note, CMV-driven *Renilla* luciferase vector was co-transfected as an internal control; however, despite a range of experimental vector to control vector ratios tested, *Renilla* luciferase activity was sensitive to co-transfected plasmids (data not shown) and, thus, withheld from normalization. Data are presented as firefly luciferase reporter values alone and are representative of at least two independent experiments.

Chromatin immunoprecipitation (ChIP)

Primary hepatocytes stimulated for 1.5 hours with 10 μM forskolin or DMSO vehicle were fixed in 1% formaldehyde for 10 min at room temperature. Crosslinking was quenched by adding glycine to a final concentration of 125 mM and rinsing twice with cold PBS. Cells were collected in PBS containing protease inhibitors followed by mild lysis [10 mM HEPES (pH 7.9),

10 mM KCl, 1.5 mM $MgCl_2$, 0.5% Igepal, 1 mM PMSF, and protease inhibitors] and centrifugation. The resulting nuclear pellets were resuspended in ChIP buffer [50 mM HEPES (pH 7.9), 140 mM NaCl, 1 mM EDTA, 1% Triton X-100, 0.1% NaDOC, 0.1% SDS, 1 mM PMSF, and protease inhibitors] and chromatin sheared by sonication with a Diagenode Biorupter for 3 cycles of 5 min (30 sec on, 30 sec off). Samples were clarified and chromatin immunoprecipitated overnight at 4°C with anti-FoxO1 (C29H4, Cell Signaling Technologies) or isotype rabbit IgG (Abcam). Immunecomplexes were recovered with Protein A magnetic beads (Dynabeads; Novex, Life Technologies) preblocked with salmon sperm DNA (Invitrogen, Life Technologies). Following extensive washes, immunoprecipitated DNA was then isolated with a Chelex 100-based DNA purification method described in (37). Input DNA was prepared from 10% of respective chromatin prior to precipitation. Immunoprecipitated DNA and input DNA were analyzed by quantitative real-time PCR with primers specific for the *G6Pc* IRE (forward: 5′-TGGCTTCAAGGACCAGGAAG-3′ and reverse: 5′-TGCAAACATGTTCAGGGTGA-3′), *Pck1* IRE (forward: 5′-TGGCTCAGAGCTGAATTTCC-3′ and reverse: 5′-CCTGTTGCTGAT-GCAAACTG-3′), and a control genomic region 17.9 kb upstream of *Cycs* (forward: 5′-GGCTC-TCCTTGCAGTTTTTG-3′ and reverse: 5′-CCGACCTTTACATCGCCTAA-3′). Enrichment of specific promoter regions after immunoprecipitation was calculated as percent of input.

Animal experiments and procedures

Mouse experiments were performed with 10-week-old male C57BL/6 mice and 8-week-old male BALB/c mice purchased from Taconic Farms and allowed at least one week of acclimation to our facilities. All mice were maintained on normal chow and housed under a 12-hour light/12-hour dark cycle at 22°C. Mice were handled for three days prior to adenovirus

infection (1.5×10^9 infectious particles per mouse) by tail vein injection under isofluorane anesthesia. All analyses were performed four days after infection. For gene expression analysis, mice were sacrificed after the indicated fasting or refeeding duration; the livers were snap-frozen in liquid nitrogen and stored at -80°C until processing. Pyruvate tolerance tests were performed on animals fasted for 16 hours prior to intraperitoneal injection of 2 g/kg sodium pyruvate dissolved in sterile PBS. Glycemia was measured by tail bleed at the indicated times using a glucometer (Precision Xtra, Abbott Diabetes Care). All studies were performed according to protocols approved by Dana-Farber Cancer Institute's Animal Care and Use Committee.

Quantitative real-time PCR analysis

Total RNA was extracted from cells or pulverized liver using TRIzol reagent (Ambion, Life Technologies), followed by cDNA preparation from 2 μg of total RNA with a High Capacity cDNA Reverse Transcription Kit (Applied Biosystems) on a MJ Mini thermal cycler (Bio-Rad). cDNA products were quantified by real-time PCR using Power SYBR Green PCR Master Mix (Applied Biosystems) on a CFX384 Real-Time PCR System (Bio-Rad). Gene expression was determined by generation of a standard curve and normalized for the expression of *36B4*. All primer sequences are available upon request.

Western blotting

Whole-cell extracts were prepared in RIPA buffer containing phosphatase inhibitors (1 mM glycerol-2-phosphate, 5 mM NaF, and 1 mM Na orthovanadate), 1 mM PMSF, and protease inhibitors (Roche). Cytoplasmic and nuclear fractionation from cells and pulverized liver were performed as previously described with minor modifications (38). Briefly, cytoplasmic fractions

were obtained from a buffer A containing 10 mM HEPES (pH 7.9), 10 mM KCl, 1.5 mM $MgCl_2$, 0.5% Igepal, phosphatase inhibitors, 1 mM PMSF, and protease inhibitors. After washing with buffer A, nuclear pellets were resuspended in a buffer B containing 20 mM HEPES (pH 7.9), 150 mM NaCl, 1.5 mM $MgCl_2$, 0.2 mM EDTA, 15% glycerol, 0.5% Igepal, 0.3% CHAPS, phosphatase inhibitors, 1 mM PMSF, and protease inhibitors. Protein concentration was determined by DC (detergent compatible) protein assay (Bio-Rad) and lysates separated by SDS-PAGE, transferred to Immobilon-P transfer membranes (Millipore), and blotted according to manufacturer's recommendations for the indicated antibodies. Antibodies for the detection of FoxO1, phospho-FoxO1 (Ser256), phospho-FoxO1 (Thr24), Akt, phospho-Akt (Thr308), phospho-Akt (Ser473), GSK3β, and phospho-GSK3β (Ser9) were from Cell Signaling Technologies. Anti-USP7 antibody was purchased from Bethyl Laboratories, Inc. Anti-HA, anti-Myc, and anti-Flag peroxidase conjugates were from Sigma. Horse peroxidase-conjugated secondary antibodies were from Jackson ImmunoResearch. Anti-Lamin B1 (Abcam) and anti-β-Tubulin (Millipore) were used as loading controls.

Co-immunoprecipitations

To assess the endogenous interaction of USP7 with FoxO1 from primary hepatocytes, nuclear extracts were prepared in RIPA buffer without SDS containing phosphatase inhibitors, 1 mM PMSF, and protease inhibitors. Clarified lysates were precleared with 20 μL of a protein A sepharose (GE Healthcare Bio-Sciences) slurry prior to incubation with anti-FoxO1 or isotype rabbit IgG overnight at 4°C. The immunecomplexes were then precipitated by addition of 20 μL protein A sepharose slurry and incubation for 2 hours at 4°C. Co-immunoprecipitations (co-IPs) of epitope-tagged USP7 and FoxO1 were performed with clarified whole-cell extracts from

HEK293A cells resuspended in co-IP buffer [20 mM HEPES (pH 7.9), 125 mM NaCl, 1 mM EDTA, 0.1% Igepal, 0.3% CHAPS, phosphatase inhibitors, 1 mM PMSF, and protease inhibitors], where complexes were captured overnight by immunoprecipitation with anti-Flag agarose (Sigma). Immunoprecipitated proteins were washed four times with respective lysis buffer, eluted with 2X SDS sample buffer and boiling, and detected by immunoblotting after separation by SDS-PAGE.

Deubiquitination assays

For detection of FoxO1 deubiquitination *in vivo*, HEK293A cells transfected with the indicated plasmids were lysed in 1% SDS buffer containing 50 mM Tris (pH 7.5), 150 mM NaCl, 0.1% Triton X-100, phosphatase inhibitors, 1 mM PMSF, protease inhibitors, and 0.5 mM *N*-ethylmaleimide (NEM; Boston Biochem), boiled for 10 min, and sonicated. Lysates were immunoprecipitated with anti-Flag agarose after dilution to 0.1% SDS and clarification. Immunoprecipitates were washed with high salt buffer [50 mM Tris (pH 7.5), 250 mM NaCl, 1% Triton X-100, 1 mM EDTA, and inhibitors], eluted as above, and analyzed by SDS-PAGE. Following transfer, membranes were autoclaved prior to immunoblotting for ubiquitinated species. For *in vitro* deubiquitination assays, Flag-tagged FoxO1 and USP7 were anti-Flag affinity purified from HEK293A cells transfected with plasmids encoding the respective proteins. HA-tagged monoubiquitinated Flag-FoxO1 was immunoprecipitated as described above, and Flag-USP7 was immunoprecipitated from cells lysed in co-IP buffer. After extensive washing, immunoprecipitates were eluted in deubiquitination buffer [50 mM Tris (pH 7.5), 150 mM NaCl, 0.001% Triton X-100, 1 mM EDTA, 10 mM DTT, 5% glycerol, and inhibitors] with 200 μg/mL 3X Flag-peptide (Sigma). Purified USP7, wildtype or CS mutant, was added to

aliquots of purified monoubiquitinated FoxO1 and reactions incubated at 30°C for 1 hour. Reactions were terminated using 6X SDS sample buffer and analyzed by western blotting.

Deubiquitinating enzyme activity analysis

The effect of hormonal stimuli on USP7 activity was tested by using HA-tagged ubiquitin vinyl methyl ester (HA-UbVME; Enzo Life Sciences), a ubiquitin derivative that binds irreversibly to active deubiquitinating enzymes (39). Primary hepatocytes were isolated in co-IP buffer supplemented with 1 mM DTT, and 20 μg of lysate reacted with 0.1 μg of HA-UbVME for 1 hour at 30°C. Pretreatment of lysates with NEM, which is an inhibitor of deubiquitinating enzymes, for 20 min at 30°C was used as a negative control in parallel extracts. Reaction was stopped by addition of 6X SDS sample buffer and boiling. Samples were subjected to SDS-PAGE analysis, where USP7 activity was assessed by detection of a shift in USP7 molecular mass by approximately 8 kDa, indicative of a stable complex with ubiquitin probe. To assess USP7 activity in nuclear and cytoplasmic fractions, the cytoplasmic fraction was isolated in absence of detergent and then subjected to buffer exchange using 10 kDa MWCO Amicon centrifual filters (Millipore) such that both nuclear and cytoplasmic proteins were resuspended in the aforementioned buffer.

Statistical analysis

Data were analyzed using Prism software (GraphPad Software, Inc) and are expressed as mean ± SEM. Two-tailed Student's *t* tests and one-way ANOVA with Newman-Keuls Multiple Comparison test were used to compare means between groups as indicated; $P < 0.05$ was considered significant.

RESULTS

USP7 interacts with and deubiquitinates monoubiquitinated FoxO1

It has been reported that USP7 targets FoxO family members FoxO3 and FoxO4, where deubiquitination of monoubiquitinated FoxO3/4 leads to nuclear exclusion and decreased activity (25). However, FoxO1 as a USP7 substrate and the effect of monoubiquitination on FoxO1 activity have not been explored. To assess whether FoxO1 is also targeted by USP7, we first determined whether USP7 interacts with FoxO1. Immunoprecipitation of FoxO1 from the nuclear fraction of cultured mouse hepatocytes showed binding of endogenous USP7 to FoxO1 (Figure 4.1A). For further mechanistic analysis, we verified this interaction in an amenable transient expression system. HEK293A cells were co-transfected with Myc-tagged USP7 (Myc-USP7) and Flag-tagged FoxO1 (Flag-FoxO1) followed by co-immunoprecipitation. As shown in Figure 4.1B, immunoprecipitation of Flag-FoxO1 clearly revealed Myc-USP7 bound to FoxO1. Notably, USP7 activity is not necessary for this interaction, as both wildtype and a catalytically inactive mutant of USP7 (C223S; CS) efficiently interacted with FoxO1.

Having established an interaction between USP7 and FoxO1, we next sought to determine whether USP7 deubiquitinates FoxO1. In evaluating the effects of USP7 on FoxO1 ubiquitination, we utilized co-expression of HA-tagged ubiquitin for visualization of ubiquitinated FoxO1 species. Immunoprecipitation of Flag-FoxO1 under denaturing conditions revealed a pattern of ubiquitination that was decreased upon overexpression of USP7 (Figure 4.1C). In contrast to this, the catalytically inactive USP7 CS actually enhanced the level of FoxO1 ubiquitination, which is likely a result of this mutant acting as a dominant-negative (27) (Figure 4.1C). Further, to assess whether the pattern of ubiquitinated bands in the immunnoprecipitate of Flag-FoxO1 reflects true monoubiquitination of FoxO1, we

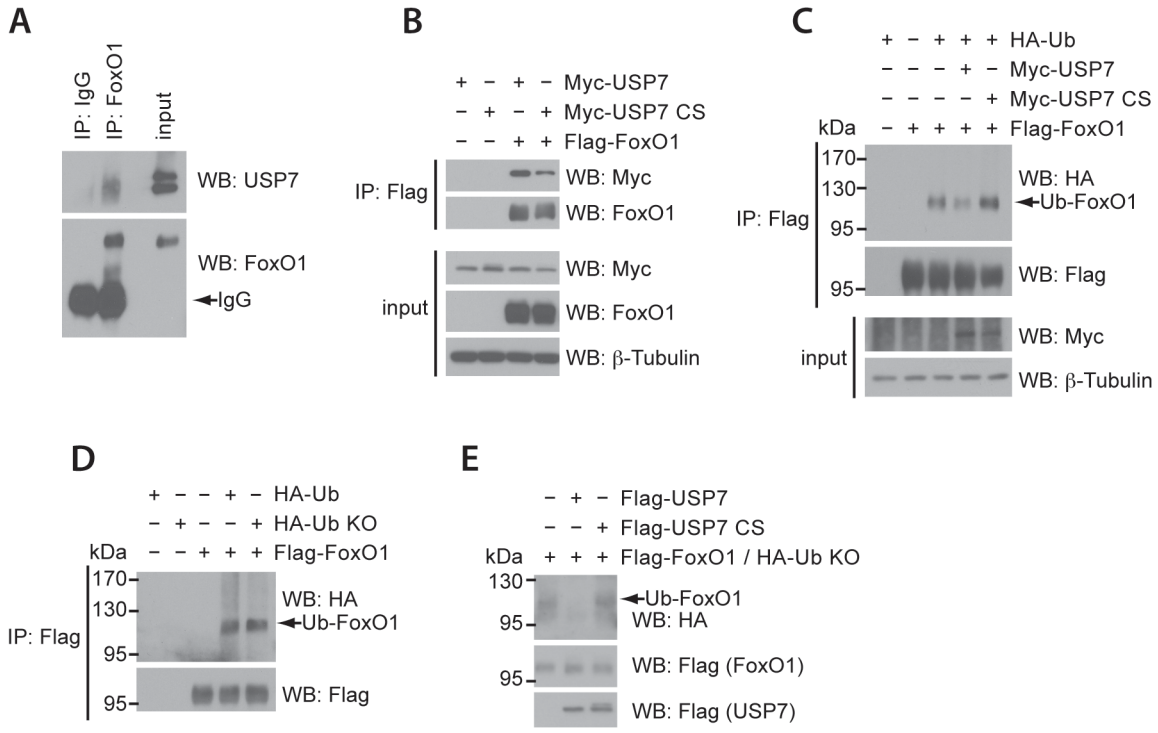

Figure 4.1. FoxO1 is a substrate of USP7. (**A**) Endogenous USP7 and FoxO1 interact. Western blot analysis of immunoprecipitated FoxO1 from nuclear extracts of primary hepatocytes that were serum-starved overnight. (**B**) USP7 catalytic activity is not required for interaction with FoxO1. Western blot analysis of whole-cell extracts (input) or following co-immunoprecipitation with anti-Flag agarose (IP: Flag) of HEK293A cells transfected with Flag-FoxO1 and Myc-USP7 constructs. (**C**) Wildtype USP7 deubiquitinates FoxO1. Western blot analysis of whole-cell extracts (input) or following immunoprecipitation with anti-Flag agarose (IP: Flag) of HEK293A cells transfected with indicated constructs. (**D**) FoxO1 is monoubiquitinated. Western blot analysis of whole-cell extracts (input) or following immunoprecipitation with anti-Flag agarose (IP: Flag) of HEK293A cells transfected with Flag-FoxO1 and HA-tagged wildtype ubiquitin or a lysine-less ubiquitin mutant (Ub KO). (**E**) USP7 deubiquitinates monoubiquitinated FoxO1 *in vitro*. Ubiquitinated FoxO1 (in the presence of HA-Ub KO) was affinity purified from HEK293A cells. Purified Flag-USP7 constructs were added and reactions incubated at 30°C for 1 hour prior to termination and analysis by SDS-PAGE.

co-transfected FoxO1 with a ubiquitin construct in which all seven lysine residues have been mutated to arginines (Ub KO). Given that this mutant ubiquitin cannot form polyubiquitin chains, the resulting similarity in pattern of FoxO1 ubiquitination in the presence of wildtype Ub and Ub KO suggests that the observed ubiquitination of FoxO1 is indeed monoubiquitination (Figure 4.1D). In order to confirm the direct deubiquitination of monoubiquitinated FoxO1 by USP7, we incubated affinity-purified monoubiquitinated FoxO1 with purified USP7 in an *in vitro* deubiquitination assay. Shown in Figure 4.1E, purified wildtype USP7, but not the USP7 CS mutant, markedly reduced the levels of monoubiquitinated FoxO1 in this cell-free assay. Taken together, these results support the conclusion that USP7 directly deubiquitinates monoubiquitinated FoxO1.

FoxO1 transcriptional activity is suppressed by USP7

To investigate the functional consequence of FoxO1 as a USP7 target, we next analyzed the effect of USP7 on the transcriptional activity of FoxO1. Unlike polyubiquitination, which impedes FoxO activity by signaling FoxO proteins for proteasomal degradation, several studies have shown that monoubiquitination of FoxO4 increases its transcriptional activity (25, 40, 41). Thus, and similar to its reported function on FoxO3/4, we hypothesized that removal of monoubiquitin moieties from FoxO1 by USP7 would attenuate FoxO1 activity. Indeed, overexpression of wildtype USP7 suppressed FoxO1 activation on a FoxO1-responsive reporter construct, whereas USP7 CS led to an increase in activation (Figure 4.2A, *top*). Importantly, these effects on transcriptional activity were in absence of an effect on FoxO1 protein levels (Figure 4.2A, *bottom*).

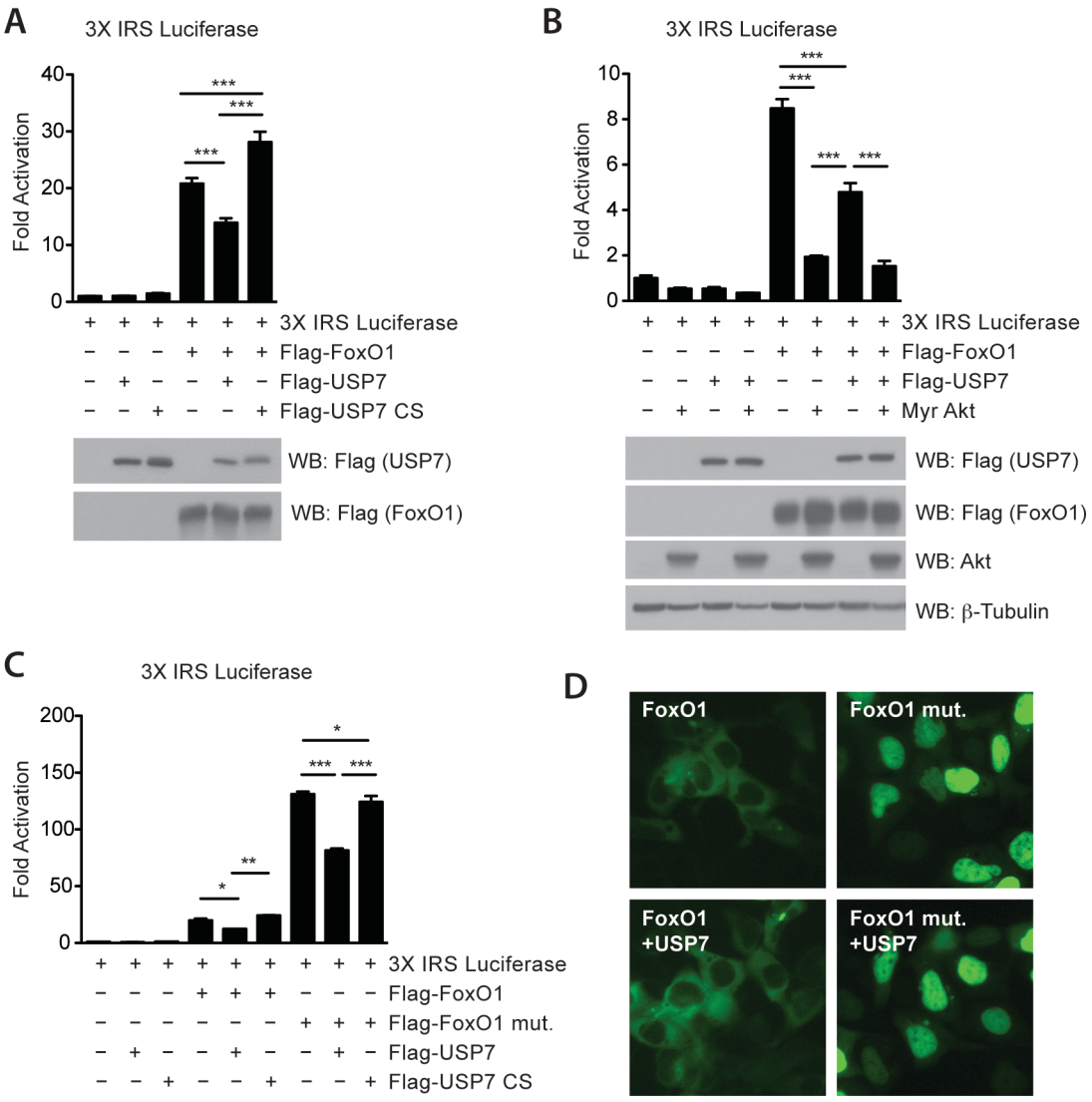

Figure 4.2. USP7 affects FoxO1 transcriptional activity. (**A**) USP7 suppresses transcriptional activation of FoxO1 on the 3X IRS FoxO1 response element-luciferase reporter construct in HEK293A cells. Data presented as relative activity and shown as ± SEM; n = 3. ***, $P < 0.001$ by one-way ANOVA with Newman-Keuls Multiple Comparison test. Effect is noted in absence of changes on FoxO1 protein levels, as indicated by included western blot analysis of whole-cell extracts. (**B**) Constitutively active Akt (Myr Akt) suppresses FoxO1 transcriptional activity to a further degree than USP7 alone. Data presented as in (**A**). (**C**) USP7 suppresses transcriptional activation of a non-insulin-sensitive FoxO1 mutant (FoxO1 mut.). Cells were deprived of serum for 6 hours prior to harvest. Data presented as relative activity and shown as ± SEM; n = 3. *, $P < 0.05$; **, $P < 0.01$; and ***, $P < 0.001$ by one-way ANOVA with Newman-Keuls Multiple Comparison test. (**D**) USP7 fails to affect FoxO1 nuclear/cytoplasmic localization. Fluorescence microscopy images showing typical nuclear and cytoplasmic localization of FoxO1-GFP. Cells were treated as in (**C**).

Since insulin is known to inhibit FoxO1 activity through Akt-mediated phosphorylation and nuclear exclusion (14, 19, 42), we wanted to examine whether USP7 could be acting downstream of insulin. A constitutively active myristoylated Akt construct potently suppressed FoxO1 activity, which was to a greater degree than USP7 alone (Figure 4.2B). However, when we used a FoxO1 mutant that is resistant to Akt-mediated phosphorylation and suppression, we found that expression of wildtype USP7 was still capable of attenuating FoxO1 transcriptional activity (Figure 4.2C). Based on previous reports that USP7-mediated deubiquitination of FoxO3/4 results in its nuclear exclusion (25), we co-transfected USP7 with a GFP-fused FoxO1 to test the effect of USP7 on FoxO1 localization. Under conditions identical to that where USP7 overexpression decreased FoxO1 transcriptional activation, we failed to observe an appreciable change in FoxO1 localization. This was true of both wildtype FoxO1 and a non-insulin-sensitive mutant (Figure 4.2D and Figure 4.3). These data suggest that USP7-mediated deubiquitination of FoxO1 leads to a suppression of its transcriptional activity.

USP7 suppresses gluconeogenesis in primary hepatocytes

Given the effect of USP7 on FoxO1 transcriptional activity, we hypothesized that USP7 might control FoxO1 activation of gluconeogenesis. To interrogate a link between USP7 and gluconeogenesis, we examined the effect of targeting USP7 with short hairpin RNA (shRNA) on gluconeogenic gene expression in primary culture of mouse hepatocytes. Primary hepatocytes were infected with adenoviruses expressing either a non-targeting scrambled control shRNA (shSCR) or one of two shRNA sequences against USP7 (designated shUSP7#1 and shUSP7#2) and treated with forskolin, a cAMP activator used to mimic the condition of fasting, alone or in combination with insulin (Figure 4.4A). These stimuli were chosen considering roles of FoxO1

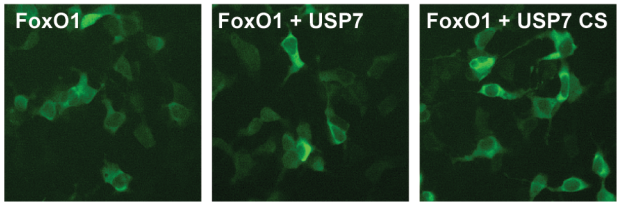

Figure 4.3. USP7 fails to affect FoxO1 nuclear/cytoplasmic localization. Fluorescence microscopy images showing typical nuclear and cytoplasmic localization of FoxO1-GFP in HEK293A cells transfected with the indicated plasmids.

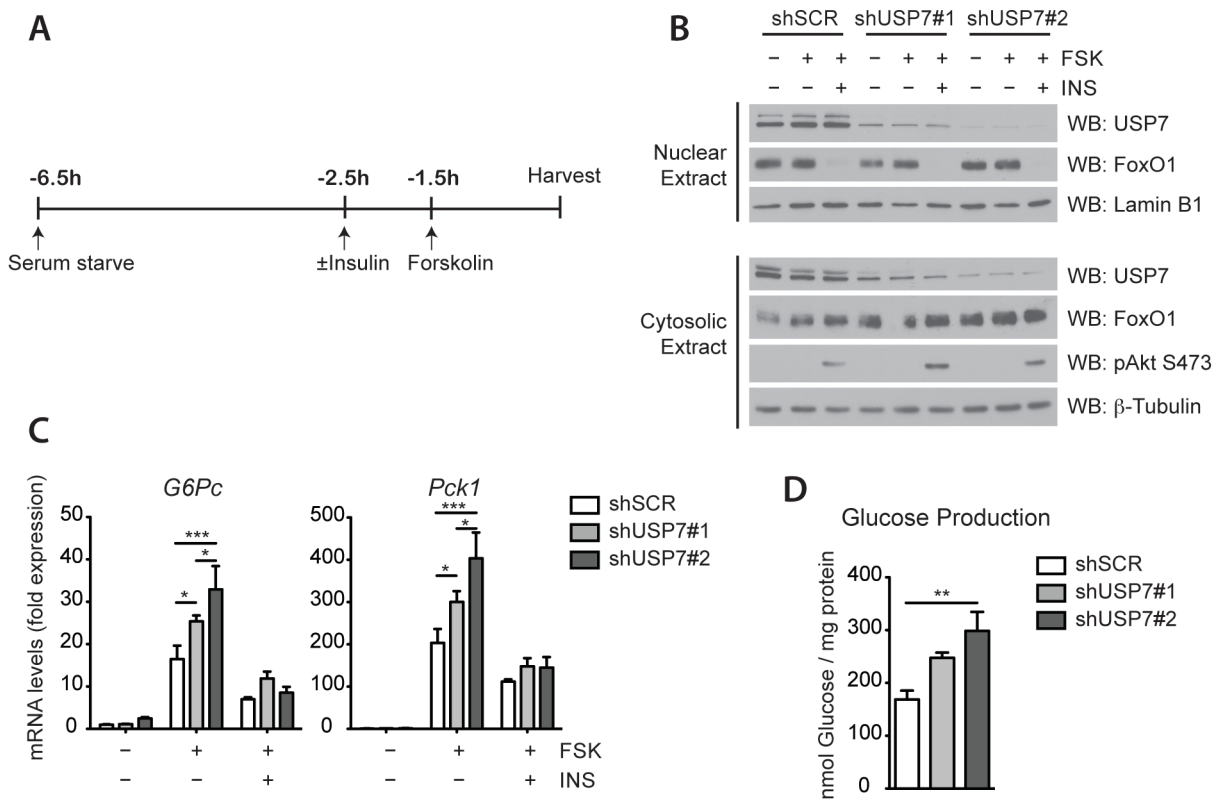

Figure 4.4. USP7 knockdown increases gluconeogenic gene expression and glucose production in primary hepatocytes. (**A**) Schematic of forskolin (FSK) and insulin (INS) treatment of primary hepatocytes. To mimic fasting conditions, cells were serum-starved in 0.2% BSA for 5 hours prior to a 1.5-hour incubation with 10 μM forskolin. To analyze the effect of insulin on suppression of gluconeogenic gene induction, cells were serum-starved for 4 hours prior to a 1-hour pretreatment with 100 nM insulin followed by a 1.5-hour incubation with both insulin and forskolin. (**B**) Insulin signaling in primary hepatocytes with USP7 knockdown. Western blot analysis of nuclear and cytosolic fractions from hepatocytes as treated in (**A**). (**C**) USP7 knockdown increases gluconeogenic gene expression upon forskolin treatment. Primary hepatocytes were infected with control (shSCR) or USP7 shRNA adenoviruses and subjected to the conditions presented in (**A**). mRNA levels are graphed relative to expression of unstimulated/serum-starved shSCR and presented as average ± SEM; n = 3. *, $P < 0.05$; and ***, $P < 0.001$ by one-way ANOVA with Newman-Keuls Multiple Comparison test. Data are representative of at least two independent experiments. (**D**) USP7 knockdown increases glucose levels in medium after overnight forskolin treatment. Glucose in medium of primary hepatocytes treated overnight with 10 μM forskolin was measured 3 hours after culturing in glucose-free medium supplemented with pyruvate and lactate. Presented as average ± SEM; n = 3. **, $P < 0.01$ by one-way ANOVA with Newman-Keuls Multiple Comparison test.

in both the cAMP induction of gluconeogenic genes and the insulin-mediated inhibition of cAMP-induced gluconeogenesis (9, 10, 13, 43). Adenoviral-mediated expression of shUSP7 sequences resulted in dramatic reduction of USP7 protein levels without altering FoxO1 amount or localization (Figure 4.4B). Supporting a role for USP7 on expression of FoxO1-target genes, knockdown of USP7 potentiated the forskolin response of *G6Pc* and *Pck1* (Figure 4.4C). These effects on gene expression corresponded with efficiency of knockdown, with increased knockdown of USP7 having the most pronounced increase on gene expression (Figure 4.4, B and C). Pretreatment with insulin prior to and during the forskolin treatment suppressed expression of *G6pc* and *Pck1* to a similar extent in both control and shUSP7 cells (Figure 4.4C). Importantly, the knockdown of USP7 did not lead to a general activation of the cAMP/PKA pathway, as the cAMP-inducible gene *Nurr77* exhibited a similar pattern of expression in shUSP7 and shSCR cells upon forskolin treatment (Figure 4.5A). To evaluate the physiological outcome coinciding with these effects on gene expression, hepatic glucose production was measured from primary hepatocytes adenovirally-infected with shUSP7 and incubated with medium including lactate and pyruvate as gluconeogenic substrates. Consistent with the observed increase in gluconeogenic genes, USP7 knockdown enhanced forskolin-induced glucose production (Figure 4.4D).

In order to better assess the role of USP7 activity on gluconeogenesis, we performed complementary gain-of-function experiments in primary hepatocytes with adenoviruses expressing USP7. A modest increase of wildtype USP7 over endogenous levels caused a significant suppression of forskolin-induced increases in *G6Pc* and *Pck1* expression (Figure 4.6, A and B). This was in contrast to overexpression of the catalytically inactive USP7 CS, which had a tendency to potentiate gluconeogenic gene expression (Figure 4.6B). Again, these changes in gene expression were in absence of a global alteration of cAMP-responsiveness, as observed

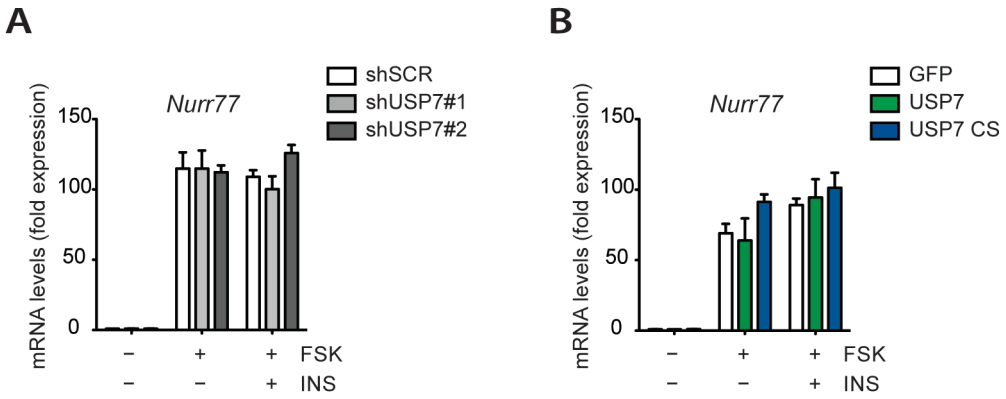

Figure 4.5. USP7 manipulation does not lead to general activation of cAMP-responsiveness. (**A**) USP7 knockdown and (**B**) USP7 overexpression were performed with the indicated adenoviruses and primary hepatocytes subjected to the conditions presented in Figure 4.4A. mRNA levels are graphed relative to expression of unstimulated/serum-starved GFP and presented as average ± SEM; n = 3. *Nurr77* expression was not statistically significant per treatment by one-way ANOVA with Newman-Keuls Multiple Comparison test. Data are representative of at least 2 independent experiments.

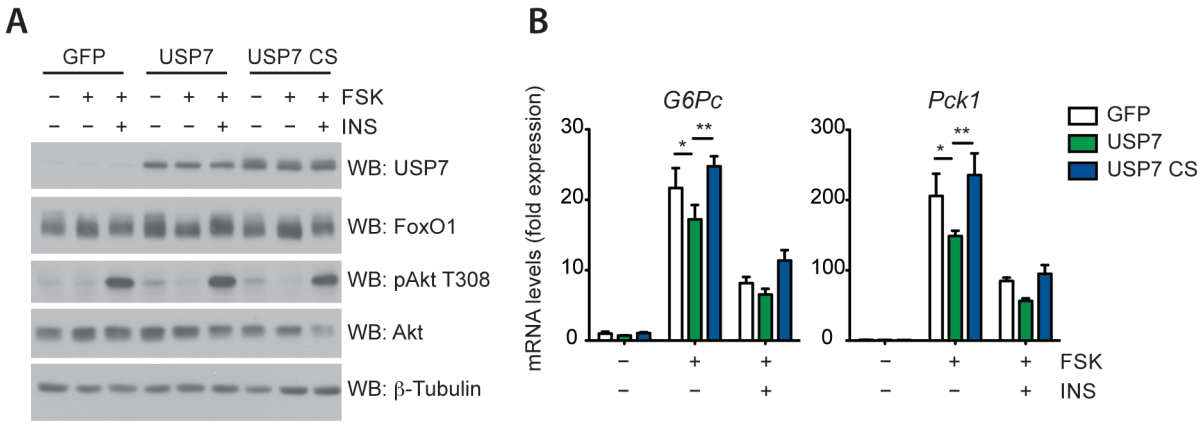

Figure 4.6. USP7 overexpression suppresses gluconeogenic gene expression in primary hepatocytes. (**A**) USP7 does not alter insulin signaling in primary hepatocytes. Western blot analysis of whole-cell extracts from primary hepatocytes infected with control (GFP), USP7 wildtype, or USP7 catalytically-inactive mutant (CS) adenoviruses and subjected to the conditions presented in Figure 4.4A. (**B**) Wildtype USP7 suppresses gluconeogenic gene expression upon forskolin treatment. Hepatocytes were treated as in (**A**). mRNA levels are graphed relative to expression of unstimulated/serum-starved GFP and presented as average ± SEM; n = 3. *, $P < 0.05$; **, $P < 0.01$; and ***, $P < 0.001$ by one-way ANOVA with Newman-Keuls Multiple Comparison test. Data are representative of at least two independent experiments.

by similar forskolin-induced *Nurr77* expression (Figure 4.5B). USP7 overexpression did not affect insulin activation of the PI3K/Akt pathway, nor did it alter the ability of insulin to suppress gluconeogenic genes (Figure 4.6, A and B). Furthermore, USP7 had no effect on total protein levels of FoxO1 (Figure 4.6A). These effects on gluconeogenic genes corroborated the results noted for transient expression of USP7 on FoxO1 transcriptional activation.

USP7 suppresses gluconeogenesis in mouse liver

We next sought to confirm whether these effects of USP7 could be recapitulated *in vivo* by altering hepatic USP7 levels. Tail vein delivery of adenoviral USP7 constructs resulted in significant increases in USP7 protein in the livers of C57BL/6 mice (Figure 4.7A). Given that liver-specific FoxO1 knockout mice exhibit hypoglycemia only after a prolonged fast (13), we decided to observe the effect of USP7 on mice that had been similarly fasted. Indeed, coincident with a role for USP7 in suppression of gluconeogenesis, mice receiving tail vein injection of wildtype USP7, and not the catalytically inactive USP7 CS, exhibited decreased expression of hepatic gluconeogenic genes after prolonged fasting (Figure 4.7B). Of note, nuclear FoxO1 levels were variable but not affected by treatment (Figure 4.7A). Also, suppression of gluconeogenic genes was not due to a disruption of insulin signaling in the livers of these animals, as the phosphorylation status of key targets in the insulin/PI3K/Akt pathway was unaffected by USP7 overexpression (Figure 4.7A).

Next, to determine the physiological consequence of USP7 perturbation in mouse liver, we performed pyruvate tolerance tests on mice with hepatic overexpression of GFP, wildtype USP7, or USP7 CS. In accordance with the change in gluconeogenic genes, overexpression of wildtype USP7 led to a decreased conversion of pyruvate to glucose after pyruvate challenge,

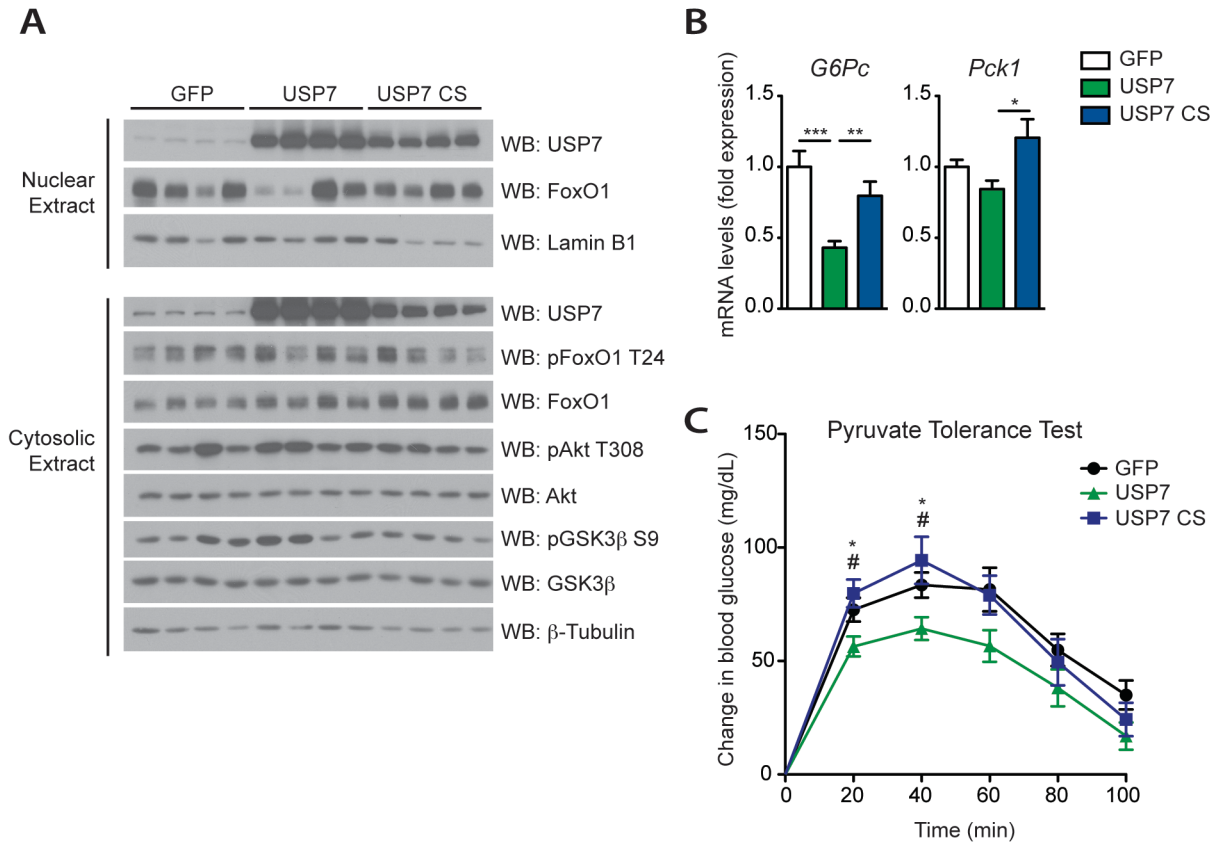

Figure 4.7. USP7 overexpression in C57BL/6 mouse liver suppresses gluconeogenesis. (**A**) Insulin signaling remains relatively unchanged in livers of mice overexpressing USP7. Western blot analysis of nuclear and cytosolic fractions from livers of 48-hour fasted mice. (**B**) Hepatic overexpression of wildtype USP7 suppresses gluconeogenic genes. Liver mRNA levels from mice in (**A**) are graphed relative to expression of GFP and presented as average ± SEM; n = 6-7. *, $P < 0.05$; **, $P < 0.01$; and ***, $P < 0.001$ by one-way ANOVA with Newman-Keuls Multiple Comparison test. (**C**) USP7 overexpression improves pyruvate tolerance. Intraperitoneal (IP) pyruvate tolerance test from mice infected with GFP, wildtype USP7, or USP7 CS adenoviruses. Mice were fasted overnight prior to injection of 2 g/kg sodium pyruvate. Data are presented as change in glycemia following pyruvate injection and are from two independent experiments. Presented as average ± SEM. n = 9-19. *, $P < 0.05$ GFP *vs*. USP7; and #, $P < 0.05$ USP7 *vs*. USP7 CS by one-way ANOVA with Newman-Keuls Multiple Comparison test per time point.

indicating suppressed hepatic gluconeogenesis in these animals (Figure 4.7C). Notably, overexpression of the USP7 CS mutant did not alter pyruvate tolerance, highlighting the importance of USP7 catalytic activity in regulation of glucose homeostasis. In aggregate, these data support a suppressive effect of hepatic USP7 on gluconeogenesis.

Effect of USP7 on gluconeogenesis is dependent on FoxO1 activity

To determine a requirement of endogenous FoxO1 for USP7's effect on gluconeogenesis, we performed double knockdown experiments with shUSP7 adenovirus and an shRNA adenovirus targeting FoxO1 (shFoxO1). As previously reported (13), shFoxO1 dramatically reduced FoxO1 levels, with a concordant reduction of gluconeogenic genes (Figure 4.8, A and B). Importantly, knockdown of FoxO1 abolished the increase in gluconeogenic gene expression observed by both shUSP7 adenoviruses (Figure 4.8B). These results indicate that USP7 depends on the presence of FoxO1 in order to affect gluconeogenic gene expression.

This then begged the question: what controls USP7 activity on FoxO1? Neither stimulation of primary hepatocytes with forskolin nor insulin, conditions where FoxO1 is active and inactive, respectively, produced significant change in USP7 protein levels (Figure 4.9A). Also, USP7 protein and mRNA levels remained constant in livers of fasted and refed mice (Figure 4.9, B and C). In addition, assessment of USP7 activity in whole-cell, nuclear, and cytoplasmic lysates of primary hepatocytes failed to recognize an appreciable effect of hormonal stimulation on catalytic activity (Figure 4.9, D and E). Thus, stimuli that dramatically affect FoxO1 transcriptional activation do not appear to alter USP7 levels or activity. In summation, these results suggest that USP7 modulation of FoxO1 transcriptional activity occurs subsequent to nuclear FoxO1 availability.

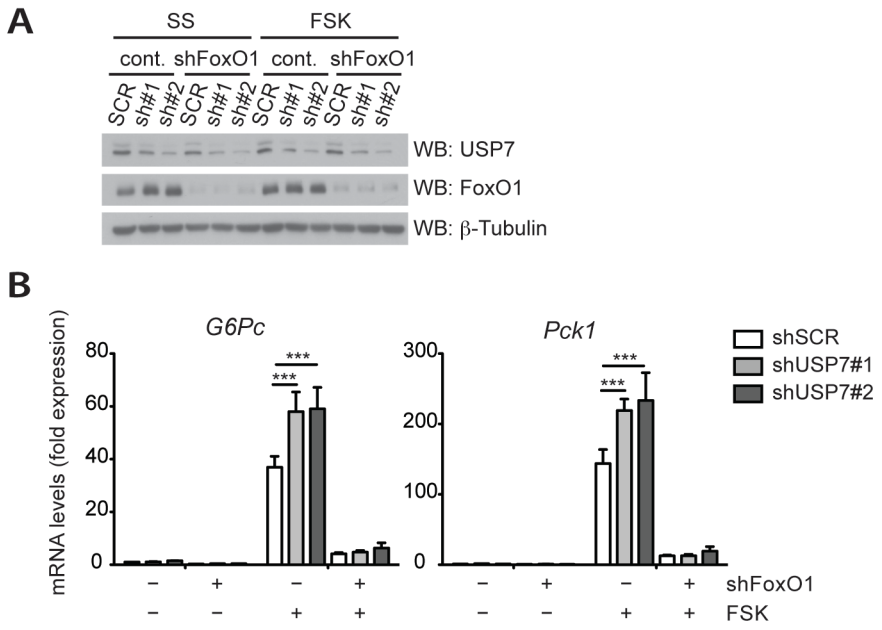

Figure 4.8. USP7's effect on gluconeogenic gene expression is dependent on FoxO1. (**A**) Efficient knockdown of FoxO1 protein upon double knockdown with USP7. Western blot analysis of whole-cell extracts from primary hepatocytes infected with the indicated adenoviruses (in the absence of shFoxO1, cells received co-infection with corresponding control shRNA adenovirus) and serum-starved in 0.2% BSA for 3 hours prior to a 1.5-hour incubation with 10 μM forskolin. (**B**) Knockdown of FoxO1 abolishes the effect of USP7 knockdown on gluconeogenic gene expression. mRNA levels are graphed relative to expression of unstimulated/serum-starved control shSCR and presented as average ± SEM; n = 3. *, $P < 0.05$; and ***, $P < 0.001$ by one-way ANOVA with Newman-Keuls Multiple Comparison test. Data are representative of at least two independent experiments.

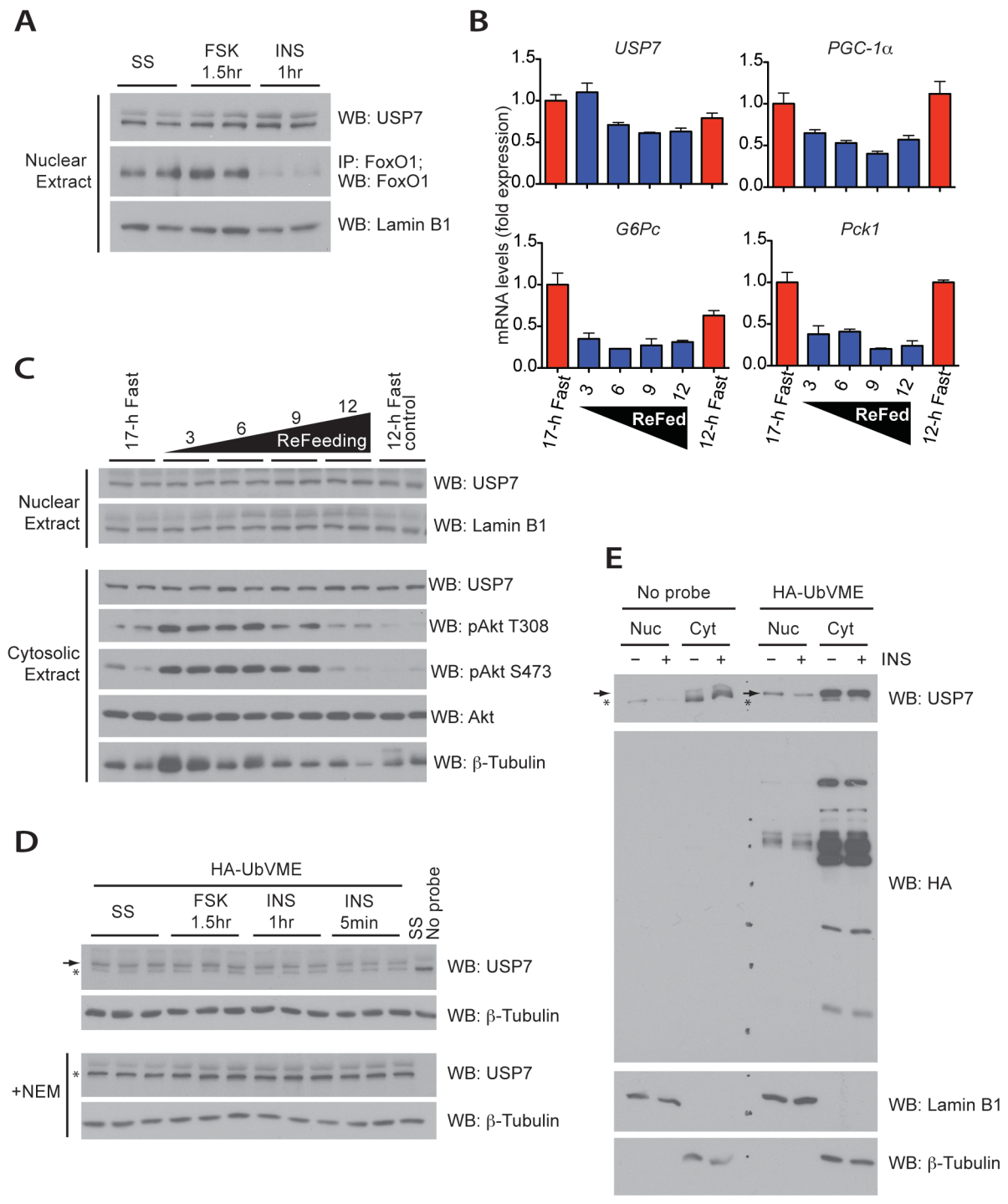

Figure 4.9. USP7 levels and activity are unchanged by fasting/feeding stimuli. (**A**) Levels of nuclear USP7 are unchanged by hormonal stimulation. Primary hepatocytes were serum-starved in 0.2% BSA prior to treatment with 10 μM forskolin (FSK) or 100 nM insulin (INS) for the indicated durations. (**B**) *USP7* mRNA levels in mouse liver are relatively unchanged during fasting/feeding. BALB/c mice were subjected to a 17-hour fast, after which food was

Figure 4.9 (Continued). reintroduced and mice sacrificed 3, 6, 9, and 12 hours after initiation of feeding. To control for effects that are predominantly circadian, one group (12-h Fast) was allowed normal overnight feeding but then subjected to a 12-hour fast in parallel with the 12-hour refeeding group. Liver mRNA levels are graphed relative to expression of the overnight 17-hour fast and presented as average ± SEM; n=3. (**C**) USP7 protein is not regulated by fasting/feeding in mouse liver. Western blot analysis of nuclear and cytosolic extracts from liver isolated from mice in (**B**). Analysis performed on two mice per time point. (**D–E**) Hormonal stimulants fail to affect USP7 activity. Primary hepatocytes were serum-starved prior to treatment with 10 μM forskolin or 100 nM insulin for the indicated durations. Extracts were incubated with deubiquitinating enzyme activity probe (HA-UbVME), followed by western blot analysis with anti-USP7 antibody. Active USP7 is indicated by a shift in USP7 molecular weight (~8 kDa) and denoted by an arrow. An asterisk indicates unlabeled (inactive) USP7. In (**D**), whole-cell extracts were analyzed; bottom panel shows samples run in parallel that received pre-incubation with NEM as a control for the assay. Treatments are shown in triplicate. In (**E**), the activity of nuclear versus cytoplasmic extracts was analyzed.

USP7 modulates FoxO1 occupancy on promoters of gluconeogenic genes

We had originally hypothesized that USP7-mediated deubiquitination of FoxO1 would lead to nuclear exclusion, as indicated for the mechanism in its interaction with FoxO3/4 (25). However, we have not seen such an effect with transient overexpression of USP7 and FoxO1 in HEK293A cells (Figure 4.3), and have failed to detect a significant change in the level of endogenous nuclear FoxO1 upon USP7 knockdown (Figure 4.4B) or overexpression (Figure 4.7A). Since USP7 did not alter the nuclear/cytoplasmic localization of FoxO1, we examined the ability of USP7 to modulate the association of FoxO1 with gluconeogenic promoters. Using primers that specifically span the IRE(s) of *G6Pc* and *Pck1* (Figure 4.10A), we performed chromatin immunoprecipitation (ChIP) of FoxO1 from primary hepatocytes infected with shSCR or shUSP7 and stimulated with forskolin. Compared to unstimulated cells, forskolin treatment resulted in increased ChIP of endogenous FoxO1 with *G6Pc* and *Pck1* promoters (Figure 4.10B). Knockdown of USP7 further potentiated the forskolin-induced FoxO1 occupancy at these promoters (Figure 4.10B). Notably, this increase in FoxO1 promoter binding by USP7 knockdown occurred irrespective of unaltered nuclear FoxO1 levels (Figure 4.11A). And consistent with elevated gluconeogenic gene expression, histone H3 acetylation at Lys9 (H3K9Ac), a marker of increased transcriptional activity recently shown to be elevated over *G6Pc* and *Pck1* in livers of fasting and diabetic animals (44), was found to be significantly higher on the *G6Pc* promoter upon USP7 knockdown (Figure 4.11B).

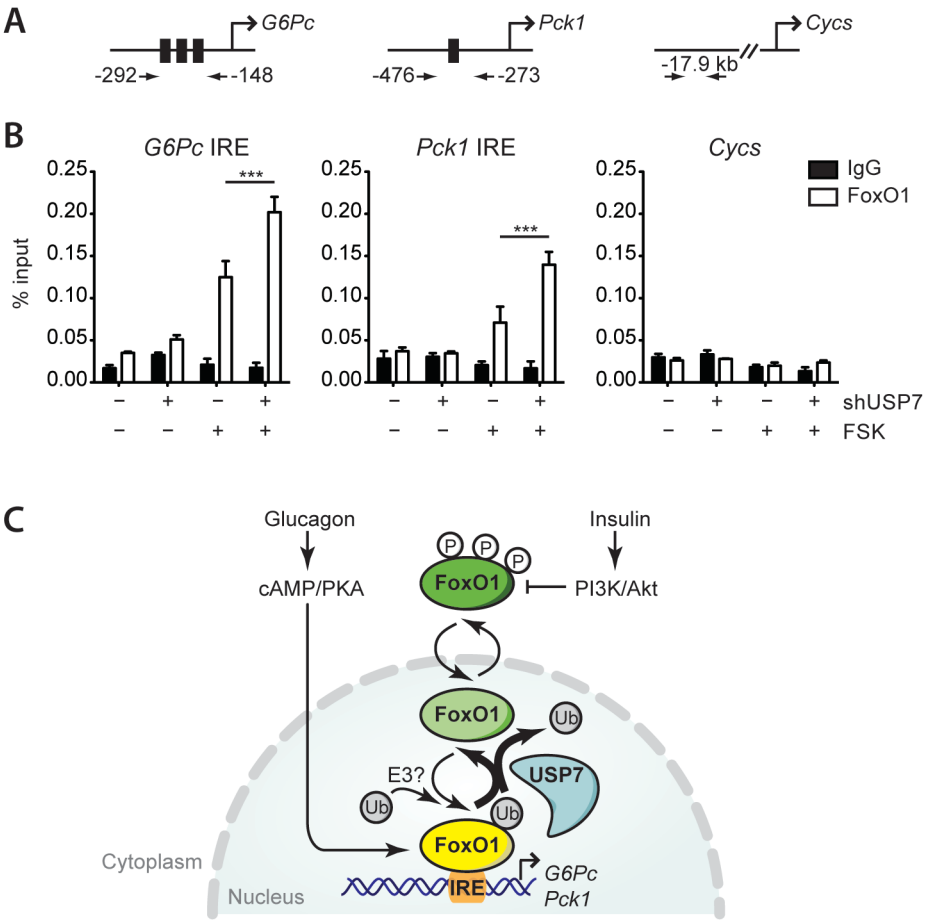

Figure 4.10. USP7 alters FoxO1 occupancy at gluconeogenic gene promoters. (**A–B**) ChIP-qPCR analysis reveals increased association of FoxO1 with *G6Pc* and *Pck1* promoters at IRE regions upon USP7 knockdown. Schematic in (**A**) indicates primers used for amplification of FoxO1 binding sites (black boxes in promoters of *G6Pc* and *Pck1*) and a control region (*Cycs*). In (**B**), cells were infected with the indicated adenoviruses and treated with 10 μM forskolin for 1.5 hours prior to harvest and ChIP assay of FoxO1. Results graphed as average ± SEM; n = 3. *, $P < 0.05$ by one-way ANOVA with Newman-Keuls Multiple Comparison test. Data are representative of at least two independent experiments. (**C**) Model illustrating novel role for USP7 in deubiquitination and suppression of FoxO1 activity. Transcriptionally active FoxO1 is presented in yellow, and inactive forms of FoxO1 are presented in shades of green. Fasting-induced glucagon stimulus through cAMP/PKA activates FoxO1 transcription of gluconeogenic genes *G6Pc* and *Pck1*. Monoubiquitination of FoxO1, through an as-of-yet unidentified E3 ligase, promotes FoxO1 activity through enhanced occupancy over binding sites (IRE) on *G6Pc* and *Pck1* promoters. During feeding, insulin suppresses hepatic gluconeogenesis through the PI3K/Akt-mediated phosphorylation and nuclear exclusion of FoxO1. Our results presented here suggest that USP7 acts as a break on nuclear FoxO1 through deubiquitination to suppress its association with promoters of gluconeogenic genes.

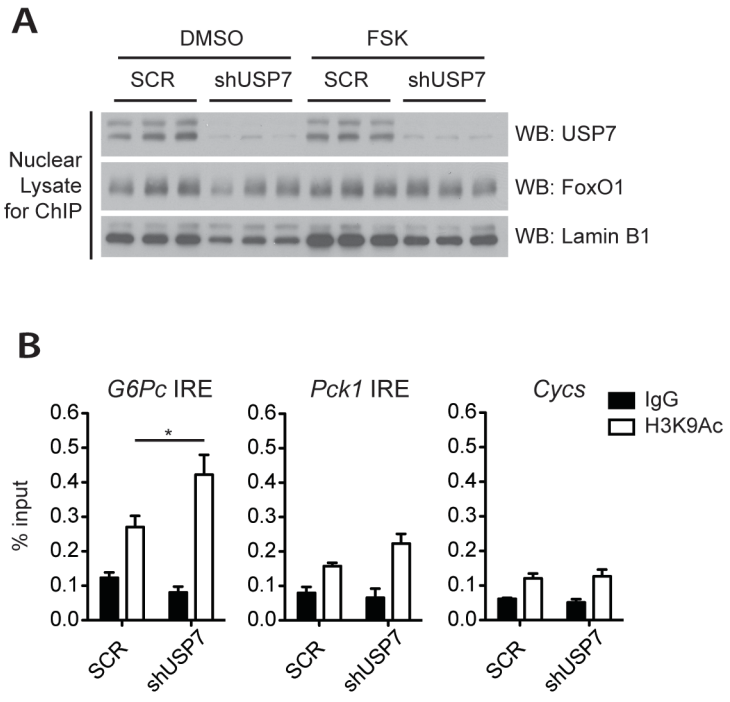

Figure 4.11. FoxO1 targets show increased H3K9Ac despite steady levels of nuclear FoxO1 upon USP7 knockdown. (**A**) Nuclear FoxO1 is unchanged in primary hepatocyte lysates from USP7 knockdown. Western blot analysis of nuclear lysate used for ChIP analysis in Figure 4.10B. (**B**) H3K9Ac is increased over gluconeogenic genes with knockdown of USP7. Cells were infected with the indicated adenoviruses and treated with 10 μM forskolin for 1.5 hours prior to harvest and ChIP with anti-histone H3K9Ac antibody (Abcam) followed by qPCR. Results graphed as average ± SEM; n = 3. *, $P < 0.05$ by one-way ANOVA with Newman-Keuls Multiple Comparison test.

DISCUSSION

Our studies expand the role of the USP7 deubiquitinating enzyme to FoxO1 modulation and regulation of glucose homeostasis. The findings presented here suggest that FoxO1 transcriptional activity is controlled by USP7-mediated deubiquitination. FoxO1-target genes were increased upon USP7 knockdown and conversely suppressed with overexpression of wildtype USP7. These changes in gene expression led to altered hepatic glucose output as assessed in cells and mouse liver. Importantly, the effect of USP7 on gluconeogenic genes required activity of FoxO1. In light of these data, we propose a model where deubiquitination of FoxO1 by USP7 leads to decreased occupancy of FoxO1 at promoters of gluconeogenic genes, thereby suppressing gluconeogenesis (Figure 4.10C).

Previous studies have looked at the effect of stress-induced monoubiquitination of FoxO proteins, having found that monoubiquitination promotes FoxO-dependent transcription. However, these studies focused on FoxO4 in the cell cycle (25, 40, 41). The present data support this model of monoubiquitination-induced increase in FoxO transactivation and broaden its biologic effects to the area of hepatic glucose metabolism. Our findings, in combination with others, suggest a common regulatory mechanism for USP7 and the family of FoxO proteins. However, contrary to its reported mechanism for FoxO3/4 (25), we found that USP7 suppresses FoxO1 activity in absence of an effect on its nuclear/cytoplasmic localization.

Altered FoxO1 transactivation despite unchanged nuclear accumulation is not an unusual concept, as FoxO proteins may exhibit reduced activity by mechanisms that do not depend on cellular redistribution. For example, insulin is still able to inhibit a mutant of FoxO1 that is rendered constitutively nuclear by mutation in the nuclear export signal (45). In addition, phosphorylation of FoxO1 residue S256 alters its in vitro binding activity by introducing a

negative charge that interferes with basic residues in the DNA-binding domain of FoxO1 (46). This disruption of FoxO1 affinity for target chromatin has also been seen with acetylation, where acetylated FoxO1 has attenuated ability to bind DNA (47). Since we observed increased FoxO1 binding to gene promoters upon USP7 knockdown—when monoubiquitination of FoxO1 is presumably elevated—the presence of ubiquitin moieties might facilitate FoxO1 association with chromatin. Related to this, a recent report has implicated a role for USP7 in the dissociation of minichomosome maintenance (MCM) complex from chromatin at the end of S-phase (48), which the authors suggest might occur subsequent to mono-deubiquitination of MCM. Thus, the ability of monoubiquitination to alter FoxO1 recruitment to DNA deserves further exploration.

An intriguing study by Nardini *et al*. has shown that monoubiquitination of the transcription factor NF-Y is necessary for active transcription of target genes by mimicking and, thus, facilitating monoubiquitination of histone H2B at Lys120, an epigenetic mark associated with transcriptional activation (49). This is important to our current findings given work originally done in flies that revealed a role for USP7 in epigenetic silencing through deubiquitination of H2B (50). Although it is disputed whether USP7 deubiquitinates H2B in mammalian cells, USP7 has also been shown to deubiquitinate and stabilize Polycomb repressive complex 1 (PRC1), which confers gene repression by H2A monoubiquitination (51). Taken together, it is interesting to speculate a function for monoubiquitination of FoxO1 in the activation of permissible histone marks and—coordinately—mono-deubiquitination of FoxO1 by USP7 in transcriptional silencing.

The binding of cofactors to transcription factors can also facilitate a transcriptionally-favorable chromatin environment. Thus, a third possibility exists where USP7 might modulate FoxO1 activity by affecting the association of FoxO1 with coregulators, such as CREB binding

protein (CBP) and its related protein p300 (CBP/p300) or PGC-1α. The binding of histone acetyltransferases CBP/p300 to FoxO proteins is essential for the transactivation of target gene promoters (52-54). This is true also of PGC-1α, which coactivates FoxO1 on gluconeogenic promoters in an insulin-sensitive fashion (10). Whether USP7-mediated deubiquitination of FoxO1 inhibits these interactions, or whether monoubiquitinated FoxO1 enhances them, is unknown.

In some cases, the same lysine residues are alternately acetylated or ubiquitinated. Of note, the specific lysines that are acetylated in FoxO1 are not the ones that get polyubiquitinated (55). Interestingly, the effect of deubiquitination on FoxO1 as reported here is the opposite of that observed by deacetylation of FoxO1, where deacetylation increases FoxO1 transcriptional activity (56, 57). Does monoubiquitination antagonize acetylation—or vice versa? Van der Horst and colleagues reported a reduction of FoxO4 monoubiquitination with mutation of lysine residues Lys199 and Lys211, which are sites of acetylation that are conserved among FoxOs (25). These findings might indicate overlapping and alternately monoubiquitinated/acetylated FoxO residues. However, this mutant did not exhibit altered transcriptional activity, and the authors did not address its function in the presence of USP7, questioning whether these residues are true targets for USP7-mediated deubiquitination. Nevertheless, the extent that monoubiquitination affects other posttranslational modifications, and where it falls in the hierarchy for eliciting functional change, requires future attention.

Our findings of unaltered USP7 protein and activity upon fasting and feeding stimuli have led us to propose a model whereby USP7 suppresses FoxO1 transactivation mainly under fasting conditions, when FoxO1 is predominantly nuclear. Given that insulin/Akt overrode effects shown by USP7 loss- and gain-of-function experiments, a role for USP7 action on FoxO1

during feeding cannot be concluded. More specifically, our data indicate that nuclear FoxO1 is requisite for USP7 function. Although a physiological role for USP7-mediated suppression of gluconeogenesis during fasting might seem counterintuitive, it is not unprecedented. In fact, a negative feedback pathway has been suggested where FoxO amplification of insulin/growth factor signaling limits prolonged FoxO activation [reviewed in (58)]. Our data suggest that USP7 is active regardless of hormonal stimulus, thus, acting as a constitutively accessible break on nuclear FoxO1. However, it is reasonable to surmise that the specific activity of USP7 on FoxO1 (as opposed to its enzymatic activity, as assessed by our assays) is subject to hormonal control. USP7 activity can be altered through interactions with different binding partners and through posttranslational modification (50, 59-61); future studies will be required to determine whether USP7-mediated deubiquitination of FoxO1 can be controlled at either of these levels. All together, the results presented here reveal USP7 as an additional node for fine-tuning FoxO1 activity, and suggest that activation of USP7 could be useful in alleviating states of excess hepatic glucose production.

Recently, Lee *et al*. reported that overexpression of USP7 in mouse liver decreased blood glucose by increasing hepatic levels of PPARγ (62). This conclusion is complicated by the fact that PPARγ levels are extremely low in non-obese liver (63), which questions the physiological relevance of a hepatic USP7-PPARγ interaction. In addition, although the authors suggested that elevated PPARγ led to the decreased glycemia upon USP7 overexpression, a causal role in glucose homeostasis was not fully explored. Given our current findings, it is likely that USP7-mediated inactivation of FoxO1 and suppression of hepatic gluconeogenesis contributed to their observed phenotype.

FoxO1 function is also of critical importance for other metabolic tissues, such as skeletal muscle and adipose tissue. Mice overexpressing FoxO1 in skeletal muscle exhibit muscle atrophy and impaired glycemic control (64), whereas inhibition of FoxO transcriptional activity prevents muscle loss (65). In adipose tissue, expression of a dominant negative FoxO1 leads to increased energy expenditure and improved glucose tolerance (66). Thus, under both scenarios, suppression of FoxO1 would be a favorable approach to improve metabolic imbalance. Whether USP7 can inhibit FoxO1 function in muscle and/or adipose tissue will be addressed in future studies. Of note, a functional interaction between USP7 and Tip60 has been reported to be required for 3T3-L1 adipocyte differentiation (67), further supporting a role for USP7 targets in the maintenance of energy/nutrient homeostasis.

The human genome encodes approximately 100 deubiquitinating enzymes, which counteract several hundred ubiquitin ligases, suggesting that ubiquitination and its reversal are subject to considerable specialization and specificity. Because of their high specificity, deubiquitinating enzymes are attractive targets for drug development (24). Our data suggest that USP7 may be important for the regulation of FoxO1 transcriptional activity during fasting/refeeding, making USP7 an excellent candidate for translational applications. The identification here of a deubiquitinase involved in glucose metabolism could provide a potent target for clinical intervention of not only hepatic glucose output in the context of diabetes, but also for broader therapeutic pathways in the treatment of obesity and other metabolic disorders.

ACKNOWLEDGEMENTS

The authors would like to thank members of the Puigserver laboratory for experimental assistance and mechanistic insight, with special thanks to Yoonjin Lee for invaluable aid in

animal experiments. We are grateful to initial work performed by Drs. J. Wade Harper and Sebastian Hayes, for whom without this project would not have been conceived. We would also like to thank Drs. Bruce Spiegelman and John Blenis for helpful discussions, and Drs. Alexander Banks and Pier Pandolfi for donation of reagents that were of critical importance to this work. This work was supported by an American Heart Association predoctoral fellowship (J.A.H.) and postdoctoral fellowship (M.T.). P.P. has support from American Diabetes Association and NIH/NIDDK (R01 069966).

REFERENCES

1. **Newgard CB** 2004 Regulation of glucose metabolism in the liver. In: DeFronzo RA, Ferrannini E, Keen H, Zimmet P eds. International Textbook of Diabetes, Third Edition. Chichester, UK: John Wiley & Sons; 253-275

2. **Zhou G, Myers R, Li Y, Chen Y, Shen X, Fenyk-Melody J, Wu M, Ventre J, Doebber T, Fujii N, Musi N, Hirshman MF, Goodyear LJ, Moller DE** 2001 Role of AMP-activated protein kinase in mechanism of metformin action. J Clin Invest 108:1167-1174

3. **Herzig S, Long F, Jhala US, Hedrick S, Quinn R, Bauer A, Rudolph D, Schutz G, Yoon C, Puigserver P, Spiegelman B, Montminy M** 2001 CREB regulates hepatic gluconeogenesis through the coactivator PGC-1. Nature 413:179-183

4. **Quinn PG, Granner DK** 1990 Cyclic AMP-dependent protein kinase regulates transcription of the phosphoenolpyruvate carboxykinase gene but not binding of nuclear factors to the cyclic AMP regulatory element. Mol Cell Biol 10:3357-3364

5. **Altomonte J, Richter A, Harbaran S, Suriawinata J, Nakae J, Thung SN, Meseck M, Accili D, Dong H** 2003 Inhibition of Foxo1 function is associated with improved fasting glycemia in diabetic mice. Am J Physiol Endocrinol Metab 285:E718-728

6. **Hall RK, Sladek FM, Granner DK** 1995 The orphan receptors COUP-TF and HNF-4 serve as accessory factors required for induction of phosphoenolpyruvate carboxykinase gene transcription by glucocorticoids. Proc Natl Acad Sci U S A 92:412-416

7. **Yoon JC, Puigserver P, Chen G, Donovan J, Wu Z, Rhee J, Adelmant G, Stafford J, Kahn CR, Granner DK, Newgard CB, Spiegelman BM** 2001 Control of hepatic gluconeogenesis through the transcriptional coactivator PGC-1. Nature 413:131-138

8. **Koo SH, Flechner L, Qi L, Zhang X, Screaton RA, Jeffries S, Hedrick S, Xu W, Boussouar F, Brindle P, Takemori H, Montminy M** 2005 The CREB coactivator TORC2 is a key regulator of fasting glucose metabolism. Nature 437:1109-1111

9. **Nakae J, Kitamura T, Silver DL, Accili D** 2001 The forkhead transcription factor Foxo1 (Fkhr) confers insulin sensitivity onto glucose-6-phosphatase expression. J Clin Invest 108:1359-1367

10. **Puigserver P, Rhee J, Donovan J, Walkey CJ, Yoon JC, Oriente F, Kitamura Y, Altomonte J, Dong H, Accili D, Spiegelman BM** 2003 Insulin-regulated hepatic gluconeogenesis through FOXO1-PGC-1alpha interaction. Nature 423:550-555

11. **Li X, Monks B, Ge Q, Birnbaum MJ** 2007 Akt/PKB regulates hepatic metabolism by directly inhibiting PGC-1alpha transcription coactivator. Nature 447:1012-1016

12. **Dong XC, Copps KD, Guo S, Li Y, Kollipara R, DePinho RA, White MF** 2008 Inactivation of hepatic Foxo1 by insulin signaling is required for adaptive nutrient homeostasis and endocrine growth regulation. Cell Metab 8:65-76

13. **Matsumoto M, Pocai A, Rossetti L, Depinho RA, Accili D** 2007 Impaired regulation of hepatic glucose production in mice lacking the forkhead transcription factor Foxo1 in liver. Cell Metab 6:208-216

14. **Nakae J, Park BC, Accili D** 1999 Insulin stimulates phosphorylation of the forkhead transcription factor FKHR on serine 253 through a Wortmannin-sensitive pathway. J Biol Chem 274:15982-15985

15. **Guo S, Rena G, Cichy S, He X, Cohen P, Unterman T** 1999 Phosphorylation of serine 256 by protein kinase B disrupts transactivation by FKHR and mediates effects of insulin on insulin-like growth factor-binding protein-1 promoter activity through a conserved insulin response sequence. J Biol Chem 274:17184-17192

16. **Goswami R, Lacson R, Yang E, Sam R, Unterman T** 1994 Functional analysis of glucocorticoid and insulin response sequences in the rat insulin-like growth factor-binding protein-1 promoter. Endocrinology 134:736-743

17. **Ayala JE, Streeper RS, Desgrosellier JS, Durham SK, Suwanichkul A, Svitek CA, Goldman JK, Barr FG, Powell DR, O'Brien RM** 1999 Conservation of an insulin response unit between mouse and human glucose-6-phosphatase catalytic subunit gene promoters: transcription factor FKHR binds the insulin response sequence. Diabetes 48:1885-1889

18. **Rena G, Guo S, Cichy SC, Unterman TG, Cohen P** 1999 Phosphorylation of the transcription factor forkhead family member FKHR by protein kinase B. J Biol Chem 274:17179-17183

19. **Brunet A, Bonni A, Zigmond MJ, Lin MZ, Juo P, Hu LS, Anderson MJ, Arden KC, Blenis J, Greenberg ME** 1999 Akt promotes cell survival by phosphorylating and inhibiting a Forkhead transcription factor. Cell 96:857-868

20. **Huang H, Regan KM, Wang F, Wang D, Smith DI, van Deursen JM, Tindall DJ** 2005 Skp2 inhibits FOXO1 in tumor suppression through ubiquitin-mediated degradation. Proc Natl Acad Sci U S A 102:1649-1654

21. **Matsuzaki H, Daitoku H, Hatta M, Tanaka K, Fukamizu A** 2003 Insulin-induced phosphorylation of FKHR (Foxo1) targets to proteasomal degradation. Proc Natl Acad Sci U S A 100:11285-11290

22. **Zhang K, Li L, Qi Y, Zhu X, Gan B, DePinho RA, Averitt T, Guo S** 2012 Hepatic suppression of Foxo1 and Foxo3 causes hypoglycemia and hyperlipidemia in mice. Endocrinology 153:631-646

23. **Zhao Y, Wang Y, Zhu WG** 2011 Applications of post-translational modifications of FoxO family proteins in biological functions. J Mol Cell Biol 3:276-282

24. **Reyes-Turcu FE, Ventii KH, Wilkinson KD** 2009 Regulation and cellular roles of ubiquitin-specific deubiquitinating enzymes. Annu Rev Biochem 78:363-397

25. **van der Horst A, de Vries-Smits AM, Brenkman AB, van Triest MH, van den Broek N, Colland F, Maurice MM, Burgering BM** 2006 FOXO4 transcriptional activity is regulated by monoubiquitination and USP7/HAUSP. Nat Cell Biol 8:1064-1073

26. **Everett RD, Meredith M, Orr A, Cross A, Kathoria M, Parkinson J** 1997 A novel ubiquitin-specific protease is dynamically associated with the PML nuclear domain and binds to a herpesvirus regulatory protein. EMBO J 16:566-577

27. **Li M, Chen D, Shiloh A, Luo J, Nikolaev AY, Qin J, Gu W** 2002 Deubiquitination of p53 by HAUSP is an important pathway for p53 stabilization. Nature 416:648-653

28. **Li M, Brooks CL, Kon N, Gu W** 2004 A dynamic role of HAUSP in the p53-Mdm2 pathway. Mol Cell 13:879-886

29. **Nicholson B, Suresh Kumar KG** 2011 The multifaceted roles of USP7: new therapeutic opportunities. Cell Biochem Biophys 60:61-68

30. **Dansen TB, Burgering BM** 2008 Unravelling the tumor-suppressive functions of FOXO proteins. Trends Cell Biol 18:421-429

31. **Tang ED, Nunez G, Barr FG, Guan KL** 1999 Negative regulation of the forkhead transcription factor FKHR by Akt. J Biol Chem 274:16741-16746

32. **Cummins JM, Vogelstein B** 2004 HAUSP is required for p53 destabilization. Cell Cycle 3:689-692

33. **Lim KL, Chew KC, Tan JM, Wang C, Chung KK, Zhang Y, Tanaka Y, Smith W, Engelender S, Ross CA, Dawson VL, Dawson TM** 2005 Parkin mediates nonclassical, proteasomal-independent ubiquitination of synphilin-1: implications for Lewy body formation. J Neurosci 25:2002-2009

34. **Qiang L, Banks AS, Accili D** 2010 Uncoupling of acetylation from phosphorylation regulates FoxO1 function independent of its subcellular localization. J Biol Chem 285:27396-27401

35. **Dominy JE, Jr., Lee Y, Jedrychowski MP, Chim H, Jurczak MJ, Camporez JP, Ruan HB, Feldman J, Pierce K, Mostoslavsky R, Denu JM, Clish CB, Yang X, Shulman GI, Gygi SP, Puigserver P** 2012 The deacetylase Sirt6 activates the acetyltransferase GCN5 and suppresses hepatic gluconeogenesis. Mol Cell 48:900-913

36. **Matsumoto M, Han S, Kitamura T, Accili D** 2006 Dual role of transcription factor FoxO1 in controlling hepatic insulin sensitivity and lipid metabolism. J Clin Invest 116:2464-2472

37. **Nelson JD, Denisenko O, Bomsztyk K** 2006 Protocol for the fast chromatin immunoprecipitation (ChIP) method. Nat Protoc 1:179-185

38. **Rodgers JT, Puigserver P** 2007 Fasting-dependent glucose and lipid metabolic response through hepatic sirtuin 1. Proc Natl Acad Sci U S A 104:12861-12866

39. **Borodovsky A, Ovaa H, Kolli N, Gan-Erdene T, Wilkinson KD, Ploegh HL, Kessler BM** 2002 Chemistry-based functional proteomics reveals novel members of the deubiquitinating enzyme family. Chem Biol 9:1149-1159

40. **Brenkman AB, de Keizer PL, van den Broek NJ, Jochemsen AG, Burgering BM** 2008 Mdm2 induces mono-ubiquitination of FOXO4. PLoS One 3:e2819

41. **Brenkman AB, de Keizer PL, van den Broek NJ, van der Groep P, van Diest PJ, van der Horst A, Smits AM, Burgering BM** 2008 The peptidyl-isomerase Pin1 regulates p27kip1 expression through inhibition of Forkhead box O tumor suppressors. Cancer Res 68:7597-7605

42. **Biggs WH, 3rd, Meisenhelder J, Hunter T, Cavenee WK, Arden KC** 1999 Protein kinase B/Akt-mediated phosphorylation promotes nuclear exclusion of the winged helix transcription factor FKHR1. Proc Natl Acad Sci U S A 96:7421-7426

43. **Wondisford AR, Xiong L, Chang E, Meng S, Meyers DJ, Li M, Cole PA, He L** 2014 Control of Foxo1 Gene Expression by Co-activator P300. J Biol Chem 289:4326-4333

44. **Ravnskjaer K, Hogan MF, Lackey D, Tora L, Dent SY, Olefsky J, Montminy M** 2013 Glucagon regulates gluconeogenesis through KAT2B- and WDR5-mediated epigenetic effects. J Clin Invest 123:4318-4328

45. **Tsai WC, Bhattacharyya N, Han LY, Hanover JA, Rechler MM** 2003 Insulin inhibition of transcription stimulated by the forkhead protein Foxo1 is not solely due to nuclear exclusion. Endocrinology 144:5615-5622

46. **Zhang X, Gan L, Pan H, Guo S, He X, Olson ST, Mesecar A, Adam S, Unterman TG** 2002 Phosphorylation of serine 256 suppresses transactivation by FKHR (FOXO1) by multiple mechanisms. Direct and indirect effects on nuclear/cytoplasmic shuttling and DNA binding. J Biol Chem 277:45276-45284

47. **Matsuzaki H, Daitoku H, Hatta M, Aoyama H, Yoshimochi K, Fukamizu A** 2005 Acetylation of Foxo1 alters its DNA-binding ability and sensitivity to phosphorylation. Proc Natl Acad Sci U S A 102:11278-11283

48. **Jagannathan M, Nguyen T, Gallo D, Luthra N, Brown GW, Saridakis V, Frappier L** 2014 A Role for USP7 in DNA Replication. Mol Cell Biol 34:132-145

49. **Nardini M, Gnesutta N, Donati G, Gatta R, Forni C, Fossati A, Vonrhein C, Moras D, Romier C, Bolognesi M, Mantovani R** 2013 Sequence-specific transcription factor NF-Y displays histone-like DNA binding and H2B-like ubiquitination. Cell 152:132-143

50. **van der Knaap JA, Kumar BR, Moshkin YM, Langenberg K, Krijgsveld J, Heck AJ, Karch F, Verrijzer CP** 2005 GMP synthetase stimulates histone H2B deubiquitylation by the epigenetic silencer USP7. Mol Cell 17:695-707

51. **Maertens GN, El Messaoudi-Aubert S, Elderkin S, Hiom K, Peters G** 2010 Ubiquitin-specific proteases 7 and 11 modulate Polycomb regulation of the INK4a tumour suppressor. EMBO J 29:2553-2565

52. **Nasrin N, Ogg S, Cahill CM, Biggs W, Nui S, Dore J, Calvo D, Shi Y, Ruvkun G, Alexander-Bridges MC** 2000 DAF-16 recruits the CREB-binding protein coactivator complex to the insulin-like growth factor binding protein 1 promoter in HepG2 cells. Proc Natl Acad Sci U S A 97:10412-10417

53. **Perrot V, Rechler MM** 2005 The coactivator p300 directly acetylates the forkhead transcription factor Foxo1 and stimulates Foxo1-induced transcription. Mol Endocrinol 19:2283-2298

54. **Yang Y, Zhao Y, Liao W, Yang J, Wu L, Zheng Z, Yu Y, Zhou W, Li L, Feng J, Wang H, Zhu WG** 2009 Acetylation of FoxO1 activates Bim expression to induce apoptosis in response to histone deacetylase inhibitor depsipeptide treatment. Neoplasia 11:313-324

55. **Kitamura YI, Kitamura T, Kruse JP, Raum JC, Stein R, Gu W, Accili D** 2005 FoxO1 protects against pancreatic beta cell failure through NeuroD and MafA induction. Cell Metab 2:153-163

56. **Daitoku H, Hatta M, Matsuzaki H, Aratani S, Ohshima T, Miyagishi M, Nakajima T, Fukamizu A** 2004 Silent information regulator 2 potentiates Foxo1-mediated transcription through its deacetylase activity. Proc Natl Acad Sci U S A 101:10042-10047

57. **Frescas D, Valenti L, Accili D** 2005 Nuclear trapping of the forkhead transcription factor FoxO1 via Sirt-dependent deacetylation promotes expression of glucogenetic genes. J Biol Chem 280:20589-20595

58. **Hay N** 2011 Interplay between FOXO, TOR, and Akt. Biochim Biophys Acta 1813:1965-1970

59. **Fernandez-Montalvan A, Bouwmeester T, Joberty G, Mader R, Mahnke M, Pierrat B, Schlaeppi JM, Worpenberg S, Gerhartz B** 2007 Biochemical characterization of USP7 reveals post-translational modification sites and structural requirements for substrate processing and subcellular localization. FEBS J 274:4256-4270

60. **Epping MT, Meijer LA, Krijgsman O, Bos JL, Pandolfi PP, Bernards R** 2011 TSPYL5 suppresses p53 levels and function by physical interaction with USP7. Nat Cell Biol 13:102-108

61. **Khoronenkova SV, Dianova, II, Ternette N, Kessler BM, Parsons JL, Dianov GL** 2012 ATM-dependent downregulation of USP7/HAUSP by PPM1G activates p53 response to DNA damage. Mol Cell 45:801-813

62. **Lee KW, Cho JG, Kim CM, Kang AY, Kim M, Ahn BY, Chung SS, Lim KH, Baek KH, Sung JH, Park KS, Park SG** 2013 Herpesvirus-associated Ubiquitin-specific Protease (HAUSP) Modulates Peroxisome Proliferator-activated Receptor gamma (PPARgamma) Stability through Its Deubiquitinating Activity. J Biol Chem 288:32886-32896

63. **Tontonoz P, Hu E, Graves RA, Budavari AI, Spiegelman BM** 1994 mPPAR gamma 2: tissue-specific regulator of an adipocyte enhancer. Genes Dev 8:1224-1234

64. **Kamei Y, Miura S, Suzuki M, Kai Y, Mizukami J, Taniguchi T, Mochida K, Hata T, Matsuda J, Aburatani H, Nishino I, Ezaki O** 2004 Skeletal muscle FOXO1 (FKHR) transgenic mice have less skeletal muscle mass, down-regulated Type I (slow twitch/red muscle) fiber genes, and impaired glycemic control. J Biol Chem 279:41114-41123

65. **Reed SA, Senf SM, Cornwell EW, Kandarian SC, Judge AR** 2011 Inhibition of IkappaB kinase alpha (IKKalpha) or IKKbeta (IKKbeta) plus forkhead box O (Foxo) abolishes skeletal muscle atrophy. Biochem Biophys Res Commun 405:491-496

66. **Nakae J, Cao Y, Oki M, Orba Y, Sawa H, Kiyonari H, Iskandar K, Suga K, Lombes M, Hayashi Y** 2008 Forkhead transcription factor FoxO1 in adipose tissue regulates energy storage and expenditure. Diabetes 57:563-576

67. **Gao Y, Koppen A, Rakhshandehroo M, Tasdelen I, van de Graaf SF, van Loosdregt J, van Beekum O, Hamers N, van Leenen D, Berkers CR, Berger R, Holstege FC, Coffer PJ, Brenkman AB, Ovaa H, Kalkhoven E** 2013 Early adipogenesis is regulated through USP7-mediated deubiquitination of the histone acetyltransferase TIP60. Nat Commun 4:2656

Chapter 5

Conclusions and Future Directions

Mammals preserve energy balance through complex homeostatic mechanisms that integrate endocrine and neural signals with metabolic gene programs across multiple organ systems. The central theme of this body of work concerns understanding key pathways at the intersection of hormonal and transcriptional control that aid in the maintenance of energy homeostasis. This work portrays two distinct pathways—one for thyroid hormone and one for insulin signaling.

Thyroid hormone signaling: D2 in adaptive thermogenesis

In Chapters 2 and 3, we explored the role of type 2 deiodinase (D2) in brown fat development and function. D2 is an enzyme that activates the prohormone thyroxine (T4) to the biologically active form of thyroid hormone, 3,5,3′-triiodothyronine (T3), in individual cells and has previously been recognized for its crucial role in amplification of thyroid hormone signaling in brown adipose tissue (BAT) during the acute thermogenic response to cold (1, 2). By analyzing BAT development in mice with inactivation of the D2 pathway (D2KO), we demonstrate in Chapter 2 that BAT D2 is necessary for coordinating the expression of key genes that contribute to the proper development and identity of BAT. Absence of D2-generated T3 results in defective differentiation of brown preadipocytes *in vitro*, which can be linked to oxidative stress and impaired insulin signaling. Chapter 3, we found that D2KO mice are more susceptible to high-fat diet-induced obesity, glucose intolerance, and hepatic steatosis. Importantly, this phenotype is only realized when the thermal stress of room temperature is eliminated by rearing mice at thermoneutrality. These findings highlight the importance of D2-generated T3 in BAT development, where it plays a crucial role in providing the mature brown

adipocyte with the molecular signature required for adaptive thermogenesis and protection from obesity.

Therapeutic potential for targeting D2 in obesity

Given the recent discovery of BAT in adult humans (3-5), targeting pathways to activate this tissue could provide a physiological model to increase energy expenditure and correct the overabundance of stored energy in obese individuals. Thyroid hormone has long been appreciated as one of the known activators of brown fat in rodents, and recent reports suggest that hyperthyroidism in humans also leads to increased BAT activity (6, 7). However, given its pleiotropic effects, general administration of T3 would be an ill-advised approach to activate adaptive thermogenesis in BAT. Previous efforts to do so have resulted in adverse effects, including tachycardia, muscle wasting, and bone loss (8). Because the TR isoform TRβ positively regulates *UCP1* expression, there have been several attempts to reap the therapeutic benefits of selective TRβ agonism, and preliminary results with TRβ-selective agonists in rodent models suggest this could be an effective approach to harness the positive effects of thyroid hormone on brown fat activation and weight loss (9-11).

Yet another alternative to selectively increase T3 in BAT would be to target D2 enzymatic activity, which could locally amplify thyroid hormone signaling in BAT and thus avoid systemic side effects. Indeed, our results showing an obesity-prone D2KO mouse suggest that D2 normally functions to protect from obesity. That D2 might play a similar protective function in humans is suggested by a common sequence polymorphism in the *Dio2* gene, which is strongly associated with insulin resistance and type 2 diabetes (12, 13). Several small molecules have been reported to increase D2 activity, such as kaempferol (14), chemical

chaperones (15), and bile acids (16), lending support to the tractability of D2 activation and its therapeutic appeal as an anti-obesity target. Activating D2 in human BAT could be effective at inducing adaptive thermogenesis, but it will also require that there is sufficient BAT mass to do so.

In Chapter 2, we discovered a role for D2 in proper brown fat development and adipogenesis, which suggests that activation of D2 could be a potential therapeutic target for the differentiation of brown preadipocytes and the expansion of human brown fat mass. However, our studies looked at the classical interscapular BAT depot of rodents, and the current understanding of adult human UCP1-positive fat cells in the neck/thoracic region is that they share more characteristics with rodent beige adipocytes than brown adipocytes (17, 18). Since beige and brown adipocytes develop from distinct cell lineages (18), it will be important to determine if D2 also plays a role in beige fat function and development. In addition, it was recently shown that human preadipocytes derived from mesenteric and subcutaneous white fat depots express D2 (19). D2 is not normally found in white adipose tissue (20), but "ectopic" D2 expression in white fat depots has been found in rodent models with resistance to diet-induced obesity (21). It is interesting to speculate that these preadipocytes actually represent a population of beige cells that could be selectively recruited and activated by a D2-targeted approach. Notably, *Dio2* expression has also been reported in both the interscapular BAT of human newborns and the supraclavicular fat of adult humans (3, 22). The fact that human fat—albeit brown or beige—expresses D2 supports a D2-targeted approach in the recruitment and development of brown/beige preadipocytes when developing new therapies to counter obesity.

Insulin signaling: USP7 in glucose metabolic control

In Chapter 4, we found the deubiquitinating enzyme USP7 to be a novel regulator of FoxO1 transcriptional activity. Through *in vitro* and *in vivo* studies, we provided data to suggest a model where USP7-mediated removal of monoubiquitin moieties from FoxO1 leads to decreased association of FoxO1 with target gluconeogenic gene promoters, thereby suppressing gluconeogenesis. Notably, this work not only expands the role of USP7 to glucose metabolic control, but it also reveals that monoubiquitination and its reversal is an important posttranslational modification controlling FoxO1 activity. The pivotal role of FoxO1 in linking insulin action to suppression of gluconeogenic genes means that manipulating the monoubiquitinated status of FoxO1 may offer alternatives to decrease hepatic glucose output during states of insulin resistance.

Therapeutic potential for targeting FoxO1 monoubiquitination in diabetes

Hyperglycemia is a hallmark of diabetes and predominately caused by an elevation of hepatic gluconeogenesis (23). Our data in Chapter 4 suggest that activation of USP7 may lead to a reduction in gluconeogenesis, which could prove therapeutically useful in the management of diabetes. This statement is best generalized from our findings with adenoviral-mediated overexpression of USP7 in mouse liver, which we found to produce a significant—yet modest—reduction in gluconeogenic gene expression and conversion of pyruvate to glucose. These relatively minor changes are expected given that even the liver-specific FoxO1 knockout mouse exhibits what has been called a “mild phenotype” and requires prolonged fasting to detect a decrease in blood glucose (24). Moreover, the effects of FoxO1 on gluconeogenesis are best appreciated in states of insulin resistance, when defective insulin action results in nuclear

accumulation and increased activity of FoxO1 (25, 26). Therefore, we anticipate that under a context of hyper-activated FoxO1, such as mice with genetically- or diet-induced diabetes, overexpression of USP7 should have a more profound suppressive effect on FoxO1-target genes and reduction of blood glucose. These studies could also provide a better indication of the clinical utility for a USP7-targeted approach in the treatment of diabetes. Similarly, future investigations could be aided by generation of liver-specific USP7 knockout mice, which, in accordance with our primary hepatocyte data, should become hyperglycemic as a result of increased FoxO1 occupancy at promoters of gluconeogenic genes. Although activation of USP7 by suppressing FoxO1 activity may provide a beneficial blood glucose lowering effect in the diabetic individual, the fact that USP7 has other targets should be heavily considered.

Currently, there are generous efforts aimed at designing USP7 inhibitors for the treatment of cancer (27). But would inhibition of USP7—in the context of a cancer therapeutic—lead to detrimental elevation of hepatic glucose production by activating FoxO1? Considering our findings that USP7 knockdown does not alter the ability for insulin to suppress gluconeogenic targets, the insulin-sensitive individual should not experience hyperglycemia on a USP7 inhibitor drug regimen. For example, hepatic overexpression of FoxO1, despite elevating gluconeogenic genes, does not increase fasting glucose because of a compensatory increase of serum insulin (26). Therefore, as long as insulin signaling is intact, then activity of FoxO1 will be kept in check; however, this may not occur for diabetic individuals with insulin resistance. Under this scenario, our data suggest that inhibition of USP7 could exacerbate elevated gluconeogenesis and further increase hyperglycemia. Because diabetics are at an increased risk for several cancers (28), this contraindication could be a potential obstacle for a substantial number of cancer patients receiving anti-USP7 therapy. Although this adverse effect may not preclude use *per se*

in the diabetic cancer patient, it would necessitate judicious blood glucose monitoring because levels could be difficult to control. Results from liver-specific deletion of USP7 on a diabetic background should be informative in this regard.

As stated above, upregulation of USP7 would be favorable in the treatment of diabetes. One potential caveat for this therapy is its connection to cancer. An example of particular importance is the report of increased USP7 levels in a hepatocellular carcinoma cell line (29), which suggests that an attempt to activate hepatic USP7 in the context of an anti-diabetes therapeutic could have oncogenic effects. Although this does not indicate causality, USP7 is in fact overexpressed in several tumor types (30, 31). Thus, USP7 itself as a therapeutic target should be carefully considered, but targeting the deubiquitination of FoxO1 could still be a viable option.

Targeting the E3 ubiquitin ligase responsible for monoubiquitination of FoxO1 is an attractive therapeutic alternative that could avoid the potential drawbacks of a USP7-targeted approach. In this regard, one would expect that inhibition of such an E3 ligase would decrease monoubiquitination of FoxO1, thereby suppressing its activity and decreasing gluconeogenesis. One potential candidate for the E3 ligase is MDM2, which has been shown to induce monoubiquitination and increase transcriptional activity of FoxO4 (32). However, this is contrary to other reports implicating MDM2 as an E3 ligase that catalyzes polyubiquitination and degradation of FoxO proteins (33, 34). This suggests that there is possibly a different E3 ligase responsible for FoxO1 monoubiquitination. To determine the particular E3 ligase involved, we could take a mass spectrometry (MS/MS) approach to identify high-confidence candidate interactors with FoxO1 (35). Importantly, we would want to enrich the system for an E3 ligase that activates FoxO1 rather than degrade it, and this experiment would best be performed with

FoxO1 immunoprecipitates from hepatocytes isolated from insulin-resistant mouse livers. Once identified and validated, small molecules that inhibit the E3 ligase activity or its interaction with FoxO1 could be designed with therapeutic intentions. Therefore, a better understanding of other players in the pathway of FoxO1 monoubiquitination could offer alternative approaches to control FoxO1 activity and could provide therapeutic benefit for states of insulin resistance.

When glucose availability or uptake is reduced, the liver aids in maintenance of energy homeostasis through production of ketone bodies. During prolonged starvation, for example, fatty acids mobilized from adipose tissue are converted in the liver to ketone bodies, which replace glucose as the predominant fuel source for the brain. Under this setting, conservation of protein is necessary for the preservation of vital functions (36). The resulting protection from protein catabolism decreases the supply of gluconeogenic substrates, reducing hepatic glucose synthesis, and the availability of ketone bodies as a fat-derived metabolic fuel promotes survival (37-39). Conversely, high levels of ketones can have deleterious effects. In diabetes, ketogenesis increases in response to the body's perceived glucose-deficiency. The consequent elevation of acidic ketone bodies decreases blood pH, which can lead to the potentially life-threatening complication of diabetic ketoacidosis (40). Whether hepatic USP7 plays a role in ketogenesis and lipid homeostasis under either of these contexts remains to be determined.

Closing remarks

Although presented as distinct sections, thyroid hormone and insulin signaling pathways are part of a vast interconnected network responsible for the maintenance of organismal homeostasis. When forced out of equilibrium, as with obesity or insulin resistance, knowledge of these pathways may provide key targets for reestablishing a healthy energy balance.

REFERENCES

1. **Bianco AC, Silva JE** 1987 Intracellular conversion of thyroxine to triiodothyronine is required for the optimal thermogenic function of brown adipose tissue. J Clin Invest 79:295-300

2. **de Jesus LA, Carvalho SD, Ribeiro MO, Schneider M, Kim SW, Harney JW, Larsen PR, Bianco AC** 2001 The type 2 iodothyronine deiodinase is essential for adaptive thermogenesis in brown adipose tissue. J Clin Invest 108:1379-1385

3. **Cypess AM, Lehman S, Williams G, Tal I, Rodman D, Goldfine AB, Kuo FC, Palmer EL, Tseng YH, Doria A, Kolodny GM, Kahn CR** 2009 Identification and importance of brown adipose tissue in adult humans. N Engl J Med 360:1509-1517

4. **van Marken Lichtenbelt WD, Vanhommerig JW, Smulders NM, Drossaerts JM, Kemerink GJ, Bouvy ND, Schrauwen P, Teule GJ** 2009 Cold-activated brown adipose tissue in healthy men. N Engl J Med 360:1500-1508

5. **Virtanen KA, Lidell ME, Orava J, Heglind M, Westergren R, Niemi T, Taittonen M, Laine J, Savisto NJ, Enerback S, Nuutila P** 2009 Functional brown adipose tissue in healthy adults. N Engl J Med 360:1518-1525

6. **Skarulis M, Celi F, Mueller E, Zemskova M, Malek R, Hugendubler L, Cochran C, Solomon J, Chen C, Gorden P** 2010 Thyroid hormone induced brown adipose tissue and amelioration of diabetes in a patient with extreme insulin resistance. The Journal of clinical endocrinology and metabolism 95:256-262

7. **Lahesmaa M, Orava J, Schalin-Jantti C, Soinio M, Hannukainen JC, Noponen T, Kirjavainen A, Iida H, Kudomi N, Enerback S, Virtanen KA, Nuutila P** 2014 Hyperthyroidism increases brown fat metabolism in humans. J Clin Endocrinol Metab 99:E28-35

8. **Baxter JD, Webb P** 2009 Thyroid hormone mimetics: potential applications in atherosclerosis, obesity and type 2 diabetes. Nature reviews Drug discovery 8:308-320

9. **Castillo M, Freitas BC, Rosene ML, Drigo RA, Grozovsky R, Maciel RM, Patti ME, Ribeiro MO, Bianco AC** 2010 Impaired metabolic effects of a thyroid hormone receptor beta-selective agonist in a mouse model of diet-induced obesity. Thyroid 20:545-553

10. **Villicev CM, Freitas FR, Aoki MS, Taffarel C, Scanlan TS, Moriscot AS, Ribeiro MO, Bianco AC, Gouveia CH** 2007 Thyroid hormone receptor beta-specific agonist GC-1 increases energy expenditure and prevents fat-mass accumulation in rats. J Endocrinol 193:21-29

11. **Bryzgalova G, Effendic S, Khan A, Rehnmark S, Barbounis P, Boulet J, Dong G, Singh R, Shapses S, Malm J, Webb P, Baxter JD, Grover GJ** 2008 Anti-obesity, anti-

diabetic, and lipid lowering effects of the thyroid receptor beta subtype selective agonist KB-141. J Steroid Biochem Mol Biol 111:262-267

12. **Peeters RP, van der Deure WM, Visser TJ** 2006 Genetic variation in thyroid hormone pathway genes; polymorphisms in the TSH receptor and the iodothyronine deiodinases. Eur J Endocrinol 155:655-662

13. **Canani LH, Capp C, Dora JM, Meyer EL, Wagner MS, Harney JW, Larsen PR, Gross JL, Bianco AC, Maia AL** 2005 The type 2 deiodinase A/G (Thr92Ala) polymorphism is associated with decreased enzyme velocity and increased insulin resistance in patients with type 2 diabetes mellitus. J Clin Endocrinol Metab 90:3472-3478

14. **da-Silva WS, Harney JW, Kim BW, Li J, Bianco SD, Crescenzi A, Christoffolete MA, Huang SA, Bianco AC** 2007 The small polyphenolic molecule kaempferol increases cellular energy expenditure and thyroid hormone activation. Diabetes 56:767-776

15. **da-Silva WS, Ribich S, Arrojo e Drigo R, Castillo M, Patti ME, Bianco AC** 2011 The chemical chaperones tauroursodeoxycholic and 4-phenylbutyric acid accelerate thyroid hormone activation and energy expenditure. FEBS Lett 585:539-544

16. **Watanabe M, Houten SM, Mataki C, Christoffolete MA, Kim BW, Sato H, Messaddeq N, Harney JW, Ezaki O, Kodama T, Schoonjans K, Bianco AC, Auwerx J** 2006 Bile acids induce energy expenditure by promoting intracellular thyroid hormone activation. Nature 439:484-489

17. **Wu J, Cohen P, Spiegelman B** 2013 Adaptive thermogenesis in adipocytes: is beige the new brown? Genes & development 27:234-250

18. **Harms M, Seale P** 2013 Brown and beige fat: development, function and therapeutic potential. Nature medicine 19:1252-1263

19. **Nomura E, Toyoda N, Harada A, Nishimura K, Ukita C, Morimoto S, Kosaki A, Iwasaka T, Nishikawa M** 2011 Type 2 iodothyronine deiodinase is expressed in human preadipocytes. Thyroid 21:305-310

20. **Leonard JL, Mellen SA, Larsen PR** 1983 Thyroxine 5'-deiodinase activity in brown adipose tissue. Endocrinology 112:1153-1155

21. **Liu X, Rossmeisl M, McClaine J, Riachi M, Harper ME, Kozak LP** 2003 Paradoxical resistance to diet-induced obesity in UCP1-deficient mice. J Clin Invest 111:399-407

22. **Lidell M, Betz M, Dahlqvist Leinhard O, Heglind M, Elander L, Slawik M, Mussack T, Nilsson D, Romu T, Nuutila P, Virtanen K, Beuschlein F, Persson A, Borga M,**

Enerbäck S 2013 Evidence for two types of brown adipose tissue in humans. Nature medicine 19:631-634

23. **Magnusson I, Rothman DL, Katz LD, Shulman RG, Shulman GI** 1992 Increased rate of gluconeogenesis in type II diabetes mellitus. A 13C nuclear magnetic resonance study. J Clin Invest 90:1323-1327

24. **Matsumoto M, Pocai A, Rossetti L, Depinho RA, Accili D** 2007 Impaired regulation of hepatic glucose production in mice lacking the forkhead transcription factor Foxo1 in liver. Cell Metab 6:208-216

25. **Altomonte J, Richter A, Harbaran S, Suriawinata J, Nakae J, Thung SN, Meseck M, Accili D, Dong H** 2003 Inhibition of Foxo1 function is associated with improved fasting glycemia in diabetic mice. Am J Physiol Endocrinol Metab 285:E718-728

26. **Qu S, Altomonte J, Perdomo G, He J, Fan Y, Kamagate A, Meseck M, Dong HH** 2006 Aberrant Forkhead box O1 function is associated with impaired hepatic metabolism. Endocrinology 147:5641-5652

27. **Nicholson B, Kumar S, Agarwal S, Eddins M, Marblestone JG, Wu J, Kodrasov MP, Larocque JP, Sterner DE, Mattern MR** 2014 Discovery of Therapeutic Deubiquitylase Effector Molecules: Current Perspectives. Journal of biomolecular screening

28. **Giovannucci E, Harlan DM, Archer MC, Bergenstal RM, Gapstur SM, Habel LA, Pollak M, Regensteiner JG, Yee D** 2010 Diabetes and cancer: a consensus report. Diabetes Care 33:1674-1685

29. **Martinez-Lopez N, Varela-Rey M, Fernandez-Ramos D, Woodhoo A, Vazquez-Chantada M, Embade N, Espinosa-Hevia L, Bustamante FJ, Parada LA, Rodriguez MS, Lu SC, Mato JM, Martinez-Chantar ML** 2010 Activation of LKB1-Akt pathway independent of phosphoinositide 3-kinase plays a critical role in the proliferation of hepatocellular carcinoma from nonalcoholic steatohepatitis. Hepatology 52:1621-1631

30. **Song MS, Salmena L, Carracedo A, Egia A, Lo-Coco F, Teruya-Feldstein J, Pandolfi PP** 2008 The deubiquitinylation and localization of PTEN are regulated by a HAUSP-PML network. Nature 455:813-817

31. **Hussain S, Zhang Y, Galardy PJ** 2009 DUBs and cancer: the role of deubiquitinating enzymes as oncogenes, non-oncogenes and tumor suppressors. Cell Cycle 8:1688-1697

32. **Brenkman AB, de Keizer PL, van den Broek NJ, Jochemsen AG, Burgering BM** 2008 Mdm2 induces mono-ubiquitination of FOXO4. PLoS One 3:e2819

33. **Yang JY, Zong CS, Xia W, Yamaguchi H, Ding Q, Xie X, Lang JY, Lai CC, Chang CJ, Huang WC, Huang H, Kuo HP, Lee DF, Li LY, Lien HC, Cheng X, Chang KJ,**

Hsiao CD, Tsai FJ, Tsai CH, Sahin AA, Muller WJ, Mills GB, Yu D, Hortobagyi GN, Hung MC 2008 ERK promotes tumorigenesis by inhibiting FOXO3a via MDM2-mediated degradation. Nat Cell Biol 10:138-148

34. **Fu W, Ma Q, Chen L, Li P, Zhang M, Ramamoorthy S, Nawaz Z, Shimojima T, Wang H, Yang Y, Shen Z, Zhang Y, Zhang X, Nicosia SV, Zhang Y, Pledger JW, Chen J, Bai W** 2009 MDM2 acts downstream of p53 as an E3 ligase to promote FOXO ubiquitination and degradation. J Biol Chem 284:13987-14000

35. **Sowa ME, Bennett EJ, Gygi SP, Harper JW** 2009 Defining the human deubiquitinating enzyme interaction landscape. Cell 138:389-403

36. **Ruderman NB** 1975 Muscle amino acid metabolism and gluconeogenesis. Annu Rev Med 26:245-258

37. **Goodman MN, Ruderman NB** 1980 Starvation in the rat. I. Effect of age and obesity on organ weights, RNA, DNA, and protein. Am J Physiol 239:E269-E276

38. **Goodman MN, Larsen PR, Kaplan MM, Aoki TT, Young VR, Ruderman NB** 1980 Starvation in the rat. II. Effect of age and obesity on protein sparing and fuel metabolism. Am J Physiol 239:E277-E286

39. **Goodman MN, Lowell B, Belur E, Ruderman NB** 1984 Sites of protein conservation and loss during starvation: influence of adiposity. Am J Physiol 246:E383-390

40. **McPherson PA, McEneny J** 2012 The biochemistry of ketogenesis and its role in weight management, neurological disease and oxidative stress. Journal of physiology and biochemistry 68:141-151